2017

Influence Of Acetyl-Coa Metabolism On Histone Acetylation And Cancer

Joyce Vivian Lee
University of Pennsylvania, joycevlee@gmail.com

Influence Of Acetyl-Coa Metabolism On Histone Acetylation And Cancer

Abstract

Cancer cells increase nutrient uptake to support viability and proliferation. The influx of nutrients alters intermediary metabolite levels, and compelling evidence shows that metabolite availability impacts cell functions through altering chromatin modifications and downstream gene expression. One such metabolic intermediate is acetyl-CoA, as the concentration of acetyl-CoA is positively correlated with histone and non-histone protein acetylation. Histone acetylation is emerging as a nutrient-sensitive process, conferring gene expression changes in response to nutrient availability. In this thesis, we examined the impact of acetyl-CoA metabolism on the epigenome. We established that histone acetylation is sensitive to acetyl-CoA concentrations, which are dynamically regulated by glucose availability. This dynamic increase in histone acetylation induces the expression of cancer-promoting genes. We hypothesized that oncogene activation could lead to increased histone acetylation through reprogrammed metabolism. In two mouse models of cancer, histone acetylation increased upon oncogene activation. Additionally, histone acetylation was positively correlated with phosphorylated AKT in human prostate tumors and glioma. To test whether AKT regulates histone acetylation through metabolic changes, we utilized glioblastoma cell lines expressing constitutively active AKT and found that AKT promotes histone acetylation in nutrient-limited conditions. Mechanistically, this occurs partly through AKT-mediated phosphorylation of ACLY at serine 455, increasing ACLY activity. These studies reveal a novel role for AKT-driven metabolic changes on global histone acetylation in cancer cells. To better understand how concentrations of acetyl-CoA could lead to differential gene expression, we investigated a subset of acetyl-CoA regulated genes. Under conditions in which intracellular acetyl-CoA is abundant, glioma cells upregulate expression of adhesion and migration genes, increase transwell migration, adhere better to ECM, and are efficient in wound healing. Genetic deletion or biochemical inhibition of acetyl-CoA generating enzyme, ACLY, abrogates nutrient-dependent adhesion and migration. We postulated that specificity for regulation of migration related gene expression would be achieved through regulation of transcription factors. Using computational analysis of our acetyl-CoA gene set, NFAT1 was predicted as the top transcription factor in promoting these genes. Through fluorescent single cell analyses, we find that acetyl-CoA triggers calcium oscillations that allow for NFAT1 nuclear localization. These findings suggest that that acetyl-CoA availability is differentially regulated in cancer cells and contributes to malignant phenotypes.

Degree Type

Dissertation

Degree Name

Doctor of Philosophy (PhD)

Graduate Group

Cell & Molecular Biology

First Advisor

Kathryn E. Wellen

Keywords

acetyl-CoA, ATP-citrate Lyase, cancer metabolism, epigenetics, gene expression, histone acetylation

Subject Categories

Cell Biology | Molecular Biology | Oncology

INFLUENCE OF ACETYL-COA METABOLISM ON HISTONE ACETYLATION AND CANCER

Joyce V. Lee

A DISSERTATION

in

Cell and Molecular Biology

Presented to the Faculties of the University of Pennsylvania

in

Partial Fulfillment of the Requirements for the

Degree of Doctor of Philosophy

2017

Supervisor of Dissertation

_____

Kathryn E. Wellen, Ph.D.
Associate Professor of Cancer Biology

Graduate Group Chairperson

_____

Daniel S. Kessler, Ph.D.
Associate Professor of Cell and Developmental Biology

Dissertation Committee

Brian Keith, Ph.D., Professor and Dean of Biomedical Studies, The Wistar Institute
Shelley L. Berger, Ph.D., Professor of Cell and Developmental Biology, UPENN
Xiaolu Yang, Ph.D., Professor of Cancer Biology, UPENN
Joseph A. Baur, Ph.D., Associate Professor of Physiology, UPENN

INFLUENCE OF ACETYL-COA METABOLISM ON HISTONE ACETYLATION AND CANCER

DEDICATION

To my dad, who inspired my scientific curiosity from an early age

To my husband and my mom, who were my greatest cheerleaders during my graduate studies.

ACKNOWLEDGEMENTS

I would like to thank the Wellen Lab, past and present members, for helping with this work. I would also like to thank the Penn community for sharing resources, ideas, and collaborating on this work. I would also like to thank the leaders and administrators of the Cell and Molecular Biology graduate group for running a great program and providing great support to the students. This work was supported by funding from the NIH (5 F31 CA 189744-2) and NIH (R01CA174761).

Please Note: excerpts from the following manuscript were included in this document (with permission from Elseiver):

Lee, J. V., Shah, S. A., & Wellen, K. E. (2013). Obesity, cancer and acetyl-CoA metabolism. *Drug Discovery Today: Disease Mechanisms*, *10*(1-2), e55–e61.

Lee, J. V., Carrer, A., Shah, S., Snyder, N. W., Wei, S., Venneti, S., et al. (2014). Akt-Dependent Metabolic Reprogramming Regulates Tumor Cell Histone Acetylation. *Cell Metabolism*, *20*(2), 306–319.

Please Note: excerpts from the following manuscript were included in this document (with permission from Taylor & Francis Group, LLC):

Lee, J. V., Shah, S., Carrer, A., & Wellen, K. E. (2014). A cancerous web: signaling, metabolism, and the epigenome. *Molecular & Cellular Oncology*, *2*(2), e965620–4

ABSTRACT

INFLUENCE OF ACETYL-COA METABOLISM ON EPIGENETICS AND CANCER

Joyce V. Lee

Kathryn E. Wellen, Ph.D.

Cancer cells increase nutrient uptake to support viability and proliferation. The influx of nutrients alters intermediary metabolite levels, and compelling evidence shows that metabolite availability impacts cell functions through altering chromatin modifications and downstream gene expression. One such metabolic intermediate is acetyl-CoA, as the concentration of acetyl-CoA is positively correlated with histone and non-histone protein acetylation. Histone acetylation is emerging as a nutrient-sensitive process, conferring gene expression changes in response to nutrient availability. In this thesis, we examined the impact of acetyl-CoA metabolism on the epigenome. We established that histone acetylation is sensitive to acetyl-CoA concentrations, which are dynamically regulated by glucose availability. This dynamic increase in histone acetylation induces the expression of cancer-promoting genes. We hypothesized that oncogene activation could lead to increased histone acetylation through reprogrammed metabolism. In two mouse models of cancer, histone acetylation increased upon oncogene activation. Additionally, histone acetylation was positively correlated with phosphorylated AKT in human prostate tumors and glioma. To test whether AKT regulates histone acetylation through metabolic changes, we utilized glioblastoma cell lines expressing constitutively active AKT and found that AKT promotes histone acetylation in nutrient-limited conditions. Mechanistically, this occurs partly through AKT-mediated phosphorylation of ACLY at serine 455, increasing ACLY activity. These studies reveal a novel role for AKT-driven

metabolic changes on global histone acetylation in cancer cells. To better understand how concentrations of acetyl-CoA could lead to differential gene expression, we investigated a subset of acetyl-CoA regulated genes. Under conditions in which intracellular acetyl-CoA is abundant, glioma cells upregulate expression of adhesion and migration genes, increase transwell migration, adhere better to ECM, and are efficient in wound healing. Genetic deletion or biochemical inhibition of acetyl-CoA generating enzyme, ACLY, abrogates nutrient-dependent adhesion and migration. We postulated that specificity for regulation of migration related gene expression would be achieved through regulation of transcription factors. Using computational analysis of our acetyl-CoA gene set, NFAT1 was predicted as the top transcription factor in promoting these genes. Through fluorescent single cell analyses, we find that acetyl-CoA triggers calcium oscillations that allow for NFAT1 nuclear localization. These findings suggest that that acetyl-CoA availability is differentially regulated in cancer cells and contributes to malignant phenotypes.

TABLE OF CONTENTS

LIST OF FIGURES

CHAPTER 1:

INTRODUCTION

1.1 Cancer Metabolism

The metabolism of a cancer cell is distinct from benign, quiescent cells. Cell proliferation requires energy and biomass, which is a reason why cancer cells consume more glucose than quiescent normal cells in our body. This altered metabolism is driven by genetic mutations in the cancer cell. Study of these changes aids in our understanding of how metabolism contributes to tumor growth.

1.1.1 Reprogrammed metabolism in cancer cells

In 1924, Otto Warburg observed that cancer cells metabolized more glucose than normal cells. Warburg documented that cancer cells tend to convert glucose into lactate under aerobic conditions, not typical of normal cells. By determining the amount of lactate produced per hour, he estimated that through "fermentation" (glycolysis), cancer cells could produce as many energy equivalents as cells undergoing full utilization of glucose through "respiration" (mitochondrial oxidative phosphorylation). This finding was perplexing because normal cells obtain much more energy by completing oxidative phosphorylation than by glycolysis alone (Warburg, 1956). Why would cancer cells opt for a less efficient metabolism? Warburg proposed that proliferative tumor cells had lost their oxidative capacity resulting in their dependence on high glycolysis. However, decades later, the carefully analysis of highly proliferative cancer cell lines generated evidence that cancer cells have intact mitochondrial oxidative phosphorylation [reviewed

in (Moreno-Sanchez et al., 2007)], leaving an explanation for Warburg's observation elusive.

In subsequent years, leading researchers in the field proposed plausible explanations. Rather than viewing this process as purely concerning energy production, or generation of adenosine 5′-diphosphate (ATP), perhaps proliferating cells have important metabolic requirements that extend beyond ATP production (Vander Heiden et al., 2009, DeBerardinis et al., 2008, Ward and Thompson, 2012). Fundamentally, a dividing cell must replicate all of its organelles, DNA, cellular membranes to create a viable daughter cell. To do this, some glucose must be diverted to form intermediates needed for biosynthetic pathways, such as acetyl-CoA for fatty acids, glycolytic intermediates for nonessential amino acids, and ribose for nucleotides. The high rate of glycolysis allows cancer cells to support biosynthetic processes and energy production during rapid proliferation.

Mitochondria oxidative phosphorylation in cancer cells continue to produce metabolites in the tricarboxylic acid (TCA) cycle. However, while normal non-proliferating cells rely on the TCA cycle to generate ATP to support their normal homeostatic functions, proliferative cells will utilize their TCA cycle intermediates for biosynthesis of different macromolecules required for cell division and contributing to tumor growth, a process called anaplerosis. For example, under nutrient-rich conditions, mitochondrial citrate is transferred out to the cytosol and converted acetyl-CoA, the primary building block for lipid synthesis and cholesterol, and OAA, by the enzyme ATP-citrate lyase (ACLY) (Hatzivassiliou et al., 2005, Parlo and Coleman, 1984). OAA can be further be converted into nonessential amino acids for synthesis of proteins and

nucleotides. Rather than relying on mitochondria for ATP synthesis, cancer cells utilize the metabolites to support biosynthesis of macromolecules required for proliferation (**Figure 1**).

1.1.2 Cancer driving mutations rewire metabolism

The human blood supply provides a constant supply of nutrients. Normal cells are instructed to take up nutrients from their environment to support homeostatic processes. Uncontrolled proliferation does not occur because nutrient uptake is tightly controlled by growth factor signaling. Genetic mutations disrupt this strict regulation, allowing cells to overcome growth factor dependence. Mutations that lead to constitutively active receptor-initiated signaling pathways allow cancerous cells to take up and metabolize nutrients that both promote cell survival and fuel cell growth. These oncogenic mutations allow for the uptake of nutrients, particularly glucose, that give them the metabolic independence to support cellular programs for growth and proliferation.

One such pathway that is altered is PI3K/Akt signaling [reviewed in (Luo et al., 2003)]. This pathway is typically responsive to growth factors binding to surface receptors, such as EGFR, which signals downstream activation of PI3K, and activating phosphorylation of phosphatidylinositol and recruitment of serine theronie kinase Akt. In normal cells, activation of the PI3K system is tightly controlled by dephosphorylation of phosphatidylinositol species by the phosphatase PTEN. However, mutations that lead to the loss of PTEN function allows cancer cells to increase the surface expression of nutrient transporters that increase uptake of glucose, amino acids, and other nutrients

[reviewed in (DeBerardinis et al., 2008, Vander Heiden et al., 2009, Ward and Thompson, 2012)]. Furthermore, Akt drives glycolysis and lactate production (Elstrom et al., 2004b, Plas et al., 2001, Rathmell et al., 2003) and to support synthesis of macromolecules in cancer cells by stimulating lipogenic genes and lipid synthesis (Bauer et al., 2005). Aberrant activation of many other oncogenes (mTORC1, MAPK, EGFR, Ras, HER2/neu, c-myc, and others) or loss of tumor suppressors (VHL, TSC, LKB1, p53, and others) also drive metabolic changes, but will not be described in this thesis.

1.2 Epigenetics and Metabolism

There is a growing interest in understanding how the environment contributes to disease progression. Epigenetic enzymes tightly control the cellular programs that are executed in the cell. They are master regulators of the genes programs that should be switched on or off. How the environment impacts this switch has been of great interest. While nutritional availability largely serves as a fuel source for growing cells, it is understood that the metabolites that result from consumption of macronutrients contributes another layer of control to epigenetic regulation.

1.2.1 Cancer Epigenetics

Epigenetic modifications are one way cells control the transcriptional programs. Chromatin modifications work together to control the expression of genes encoded in DNA. While a person's genome is completely identical in the entire body, epigenetic regulators provide information on what cell type or function a cell should perform. Furthermore, epigenetic regulation of gene expression allows cells to adapt and integrates intrinsic and environmental signal (Jaenisch and Bird, 2003, Berger and

Sassone-Corsi, 2016). This information is relayed in the "histone code" (Jenuwein and Allis, 2001, Berger, 2007), which defines certain marks on histone tails as gene transcription activating or repressing. While histone methylation on lysine tails can be either transcription activating or transcription repressing, acetylation generally "codes" for transcription activation. The relationship of these modifications makes up the "epigenetic landscape" (Goldberg et al., 2007, Waddington, 1957) that controls the manifestation of the genome, which is often deeply altered in diseases such as cancer (Jones et al., 2016).

Human cancer cells are driven by genetic alterations as well as global epigenetic abnormalities. These genetic and epigenetic changes contribute to cancer development. Human cancers have many global epigenetic abnormalities. For example, we know that acetylation and methylation are deeply altered on a global level and large correlations studies have been performed to identify how these epigenetic changes correlate with prognosis (Chervona and Costa, 2012). However, we do not fully understand how much these changes contribute to progression. Notably, these epigenetic modifications are reversible. To begin to understand this, it is vital to understand how cancer epigenetics is regulated.

Epigenetic control of gene expression is governed by the activity of "writers" and "erasers" of histone marks. Expression levels of writers and erasers are frequently altered in cancer and thus many drug targets include targeting these epigenetic enzymes (Jones et al., 2016). However, one may consider the cofactors required for epigenetic enzymes to catalyze their reactions often come from metabolism. A less studied but important factor to epigenetic control is metabolite availability, from breakdown of

macromolecules, which is often deregulated in cancer. Perhaps information about a cell's metabolic state can be assimilated into the regulation of epigenetics and transcription (Lu and Thompson, 2012b).

1.2.2 Metabolite regulation of chromatin

Many enzymes that regulate post-translational modifications on proteins rely on metabolites as co-factors, and in some cases, the activities of these enzymes can be regulated by availability of their metabolite co-factors. This is true in the case of sirtuin deacetylases (class III KDACs), which utilize NAD+ as a co-factor to remove acetylation from proteins and are activated as the NAD+/NADH ratio rises, as occurs during nutrient deprivation (Houtkooper et al., 2012).

In certain cases, it is already established that metabolites regulate the cancer cell epigenome. Tumors with IDH1/2 mutations, for example, generate high levels of (R)-2-hydroxyglutarate, which interferes with normal activities of α-ketoglutarate-dependent enzymes such as tet-methylcytosine dioxygenase 2 (TET2), increasing global methylation and resulting in epigenetic and transcriptional deregulation (Lu et al., 2012).

Even beyond pathological circumstances such as this, accumulating evidence indicates that metabolic modulation of signaling, transcription, and chromatin can dramatically impact cellular activities. Metabolites can thus exert dual functions in providing both building blocks and instructions to the cell. There are many examples of posttranslational histone modifications that rely on metabolites such as methylation, crotonylation, other acylations, glycosylation, phosphorylation, and others that will not

be described in detail in this thesis [reviewed in (Sabari et al., 2017, Kinnaird et al., 2016, Lu and Thompson, 2012b)]

Emerging at the forefront of such regulation is acetyl-CoA, a metabolite that plays key roles in glucose, amino acid, and lipid metabolism, but is also required for posttranslational modification on lysine acetylation and for N-terminal acetylation. Studies in yeast have provided evidence that acetyl-CoA levels may fluctuate within a range to limit the activity of the lysine acetyltransferase (KAT) Gcn5 (Cai et al., 2011), based on its dissociation constant (Kd) for acetyl-CoA (8.5 μM). While mammalian concentrations of acetyl-CoA have been determined (see Chapter 3), it is noteworthy that many KATs, including human GCN5 and p300/CBP, are subject to product inhibition by free coenzyme A (CoASH), indicating that the acetyl-CoA/CoASH ratio could be the relevant regulator of KAT activity instead of absolute levels of acetyl-CoA (see Chapter 3).

1.3 Acetyl-CoA and the regulation of gene expression

1.3.1 Acetyl-CoA at metabolic crossroads

Acetyl-CoA is compartmentalized into mitochondrial and nuclear-cytoplasmic pools in eukaryotic cells, and these pools are functionally distinct (Takahashi et al., 2006). The nuclear-cytoplasmic level of acetyl-CoA in mammalian cells is established primarily by the combined actions of two enzymes: ATP-citrate Lyase (ACLY), which converts nutrient-derived citrate into acetyl-CoA and oxaloacetate, and acetyl-CoA synthetase 2 (ACSS2), which utilizes acetate for acetyl-CoA synthesis (Wellen and Thompson, 2012). Acetyl-CoA is positioned at the metabolic crossroads of glycolysis,

fatty acid oxidation, amino acid metabolism, the TCA cycle, and lipid synthesis, suggesting that acetyl-CoA may be an ideal metabolite for the cells to sense their nutrient status (**Figure 2**). Indeed, glucose-dependent production of acetyl-CoA has been shown to regulate global levels of histone lysine acetylation in both yeast and mammals (Friis et al., 2009, Wellen et al., 2009).

Nuclear-cytoplasmic acetyl-CoA production is impacted by metabolic state in a complex manner. ACLY is important for continuous production of extra-mitochondrial acetyl-CoA in mammalian cells in nutrient rich conditions (Wellen et al., 2009). ACLY is overexpressed in several cancers, including those of the lung, prostate, bladder, breast, liver, stomach, and colon (Chypre et al., 2012). Knockdown of ACLY impairs cancer cell proliferation (Bauer et al., 2005, Hatzivassiliou et al., 2005). ACLY is also subject to allosteric activation by sugar phosphates, and ACLY phosphorylation at Ser455, a site regulated by AKT and protein kinase A, enhances its activity in vitro assays (Potapova et al., 2000). Hence, ACLY may serve as an integration point for signaling and metabolic cues when metabolic conditions are favorable (**Figure 3**).

Alternatively, ACSS2 may become more active when nutrients are scarce, since it is deacetylated by SIRT1, allowing for its activation (Hallows et al., 2006). For example, under hypoxia, acetate supplementation to cancer cell lines activated expression of lipogenic genes, which occurred with acetylation of lysine 9, 27, and 56 on histone H3 (Gao et al., 2016). ACSS2 has also been linked to the development and progression of several cancer types (Comerford et al., 2014, Mashimo et al., 2014, Schug et al., 2015).

1.3.2 Nutrient sensitive histone acetylation and gene expression

Acetyl-CoA availability has been shown to regulate global levels of histone lysine acetylation and alter of gene expression in both yeast and mammals. Pivotal work linking metabolism and histone acetylation in mammalian cells was first demonstrated in mouse adipocytes (Wellen et al., 2009), establishing that acetyl-CoA can be limiting in the cell when glucose is low or when acetyl-CoA producing enzyme ACLY expression is reduced in the cell. These changes led to global reduction in histone acetylation (H3K9,14ac; H4K5,8,12,16ac) and reduced adipocyte specific gene expression, leading to defective cellular differentiation. These effects were all rescued with media supplementation of acetate, indicating that cells could sense acetyl-CoA availability to promote these processes.

In *Saccharomyces cerevisiae*, histone acetylation increased in response to an increase of acetyl-CoA when yeast cells were stimulated to enter their metabolic cycle (Cai et al., 2011, Kuang et al., 2014). In the middle of the OX (oxidative) phase, acetyl-CoA began to rise and continued to rise until the middle of the RB (reductive building) phase, the phase for cell division. During this time, global histone acetylation on several H3 and H4 lysine tails was also the highest. Using genome-wide assessment of H3K9 acetylation, the authors demonstrated the acetylation was enriched near growth genes and was dependent on generation of acetyl-CoA (Cai et al., 2011). Using this system, subsequent studies identified distinct histone acetylation peaks that occur across the yeast metabolic cycle (Kuang et al., 2014). H3K9ac, H3K14ac and H4K5ac all appeared in parallel with the RNA-seq peak (Kuang et al., 2014). Of note, H3K14ac and H4K5ac began to increase about 1 hour before the RNA peak, still within the phase of high

intracellular acetyl-CoA, hinting at differential nutrient sensitivities of chromatin-modifying enzymes.

While direct histone acetylation is one mode of gene regulation, acetyl-CoA regulation of transcription factor activity, which could also contribute to acetyl-CoA dependent gene expression, is relatively less well explored. It is clear that thousands of proteins are acetylated including metabolic enzymes and epigenetic modifying enzymes (Zhao et al., 2010, Choudhary et al., 2009, Kim et al., 2006). Many metabolic enzymes are acetylated in response to glucose availability (Zhao et al., 2010), and it's important to note that not all proteins are differentially acetylated in response to acetyl-CoA. For example, while histone acetylation is ACLY dependent, acetylation of p53 and tubulin are not reduced upon ACLY silencing in colorectal carcinoma cell line HCT116 (Wellen et al., 2009). This supports the idea that certain processes may be more sensitive to nutrients than others. Acetyl-CoA availability can impact transcription factors is potentially on protein stability, with acetylation and ubiquitination on the same lysine promoting opposing effects on the protein stability, as seen in p53 (Li et al., 2002), NFkB (Li et al., 2012), and Smad7 (Gronroos et al., 2002). Whether these acetylation sites are nutrient regulated is of great interest. Few cases of nutrient-dependent transcription factor localization have been documented. Glucose-dependent acetylation can regulate β-catenin (Chocarro-Calvo et al., 2013). Additionally, ACSS2-dependent acetylation controls HIF2α regulation of *EPO* gene expression (Xu et al., 2014). While nutrient-dependent acetylation of metabolic proteins can coordinate multiple signaling pathways to adapt cells to changes in stimuli, understanding the mechanisms of acetyl-CoA guided transcriptional programs will unveil new layers of regulation on gene expression.

1.4 Hypothesis and Aims

It is becoming increasingly apparent that acetyl-CoA sits at the hub of both metabolic and signaling processes within the cell, as its concentrations are modulated by both extracellular nutrient availability and growth factor signaling. The points outlined in this thesis will shed light on how acetyl-CoA contributes to these processes for tumor growth and survival.

1.4.1 Sensing levels of acetyl-CoA

Given that nutrient availability positively correlates with histone acetylation and expression of growth-related genes in yeast, we hypothesize that cancer cells also rely on nutrient-derived acetyl-CoA for histone acetylation and gene expression. In Chapter 3, we characterize histone acetylation in several cancer cell lines and determine the genes that are sensitive to acetyl-CoA availability. Secondly, we measure the concentrations of acetyl-CoA in mammalian cells, determining the absolute concentrations of acetyl-CoA in the cell to understand whether mammalian cellular concentrations of acetyl-CoA are within the range of known dissociations constants of KAT enzymes. Additionally, we explore whether acetyl-CoA:CoA ratio can regulate histone acetylation in vitro.

1.4.2 Oncogene induced changes in acetyl-CoA regulated histone acetylation

It has also become increasingly clear that certain post-translational modifications are sensitive to metabolite availability, raising the possibility that metabolic alterations in cancer cells could have a profound influence on signal transduction and epigenetics. AKT is known to promote signaling to increase glucose uptake. We hypothesize that

histone acetylation is high in AKT-driven cancer cells through increased glucose uptake and phosphorylation of ACLY (**Figure 3**). In Chapter 3, we determine whether AKT activation leads to increased histone acetylation using in vivo models of cancer and patient samples. we also determine the mechanism for how AKT promotes histone acetylation.

1.4.3 Metabolite directed changes in cell behavior

In Chapter 4, we investigate the mechanisms by which acetyl-CoA concentrations modulate gene expression. From a list of top acetyl-CoA regulated genes identified by RNA-sequencing, we hypothesize that the availability of acetyl-CoA contributes to signaling that supports the expression of these genes. In chapter 4, we determine whether the expression of these genes is regulated by acetyl-CoA, through acetylation at gene promoters and/or via regulation of transcription factor localization.

Figure 1: Quiescent cell versus proliferating cell metabolism.

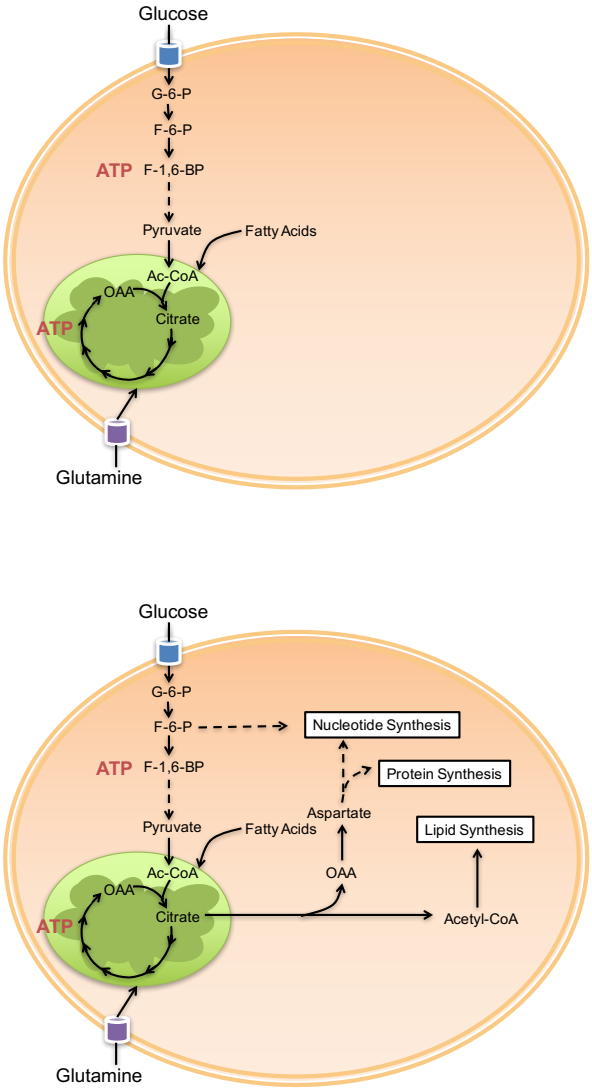

Benign quiescent cells in our body generally take up nutrients to support ATP production to support homeostatic functions. In proliferating cells, such as cancer, metabolism is increased to support energy production as well as biosynthetic pathways.

Figure 2: A cancerous web

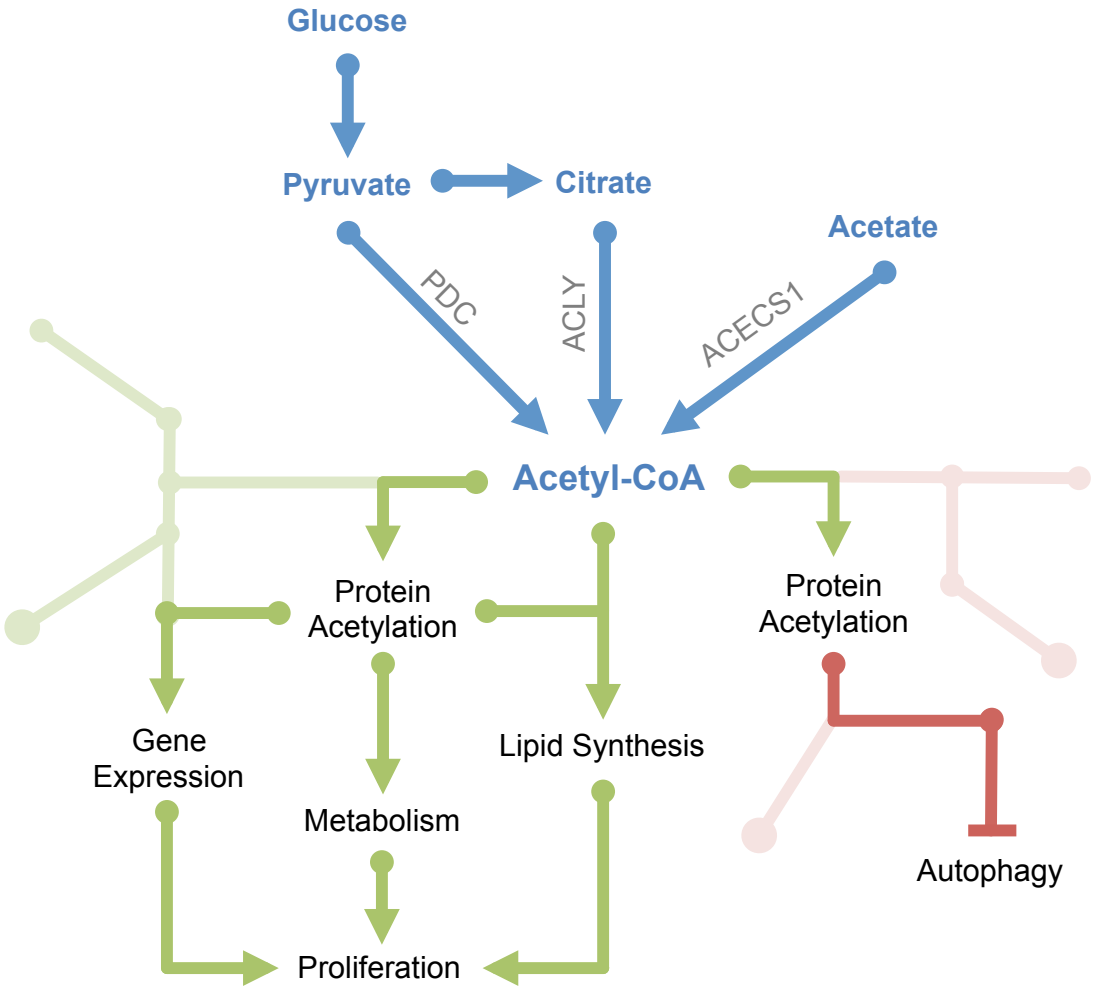

Acetyl-CoA promotes growth and proliferation through multiple mechanisms. Outside of mitochondria, acetyl-CoA can be generated from citrate by ATP-citrate lyase (ACLY), from acetate by acyl-CoA synthetase short chain family member 2 (ACSS2), and from pyruvate by the pyruvate dehydrogenase complex (PDC), which was recently reported to translocate from mitochondria into the nucleus. Acetyl-CoA has long been known to support growth and proliferation through its roles in the synthesis of fatty acids and cholesterol. Acetyl-CoA also participates in the regulation of histone acetylation and gene expression, is required for acetylation of numerous metabolic enzymes, and suppresses autophagy. Although many details remain to be elucidated, it is clear that acetylation plays crucial roles in modulating cellular activities, including decisions to grow and divide, in accordance with metabolic resources.

Figure 3: Akt promotes acetyl-CoA production

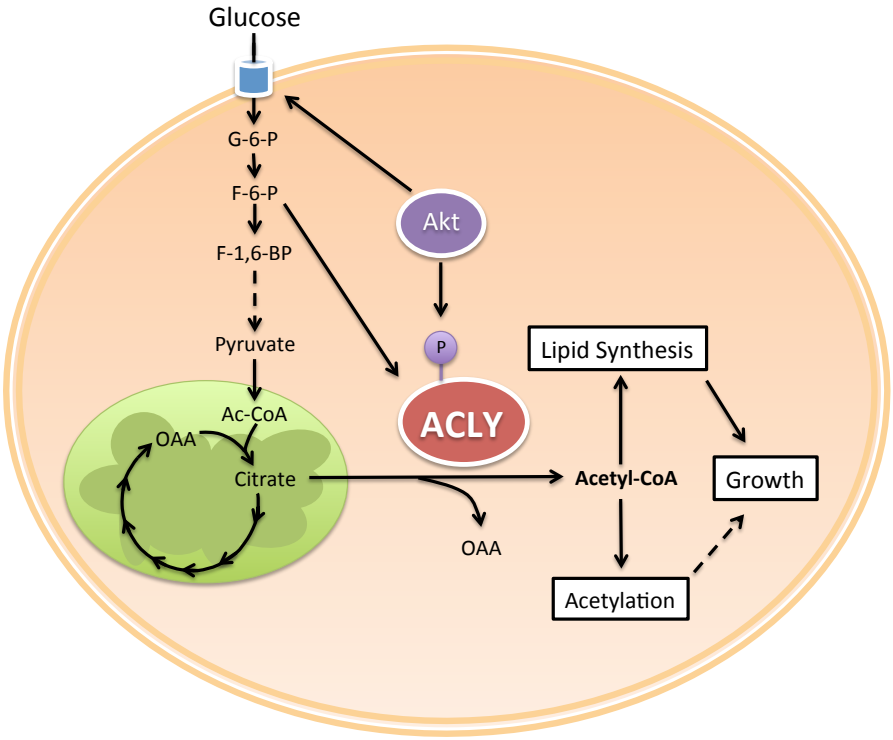

Akt promotes glucose uptake which can lead to increased production of acetyl-CoA via phosphorylation of ACLY. Acetyl-CoA is important for lipid synthesis and protein acetylation which support tumor growth.

CHAPTER 2:

MATERIALS AND METHODS

2.1 Reagents and Cell Lines

All cell lines used in this study were regularly checked for mycoplasma and authenticated using STR profiling. LN229 cells were normally cultured in RPMI with 10% CS (Hyclone) and supplemented with 1% L-glutamine (GIBCO). LN229-myrAkt cells have been previously described (Elstrom et al., 2004a). LN229-myrAkt and SF188-myrAkt cells were a gift of C.B. Thompson, MSKCC. LN229-ACLY, -S455A, and –S455D and empty vector stable cell lines were generated by transfecting cells with pEF6, pEF6-ACLY(Wild Type), pEF6-ACLY(S455A), or pEF6-ACLY(S455D) constructs and selecting. U251 cells were normally cultured in DMEM (GIBCO) with 10% heat-inactivated FBS (Gemini Bio-products) and supplemented with 1% L-glutamine (GIBCO). For experiments, cells were grown in glucose free media, supplemented with 10% dialyzed FBS (GIBCO) and indicated amounts of glucose and acetate. Cells were cultured at 37 °C and 5% CO2.

2.2 Antibodies

Tubulin (Sigma), NFAT1 (Cell Signaling, Abcam), HA (Thermo-Scientific), H3K27ac (Abcam), H4K12ac (Millipore), AcH3, AcH4, H3, H4 (from Millipore), pAktSer473, Akt, pACLY-Ser455, pERK, ERK, pS6, S6 (Cell Signaling), ACLY (previously described (Wellen et al., 2009)). Antibodies used for IHC on murine tissues: AcH4 (1:2000; clone 06-759-MN, Millipore), AcH3 (1:500; clone 06-599, Millipore), H3K4me1 (1:2000; #ab8895, Abcam), Ki67 (1:100; Abcam #ab16667).

AbCam) pACLY (1:100; #SAB4504020, Sigma), and pAkt (1:100; clone 736E11, Cell Signaling).

2.3 Expression vectors

NFAT1 shRNA was in a plko.1 backbone with the following sense sequences- #47: 5'-GTGAACTTCTACGTCATCAAT -3', Sho: 5'- CTGATGAGCGGATCCTTAA -3' previously published (Shoshan et al., 2016). ACLY shRNA #12 and #13 were previously published (Sivanand et al., 2017, Lee et al., 2014). ACLY-targeting siRNA pools were obtained from Dharmacon and transfected with RNAimax reagent, according to manufacturer's instruction. shRNA for stable silencing of murine Acly [previously described (Hatzivassiliou et al., 2005)] HA-tagged NFAT1 constructs were purchased from Addgene (CA-NFAT1: Plasmid #11792; WT-NFAT1: Plasmid #11791) and subcloned into pLX303 by Gateway Cloning kit (Invitrogen).

Lentivirus was produced by transfecting 293T cells with the indicated expression plasmid, pMD2.G and psPAX2 plasmids using Lipofectamine 2000 (Invitrogen). Virus was harvested 48 hours and 72 hours after transfection. For viral infection, cells were incubated with medium containing virus and 8μg/ml polybrene for 16 hours. Cells were allowed to recover for 24 hours before antibiotic selection, and surviving pools were utilized for downstream analyses.

2.4 Drugs

ACLY inhibitor (BMS303141) was dissolved in ethanol. C646 (p300i) was dissolved in DMSO. Akt inhibitor VIII (Calbiochem), LY294002 (Cayman Chemical), PD325901 (LC Laboratories), rapamycin (50 nM).

2.5 Preparation of whole cell protein lysate

Nuclear and cytoplasmic fractionation protocol was followed as previously published (Sivanand et al., 2017). Whole cell lysate was prepared with RIPA buffer or direct lysis with 2X LDS (Invitrogen). All buffers were supplemented with protease inhibitor cocktail (Sigma) and phosphatase inhibitor tablets (Roche).

2.6 Acid extraction of histones

Adherent cells were cultured to 80% confluency in 6-well plates and nuclei were harvested by gentle lifting in cold NIB buffer (15mM Tris-HCL pH7.5, 60mM KCl, 15mM NaCl, 5mM MgCl2, 1mM CaCl2, 250mM sucrose, freshly added: 1mM DTT, 1X protease inhibitors, 10mM sodium butyrate, 0.1% NP-40). Nuclei were pelleted at 600 rcf for 5 min at 4 °C and washed twice using NIB buffer without NP-40. The pellets were immediately resuspended in 0.4N H2SO4 and rotated for at least 30 minutes at 4 °C in. After centrifugation at 11,000 rcf for 10 min at 4 °C, histones were precipitated from the supernatant by addition of 20% tricholoracetic acid (TCA) for at least 1 hour, followed by centrifugation at 16,000 rcf for 10 min at 4 °C. The pellet (or white film) was washed once with acetone containing 0.1% HCl, and finally with 100% acetone. Histone proteins were dried at room temperature and resuspended in water.

2.7 RT-qPCR

RNA isolated with Trizol was quantified and 1-2ug was used for cDNA synthesis using a reverse transcriptase kit (Invitrogen). qPCR was completed with Power SYBR (Invitrogen) on ViiA 7 (Applied Biosystems) for a total of 40 cycles. Results were analyzed using $\Delta\Delta$Ct. List of primers can be found in the Appendix as Table 1.

2.8 Chromatin Immunoprecipitation (ChIP)

Cells were grown to 80% confluency on 10 cm2 dishes on day of harvest and were fixed on the dish with 1% formaldehyde for 10 minutes at room temperature. The reactions were quenched with 0.125 M glycine. The cells were then washed twice with 1X PB and scraped in cell lysis buffer (10 mM Tris-HCl pH8.1, 10 mM NaCl, 1.5 mM MgCl2, 0.5% NP-40), supplemented with protease inhibitors (Roche). The cell lysate was then incubated for 15 minutes on ice and crude nuclear extracts were collected by centrifugation at 600 rcf for 5 min at 4 °C. The pellet was resuspended in 0.5 mL of nuclear lysis buffer (50 mM Tris-HCl pH 8.1, 5 mM EDTA, 1% SDS) supplemented with protease inhibitors. The chromatin was fragmented with a Diagenode Bioruptor 300 (60 cycles of 30 sec on followed by 30 sec off, at 4 °C). To remove insoluble components, the samples were centrifuged at 13,000 rcf for 15 min at 4 °C and the supernatant were recovered. The supernatants were diluted 1:1 with dilution buffer (16.7 mM Tris-HCl pH 8.1, 1.1% Triton X-100, 0.01% SDS, 167 mM NaCl, 1.2 mM EDTA) supplemented with protease inhibitors and quantified by BCA. For each sample, 15 uL of protein G magnetic beads (Millipore 16-662) was added to 100 ug of protein in 500 uL of dilution buffer and incubated with 2 uL of AcH4 antibody (Millipore 06-866) overnight at 4 °C. The next

day, samples were washed with each of the following buffers, once, in the order of: low salt (0.1% SDS, 1% Triton X-100, 2 mM EDTA, 20 mM Tris HCl pH 8.1, 150 mM NaCl), high salt (0.1% SDS, 1% Triton X-100, 2 mM EDTA, 20 mM Tris HCl pH 8.1, 500 mM NaCl), LiCl (1% NP-40, 1% deoxycholate, 1 mM EDTA, 10 mM Tris-HCl pH 8.1, 250 mM LiCl), and TE (10mM Tris-HCl pH 8.1, 1 mM EDTA). ChIP DNA was eluted off the beads by incubating beads in 125 uL elution buffer (10 mM Tris-HCl pH 8.1, 1 mM EDTA, 1% SDS, 150 mM NaCl), supplemented with DTT to a final concentration of 5 mM, for 10 minutes at 65 °C. The supernatant was removed and ChIP DNA was eluted a second time in the same fashion. The combined supernatant was then incubated overnight at 65 °C to reverse crosslinks and proteinase K treated for 1 hour the next morning. Samples were purified using Macherey-Nagel DNA purification kit, with NTB binding buffer (for purification of DNA in high SDS).

ChIP samples were diluted 1:20 in water and used as template in the Power Sybr Master Mix (Invitrogen) and DNA was amplified using the ViiA-7 Real-Time PCR system. Results were calculated as percent input. All primers were designed for the human gene at -1 kb upstream of the TSS, unless otherwise indicated. For primer set, the sequence from 5' -> 3' are: *SERPINA5* - Forward: GGATATCCAACAGCCACATAATTG; Reverse: GTTCAGCAAACACTGTCCATC. *PDGFRA* - Forward: GGGAGAAGGATGAAGGATGAC; Reverse: GATGCTCCAGGAACCAGAC. *E2F2* - Forward: GGAGAATCACTTTAACCCAGGA; Reverse: GTCTGAGGCAAGGTCTCTTT. *MCM10* - Forward: CAGCTCTCAGAAATGGTTGTATTC; Reverse: AACAGTCCTGATGCCATCTAC.

2.9 YSI metabolite and doubling time measurements

Glucose and glutamine consumption and lactate production were measured using a YSI 7100 Bioanalyzer. Measurements were conducted over a 24-hour time period and normalized to cell number area under the curve, as previously described (Londono Gentile et al., 2013, Jain et al., 2012). Briefly, metabolite consumption was defined as $v = V(x_{medium\ control} - x_{final})/A$, where v is metabolite consumption/production, V is culture volume, x is metabolite concentration, and A is cell number area under the curve. A was calculated as $N(T)d/ ln2(1-2^{-T/d})$, where $N(T)$ is the final cell count, d is doubling time, and T is time of experiment. Doubling time was calculated as $d = (T)[log(2)/log(Q2/Q1)]$, where $Q1$ is starting cell number and $Q2$ is final cell number, as determined by manual counting using a hemocytometer.

2.10 Mass spectrometry analysis of histones

For ^{12}C study, LN229 cells in triplicate wells were incubated for 24 hours in 1 mM or 10 mM glucose. For ^{13}C study, LN229 cells were first cultured in 1 mM glucose overnight. Triplicate wells of cells were then treated with 1 or 10 mM [U-^{13}C]-glucose for 2 or 24 hours. Histones were acid, as described above. Total histones were subjected to chemical derivatization using propionic anhydride (Sigma-Aldrich) and digested with sequencing grade trypsin at a 10:1 substrate to enzyme ratio for 6 hours at 37°C. The digested peptides were treated with an additional round of propionylation for the purpose of adding propionyl group to the newly generated N-terminus. Peptides were desalted using C18 extracted mini disk (Empore 3M, MN, USA) and dissolved in 0.1% formic acid. Approximately 1ug of each sample was loaded via an autosampler (EASY-

nLC, Thermo Fisher Scientific Inc) onto a homemade 75μm reversed phase analytical column packed with 15cm C18-AQ resin (3μm particle sizes, 120 Å pore size) at a rate of 550nl/min. Peptides were chromatographically resolved on a 66-min 2-98% solvent B gradient (solvent A = 0.1% formic acid, solvent B = 100% acetonitrile) at a flow rate of 250 nL/min. The eluted peptides were electrosprayed through a PicoTip emitter (New Objective Inc, Woburn, MA) into and detected by LTQ Orbitrap Velos mass spectrometer (Thermo Fisher Scientific Inc) with a resolution of 60,000 for full MS spectrum followed by MS/MS spectra obtained in the ion trap.

After the MS data were generated, an in-house program was developed to calculate the relative intensity of ^{13}C enriched acetyl groups. For example, there are four acetyl groups in H4 4-17 4ac, with 2-Dalton mass shift between adjacent groups. Because the isotope patterns of adjacent groups overlap, the intensity from the former group should be subtracted. After calibration, the intensity of each group divided by the total intensity is the relative intensity.

2.11 RNA-sequencing

LN229 cells were incubated for 24 hours in 1 mM or 10 mM glucose, or 1 mM glucose + 5 mM sodium acetate. RNA was isolated using Trizol reagent and submitted to the Functional Genomics Core at the University of Pennsylvania for library preparation and sequencing. Details of data analysis and clustering may be found in the supplement. Data is deposited in GEO under accession number GSE57488.

2.12 LC-MS metabolite measurements

Acetyl-CoA and CoASH measurements were conducted as previously described (Basu and Blair, 2012, Basu et al., 2011). For molar concentrations, measurements were normalized to cell volume, as determined using a Coulter Z2 particle counter. Protocol for citrate and glutamate analysis followed a 90:10 Methanol:water extraction and is also described in (Lee et al., 2014).

Metabolomics: PEP and Citrate: Cells were grown on 6 well dish format. After treatment with 1 mM glucose overnight, glucose and/or acetate was added to the media for indicated amount of time. At harvest, aspirate media off cells and scrape directly into 1 ml super cold 80:20 MetOH:water. Samples were transferred to 1.5 ml tube. Standards for PEP were added to 1 ml MetOH:water. Internal standard (20 uL of U-^{13}C-Citrate 0.05 ug/ul) was added to every sample and standard. Samples were centrifuged 17,000 rcf 4 C 10 min and the supernatant was transferred to glass tubes for drying under nitrogen. Pellets were resuspended in 100 ul of water and mass analysis was determined on TSQ instrument.

2.13 Histone acetylation in isolated nuclei assay

Nuclei were isolated from approximately 9 x 10^6 adherent LN229 cells by using a cell lifter and cold NIB buffer (15mM Tris-HCL pH7.5, 60mM KCl, 15mM NaCl, 5mM $MgCl_2$, 1mM $CaCl_2$, 250mM sucrose, 0.1% NP-40). Nuclei were pelleted at 600 rcf for 5 min in 4°C and followed by two washes using NIB buffer without NP-40. Nuclei were suspended with indicated concentrations of acetyl-CoA and CoASH in 200 μL NIB buffer

without NP-40 for 1 hour at 37°C. After incubation, nuclei were pelleted at 600 rcf for 5 min and subject to acid extraction (described in Supplement).

2.14 Immunohistochemistry and scoring of murine tissues

For histological evaluation, tissue samples were harvested as described (Gunther et al., 2002, Rhim et al., 2012). Immunohistochemistry was performed on paraffin-embedded sections. Tissue sections were dewaxed and rehydrated. Antigen retrieval was performed by boiling samples in Citrate Buffer pH6 for 20 min (for AcH4, AcH3 and H3K4me) or in Tris-EDTA 10mM Buffer pH9 for 45 min (pACL), and endogenous peroxidase was blunted by incubating samples with 3% H_2O_2 for 10 min. After incubation with the primary antibody, slides were rinsed in PBS and signals were developed using the Vectastain Elite Kit and 3,3′-diaminobenzidine as a substrate for the peroxidase chromogenic reaction (Vector Laboratories, Burlingame, CA). At least 3 animals/group were evaluated. All animal studies were approved by the University of Pennsylvania Institutional Animal Care and Use Committee (IACUC).

Quantification of AcH4 positivity in acinar cells in Kras WT and KPCY mice (n=5/ group) was performed in a semi-automated manner using ImageJ software. For each animal, 5 to 10 images from different, non-overlapping microscopic fields were analyzed. Images containing malignant or pre-malignant lesions were excluded from the analysis. Count of nuclei within each image was calculated using ImageJ while positive nuclei were scored by a blinded evaluator. Ductal and islet cells were excluded by the evaluator.

2.15 Immunohistochemistry and automated scoring for human gliomas

Cases were obtained from the University of Pennsylvania following approval from the institutional review board. All cases were de-identified prior to analysis and were contained in a previously well-characterized tissue microarray sections (Venneti et al., 2013a). The cohort consisted of a total of 56 glioma samples (4 WHO grade II oligodendrogliomas, 5 grade III anaplastic oligodendrogliomas, 6 grade II oligoastrocytomas, 4 grade I pilocytic astrocytomas, 4 grade II diffuse astrocytomas, 9 grade III anaplastic astrocytomas, 14 grade IV glioblastomas, 2 grade I gangliogliomas and 8 grade II ependymomas). A neuropathologist evaluated all cases. Immunohistochemical studies and quantification were performed as previously described (Venneti et al., 2013b). Details may be found in Supplement.

2.16 Immunohistochemistry and scoring of human prostate tumors

Cases were obtained from the University of Pennsylvania following institutional review board approval. TMAs were assembled from primary tumors from 49 patients with either metastatic (n=25) or localized (n=24) disease. 5 μm sections from formalin-fixed paraffin-embedded (FFPE) TMA (Tissue Microarray) tissue blocks were prepared for immunohistochemical stain. Details of staining and scoring provided in Supplement.

2.17 Transwell Migration Assay

Transwell migration assays were completed on 8 μm pore membranes in 6-well format (Corning). Cells were pretreated with 1 mM glucose and 250,000 cells were seeded with glucose and/or acetate in the upper and lower chambers and dFBS was only added to the

lower chamber as a chemoattractant. After 24 hours, cells that did not migrate were cleaned off the top of the membrane with a cotton swab, and migrated cells were fixed, then stained with DAPI. Quantification was done with ImageJ using the automated cell counting feature.

2.18 Scratch Assay

Cells were grown in a monolayer to 80% confluency and then scratched with a p200 pipet tip on a 6-well plate (Sarstedt) and incubated overnight with indicated media conditions. Cell positions were recorded on Leica microscope for accurate measurements. Area of wound was quantified with ImageJ.

2.19 Brain ECM Adhesion Assay

LN229 glioblastoma cells were pretreated as described above. Cells were then trypsinized and reseeded for adhesion experiments on coverslips prepared as previously described (Barney et al., 2015) with brain-inspired ECM proteins: 50% fibronectin (EMD Millipore), 25% vitronectin (R&D Systems), 20% tenascin C (R&D Systems), and 5% laminin (Life Technologies) (all weight%). Briefly, glass coverslips were UV ozone-treated for 10 minutes (Bioforce Nanoscience), and functionalized through sequential deposition of (3-Aminopropyl)triethoxysilane (Sigma), N,N-disuccinimidyl carbonate (Sigma) and diisopropylethylamine (Sigma), then ECM proteins. For adhesion experiments, cells were seeded at 4000 cells/cm2 in low glucose medium and imaged 10 minutes after seeding, in 5 minute intervals, for 2h using a Zeiss Axio Observer Z1 microscope (Carl Zeiss). ImageJ (National Institutes of Health) was used to manually trace cell areas.

2.20 Statistical Analyses

Unless otherwise indicated, Student's 2-tailed t-tests were used for all analyses directly comparing 2 datasets. For in vitro assay testing AcCoA and CoASH effects on histone acetylation, repeated measures one-way ANOVA was used, with posttest for linear trend. For correlations shown for human IHC, Pearson's product-moment correlation coefficient (Pearson's r) and corresponding 2-tailed significance (p value) was determined.

2.21 Calcium Imaging

LN229 cells stably expressing (G418 selected) pGP-CMV-GCaMP6f (Chen et al., 2013a) were adhered to X and Y coated coverslips and maintained in culture medium (RPMI, 10% dFBS, supplemented with L-glutamine) in a temperature and CO_2 controlled chamber mounted on the stage of a fluorescence microscope and GCaMP6f images of individual cells were captured every 15 seconds for 1 hour following addition of medium containing 1 mM glucose, 1 mM glucose with 5 mM acetate, or 10 mM glucose.

2.22 Immunofluorescent detection of NFAT1

Cells were grown on 22 mm glass coverslips in a 6 well dish. Cells were fixed with 3% formaldehyde in 1X PBS for 10 minutes at room temperature. Each well was washed 2X with 1X PBS to remove traces of formaldehyde then permeablized for 5 minutes on ice with 0.1% Triton in PBS (PBS-T). The following steps were all performed at room temperature. Coverslips were blocked with 3% nonfat milk in PBS-T (filtered) for 15 minutes followed by incubated with antibody at 1:100 in 3% milk in PBS-T for 30

minutes. After incubation, coverslips were washed 3X with PBS-T for 1 minute and incubated with secondary antibody diluted in 3% milk in PBS-T at 1:1250 for 30 minutes, protected from light. Coverslips were washed 3X with PBS-T for 1 minute, stained with Hoechst, and then washed 2X with PBS-T, and mounted. Photos were taken on Olympus inverted microscope. Quantification of percent nuclear was completed by counting in a blinded to treatment conditions.

2.23 Animals

Xenograft tumor experiments were approved by the Animal Care and Use Committee at the University of Pennsylvania. Briefly, seven female athymic nude mice (Charles River, 7 weeks old) were injected subcutaneously with 1.5 million of vector control LN229 cells or sg3.8 cells in the left or right flank, respectively. Before each injection, cells were resuspended in 200 μL DMEM mixed with an equal volume of matrigel (BD Bioscience). Once palpable tumors were established, tumors size was measured twice a week with a digital caliper. After 6 weeks mice were sacrificed by CO_2 euthanasia, and xenograft tumors were dissected, weighed, and snap frozen with liquid nitrogen until further analysis.

2.24 Transcription factor identification

The upregulated subset of genes from the 881 acetyl-CoA regulated genes (Lee et al., 2014) were entered into the Broad Institute's Molecular Signatures Database (MSigDB) v4.0 with FDR q-value set to below 0.05. Top 10 transcription factor targets (TFT) was queried. FDR q-value was calculated by MSigDB. The 881 genes were then tested for

enrichment of TGGAAA_V$NFAT_Q4_01 using GSEA v3.0 with 1000 permutations and gene set permutation type, as recommended on the GSEA user guide.

CHAPTER 3:

AKT-DEPENDENT METABOLIC REPROGRAMMING REGULATES TUMOR CELL HISTONE ACETYLATION

Chapter 3 is based on and mostly a reprint of the paper: Lee, J. V., Carrer, A., Shah, S., Snyder, N. W., Wei, S., Venneti, S., et al. (2014). Akt-Dependent Metabolic Reprogramming Regulates Tumor Cell Histone Acetylation. Cell Metabolism, 20(2), 306–319.

3.1 Introduction

Rewiring of cellular metabolism in cancer cells is crucial for increased macromolecular biosynthesis, growth, and proliferation, and metabolic deregulation is now considered a hallmark feature of cancer cells (Hanahan and Weinberg, 2011, Ward and Thompson, 2012). In addition to directly supporting energetics and biosynthesis, a growing body of evidence suggests that metabolic enzymes may also promote tumorigenesis through functions that are not overtly metabolic. For example, the M2 isoform of pyruvate kinase, a glycolytic enzyme, has been reported to enter the nucleus and serve as transcriptional coregulator (Luo and Semenza, 2012). ATP-citrate lyase (ACLY), a lipogenic enzyme, is also present in the nucleus and plays a crucial role in regulating nuclear acetylation events, including histone acetylation (Wellen et al., 2009).

Metabolic changes in cancer cells are typically mediated by activation of oncogenes and/or loss of tumor suppressors (Metallo and Vander Heiden, 2010, Vander Heiden et al., 2009). Hence, mutations that drive tumorigenesis also cause metabolic

alterations. In addition to genetic mutations, epigenetic alterations play a key role in enabling malignant transformation and tumor growth (Shen and Laird, 2013, Azad et al., 2013), although mechanisms underlying epigenetic alterations in cancer are not fully clear. Notably, many chromatin-modifying enzymes depend on metabolic intermediates as cofactors or substrates and certain chromatin modifications have been shown to be sensitive to the cellular metabolic state [reviewed in (Katada et al., 2012, Kaelin and McKnight, 2013, Lu and Thompson, 2012a, Yun et al., 2012)]. Links between cancer cell metabolism and DNA and histone methylation have been recently identified in tumors with specific mutations, such as those in isocitrate dehydrogenase (*IDH1* and *IDH2*). Mutant IDH enzymes exhibit altered enzyme activity favoring conversion of α-ketoglutarate (αKG) into (*R*)-2-hydroxyglutarate, a metabolite that inhibits the activity of αKG-dependent JmjC-domain histone demethylases and TET enzymes, resulting in hypermethylation of DNA and histones [reviewed in (Ward and Thompson, 2012, Losman and Kaelin, 2013)]. Succinate dehydrogenase (*SDH*) mutations and nicotinamide N-methyltransferase (NNMT) overexpression also result in methylation changes in cancer cells (Ulanovskaya et al., 2013, Killian et al., 2013, Letouze et al., 2013, Xiao et al., 2012). In these specific cases, the epigenetic alterations are a direct result of altered activity of a particular metabolic enzyme. However, it is not known whether metabolism might more universally contribute to tumor epigenetic deregulation.

Histone acetylation is a dynamic chromatin mark, with important roles in gene regulation, DNA damage repair, and DNA replication. Global histone acetylation has also been implicated in contributing to pH balance and postulated to serve as a depot for acetate that could be mobilized as an energy source (Martinez-Pastor et al., 2013,

McBrian et al., 2013). The metabolite acetyl-coenzyme A (acetyl-CoA) is the required donor substrate used by lysine acetyltransferase (KAT) enzymes. In cells cultured under standard conditions, glucose-derived carbon supplies the majority of acetyl-CoA used for histone acetylation, although glutamine and acetate also contribute (Evertts et al., 2013). In some conditions, fatty acid breakdown can also contribute to nuclear acetyl-CoA and histone acetylation (Donohoe et al., 2012). Acetyl-CoA is compartmentalized into mitochondrial and nuclear-cytoplasmic pools (Takahashi et al., 2006). Production of nuclear-cytoplasmic acetyl-CoA from glucose, glutamine, or fatty acids depends on export of citrate from the mitochondria, where it is cleaved by ACLY to generate acetyl-CoA and oxaloacetate. Acetate also supplies nuclear-cytoplasmic acetyl-CoA through acetyl-CoA synthetase (AceCS1/ ACSS2). Together, ACLY and AceCS1 are the primary enzymatic sources of acetyl-CoA outside of the mitochondria. Several studies have demonstrated that histone acetylation levels are highly sensitive to the availability of acetyl-CoA, in cell types from yeast to human (Cai et al., 2011, Takahashi et al., 2006, Wellen et al., 2009).

Given that production and utilization of metabolites is dramatically altered in cancer cells, and that histone acetylation is responsive to acetyl-CoA availability, we postulated that metabolic reprogramming in tumor cells might alter acetyl-CoA and histone acetylation levels in tumors. In this study, we provide evidence that metabolic reprogramming orchestrated by oncogenic activation of Akt drives changes in acetyl-CoA production and histone acetylation that are reflected in total histone acetylation levels in tumors. To our knowledge, this study is the first demonstration that metabolic reprogramming mediated by oncogenic activation of a signal transduction pathway plays a major role in regulation of the cancer cell epigenome.

3.2 Results

3.2.1 Histone acetylation is variably sensitive to glucose in cancer cells

We previously showed that ACLY plays a key role in determining global histone acetylation levels in cancer cells. Histone acetylation is markedly reduced upon silencing of ACLY and can be restored by supplementing cells with the alternate acetyl-CoA source acetate, indicating that the ability of cells to produce acetyl-CoA can limit histone acetylation (Wellen et al., 2009). To determine whether glucose availability regulates histone acetylation levels in cancer cells, we examined a panel of cancer cell lines, including glioblastoma, prostate cancer, and breast cancer cell lines. Histone acetylation was sensitive to glucose availability in each of the cell lines examined, to varying degrees (**Figure 4A and Figure 5A**). As we have previously shown in other cell types (Wellen et al., 2009), silencing of ACLY inhibited glucose-dependent histone acetylation in LN229 cells (**Figure 5B**).

In LN229 glioblastoma cells, proliferation slowed when cultured in 1 mM glucose, but between 2 and 25 mM glucose doubling time was equal, indicating that histone acetylation patterns are regulated by glucose independently of cell proliferation (**Figure 5C**). Cells remained viable in all conditions (**Figure 5C**). As glucose was progressively limited, glutamine consumption increased (**Figure 5C**). Although glutamine can be used to supply nuclear-cytoplasmic acetyl-CoA, LN229 cells failed to sustain high histone acetylation levels in low glucose despite increased consumption of glutamine (**Figure 4A**).

We next sought to define which histone lysines are most sensitive to glucose availability. LN229 cells were incubated for 24 hours in 1 mM or 10 mM glucose and histone modifications analyzed by mass spectrometry. Higher acetylation in 10 mM than 1 mM glucose was observed at all H2A, H3, and H4 tail lysines analyzed (**Figure 5D**). To confirm that this is due to reduced glucose carbon incorporation into acetylated histones, this analysis was repeated in 1 mM or 10 mM [U-$^{13}C_6$]-glucose. After 24 hours, enrichment was reduced in low glucose for all lysines analyzed. However, the effects of glucose limitation became more pronounced as more lysines were acetylated in *cis*. For example, the histone H4 tail can be acetylated at lysines 5, 8, 12, and 16. In 1 mM [U-$^{13}C_6$]-glucose, significantly more tetra-acetylated histone H4 (AcH4) tails were enriched at 0 or 1 acetyl group, while in 10 mM, 3 or 4 acetyl groups were more frequently enriched (**Figure 5E**). Thus, these data indicate 1) that on all tail lysines examined, acetylation is sensitive to glucose availability and 2) that glucose limitation has a greater impact on histone tails with multiple lysines acetylated in *cis*.

Supplementation of acetate restored histone acetylation levels in low glucose conditions (**Figure 4B**). Correspondingly, acetyl-CoA levels were reduced in low glucose conditions and significantly rescued by addition of acetate (**Figure 4C**). To determine whether specific gene sets correlated with these effects on histone acetylation, we performed RNA-sequencing to identify acetyl-CoA regulated genes (genes suppressed or induced by low glucose and reversed by acetate). Approximately 10% of glucose-regulated genes were also significantly regulated by acetate (**Figure 4D**). Clustering analysis revealed that acetate regulated most genes in the same direction as glucose, suggesting that acetyl-CoA is a key mediator of glucose-dependent gene expression (**Figure 4E**). Expression was confirmed for select acetyl-CoA-regulated genes by qPCR

(**Figure 7A**), and ChIP analyses at these genes showed that promoter histone acetylation correlated with expression (**Figure 7B**). Analysis of curated pathways revealed enrichment for genes involved in cell cycle and DNA replication among acetyl-CoA-induced genes, suggesting that acetyl-CoA stimulates a pro-proliferative gene expression profile (**Figure 4F**). Analogously, prior studies in yeast showed that acetyl-CoA promotes cell growth and division by promoting expression of genes involved in these processes (Cai et al., 2011). Although acetate supplementation was not sufficient to restore normal doubling time in low glucose conditions in LN229 cells (**Figure 4G**), we considered that additional glucose-derived components might be required. Indeed, supplementation of acetate together with nucleosides (synthesis of which requires ribose generated in the pentose phosphate pathway), rescued doubling time, while neither component alone did so (**Figure 4G**). These data suggest that acetyl-CoA facilitates expression of proliferation-related genes, as part of an integrated growth response.

3.2.2 Acetyl-CoA and Coenzyme A are key determinants of histone acetylation in cancer cells

If acetyl-CoA serves as a signal of nutrient sufficiency to promote growth and proliferation, cells must have mechanisms to detect changes in acetyl-CoA abundance. Work in yeast has shown that Gcn5 is crucial for mediating histone acetylation in response to acetyl-CoA availability (Cai et al., 2011, Friis et al., 2009). In yeast, acetyl-CoA concentrations oscillate within a range that could plausibly regulate yeast Gcn5, which has a K_d of 8.5 μM (Cai et al., 2011). However, human GCN5 binds acetyl-CoA much more tightly (K_d of 0.56 μM) (Langer et al., 2002). This suggests either that levels of acetyl-CoA are lower in human cells than in yeast or that the absolute concentration of

acetyl-CoA is not the key regulatory factor for overall histone acetylation levels in human cells. Of note, many HATs including GCN5 are inhibited by the product coenzyme A (CoA) and bind acetyl-CoA and CoA with similar affinities. Hence, it has been postulated that the ratios of these metabolites might be the critical determinant for overall histone acetylation levels (Albaugh et al., 2011).

We therefore measured absolute acetyl-CoA and CoASH (reduced CoA) concentrations, normalizing to cell volume, in LN229 cells cultured in 1 or 10 mM glucose. Acetyl-CoA was measured at 6-13 μM in high glucose conditions and fell to 2-3 μM in low glucose. CoASH tended to rise in low glucose, and the ratio of acetyl-CoA: CoASH was found to be ~1.5- 2 throughout the time course in high glucose conditions and to fall below 1 under low glucose (**Figure 6A**). We also examined acetyl-CoA and CoASH levels in a second cell line, IL-3-dependent hematopoietic cells, since the volume of these cells under standard conditions and during nutrient and growth factor withdrawal has been extensively characterized (Wellen et al., 2010) A similar range of acetyl-CoA concentrations (~3-12 μM) were measured in these cells as in LN229 cells, and both acetyl-CoA and acetyl-CoA: CoASH were significantly reduced when cells were deprived of either glucose or growth factor (**Figure 6B**). The range of acetyl-CoA concentrations observed in each of these cell lines is comparable to that reported over the yeast metabolic cycle (Cai et al., 2011).

To specifically test whether histone acetylation levels respond to both acetyl-CoA and CoA levels, nuclei were isolated from LN229 cells and incubated with defined concentrations of acetyl-CoA and CoASH, which can freely enter the nucleus through the nuclear pore complex. We observed that in the presence of high acetyl-CoA, addition of

CoASH suppressed histone acetylation in a dose-dependent manner (**Figure 6C**). Together, these data indicate that levels of both acetyl-CoA and CoA in the nucleus can impact histone acetylation levels. Moreover, the ratio of acetyl-CoA: CoASH is glucose-sensitive and tracks with total acetyl-CoA.

Figure 4: Glucose Availability Regulates Histone Acetylation in Several Cancer Cell Lines

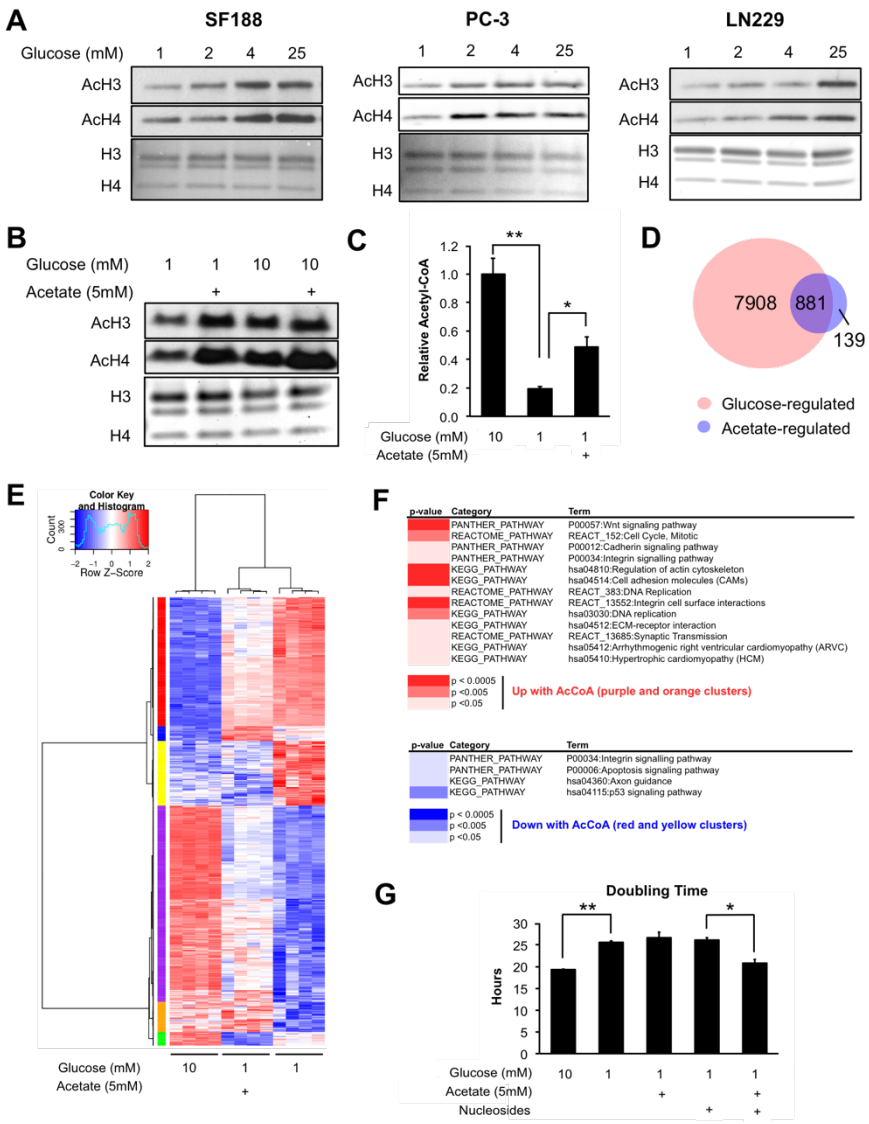

(A) Acetylation of acid-extracted histones from cells cultured under indicated glucose conditions for 24 hours. Total histones were stained by Coomassie or Ponceau. (B) Acetylation of acid extracted histones from LN229 cells treated with 1 or 10 mM glucose, +/− 5 mM NaOAc for 24 hours (C) Relative levels of acetyl-CoA in LN229 cells after 24 hours of indicated treatment, mean +/− SEM of triplicates (*, p<0.05; **, p<0.005) (D) Venn diagram of genes regulated by glucose and/or acetate in LN229 cells, with the overlap representing genes designated as acetyl-CoA-regulated (E) Heatmap of 881 genes represented in the overlap from the Venn diagram. (F) DAVID functional annotation of pathways regulated by acetyl-CoA, using the gene list identified from the indicated clusters on the heatmap. (G) Doubling time for LN229 cells treated as indicated for 24 hours, mean +/− SEM of triplicates (*, p<0.05; **, p<0.005).

Figure 5: Glucose derived acetyl-CoA regulates histone acetylation

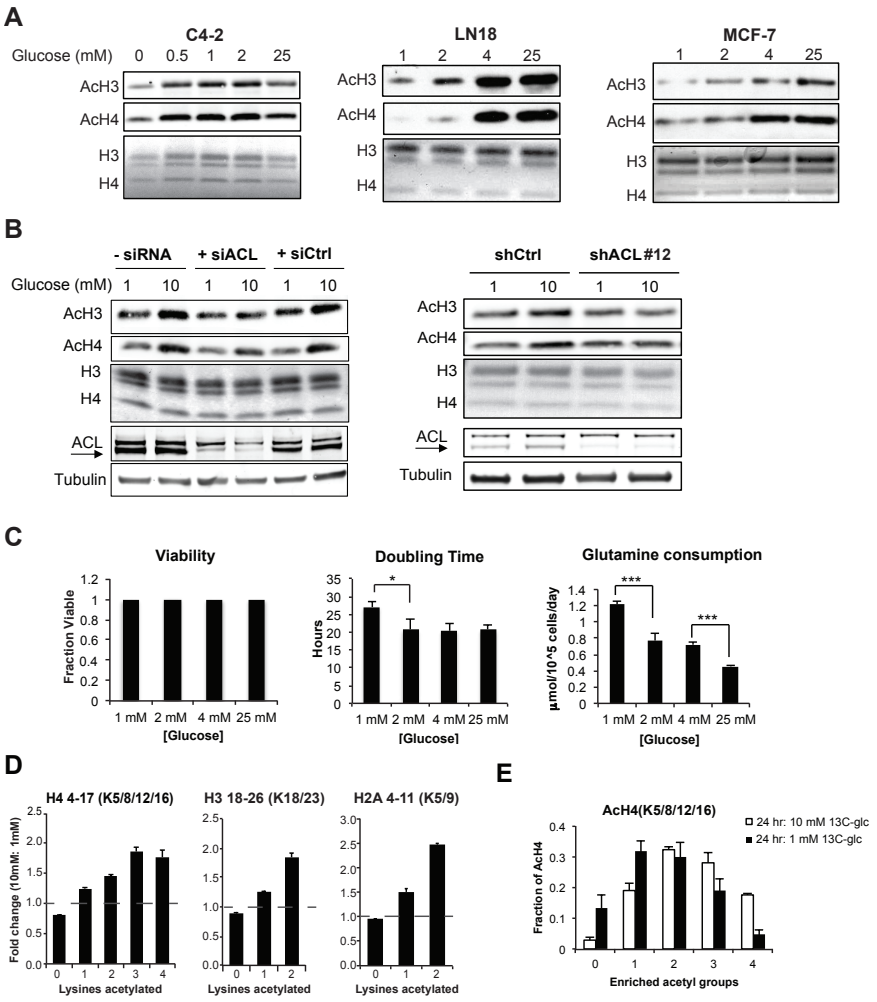

Glucose availability regulates histone acetylation in cancer cells. (A) Western blot analysis of histones acetylation in cancer cell lines cultured under indicated glucose conditions for 24 hours. Total acid-extracted histones were stained by Coomassie or Ponceau. (B) LN229 cells were transfected with Ctrl or ACLY-targeting siRNA (left panel) or transduced with Ctrl or ACLY-targeting shRNA (right panel). Cells were starved in 1 mM glucose, then treated with 1 mM or 10 mM glucose for 24 hours. Western blot analysis of acid extracted histones and other signaling components in whole cell lysates. (C) Viability, doubling time, and glutamine consumption were measured in LN229 cells after 24 hours of growth under indicated glucose concentrations, mean +/- SEM of triplicates (*, $p<0.05$; ***, $p<0.0005$). (D) Indicated histone tail peptides were analyzed by mass spectrometry. Fold change in acetylation between 10 mM: 1 mM glucose is graphed, mean +/- SEM of 10 mM sample triplicates over average 1 mM value. See Table S1 for complete data set. (E) MS analysis of acid extracted histone proteins from LN229 cells incubated with [U-13C$_6$]- glucose for 24 hours. Enrichment of tetra-acetylated H4 after 24 hours in 1mM and 10mM [U-13C$_6$]-glucose, mean +/- SD of triplicates.

Figure 6: Acetyl-CoA:CoASH Ratio Is a Determinant of Histone Acetylation in Cancer Cells

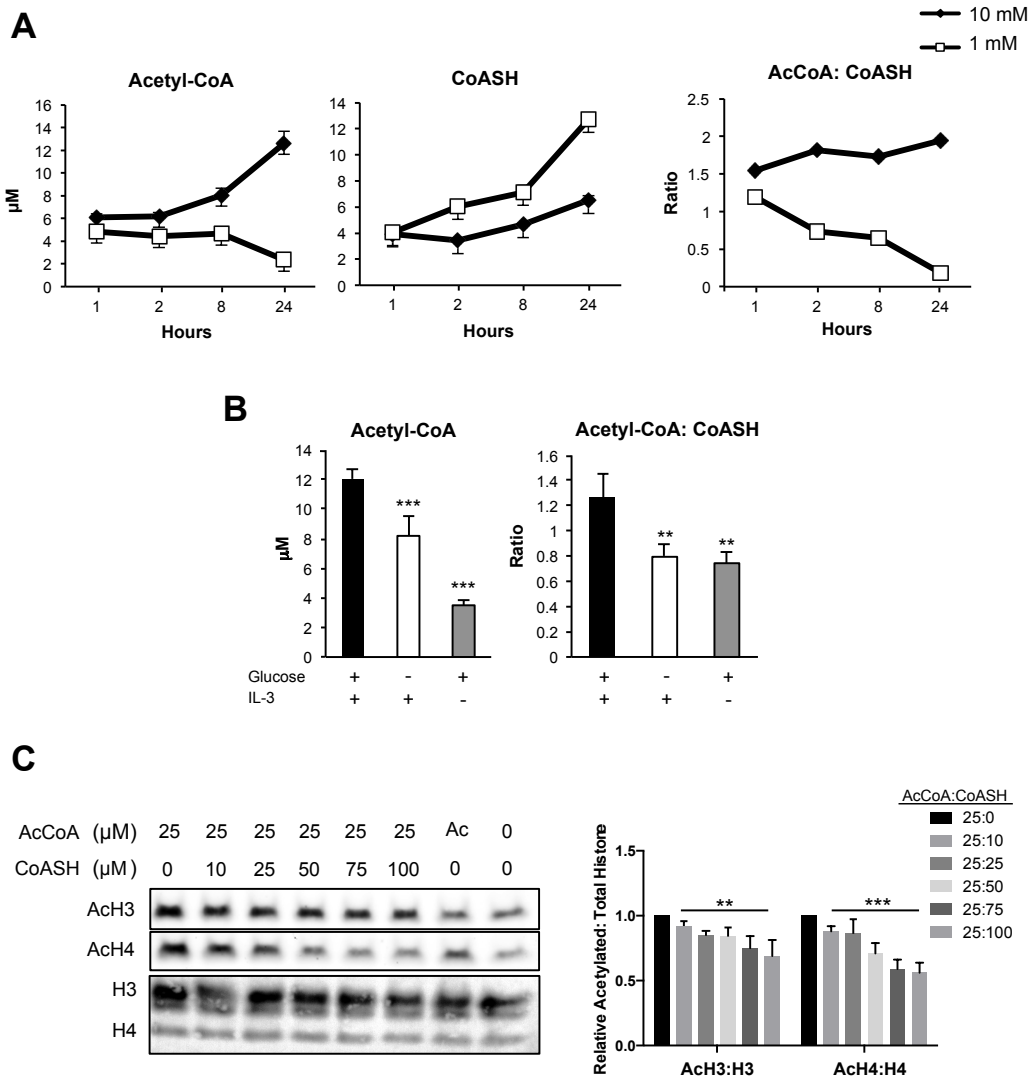

(A) Molar concentrations of acetyl-CoA, CoASH, and ratio of acetyl-CoA: CoASH over 24 hours in LN229 cells, mean +/− SEM of triplicates. Result is representative of 3 independent experiments. (B) IL-3-dependent *bax−/−bak−/−* cells were cultured for 48 hours +/− glucose, +/− IL-3 as indicated. Acetyl-CoA and CoASH were measured and normalized to cell volume, mean +/− SD of triplicates. Significance as compared to Glc+IL-3+ samples (**, p<0.005, ***, p<0.0005) (C) Representative Western blot of acetylated histones upon incubation of isolated nuclei with varying concentrations of acetyl-CoA and CoASH. Total histones were stained by Ponceau. Data was quantified from four independent experiments with 25:0 value set to 1, mean +/− SEM. Repeated measures one-way ANOVA with post test for linear trend was performed for 25:10–25:100 values. Post test for linear trend significance for AcH4: H4, p<0.0001 (***); for AcH3: H3, p=0.0034 (**)

Figure 7: Histone acetylation at relevant loci is regulated by acetyl-CoA availability.

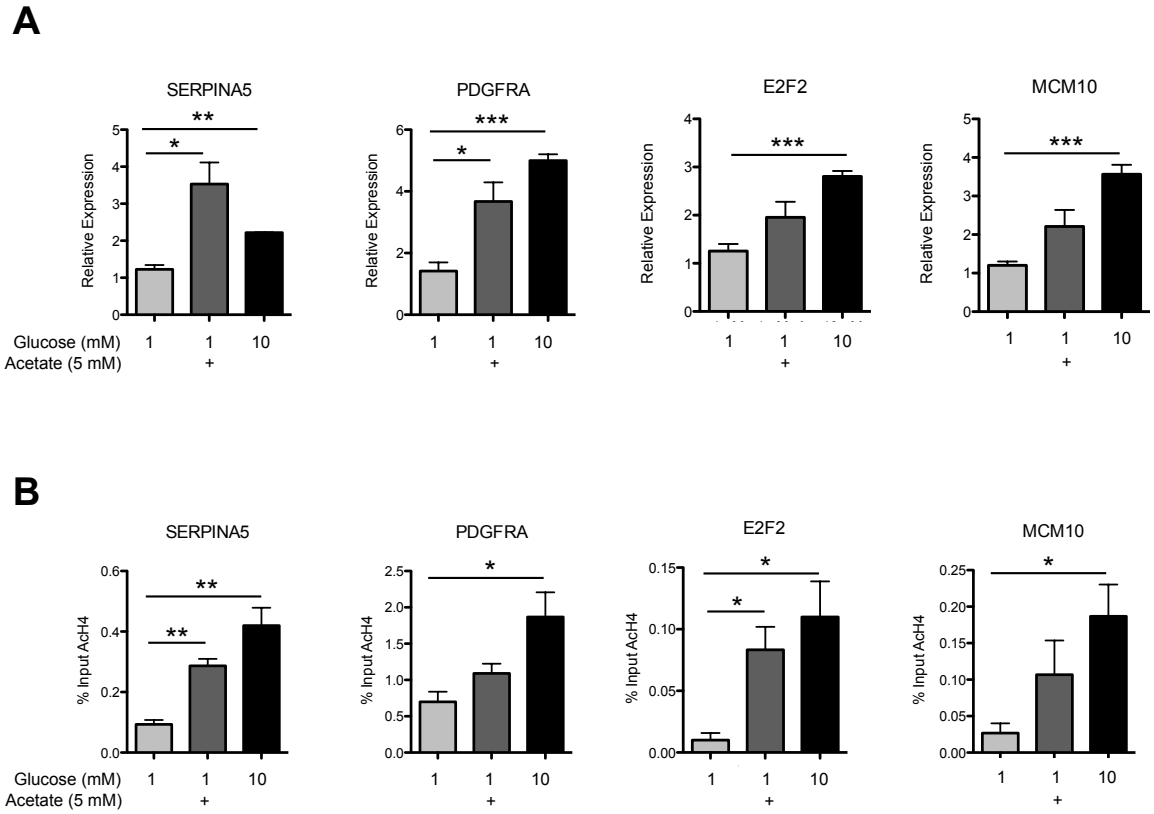

A) QPCR validation of select genes identified by RNA-Seq as glucose- and acetate-regulated, mean +/- SEM of triplicates (*, p<0.05; **, p<0.005; ***, p<0.0005) (B) AcH4 ChIP at promoter of each of genes in part (A) normalized to input, mean +/- SEM of triplicates (*, p<0.05; **, p<0.005).

3.2.3 Expression of KrasG12D in the mouse pancreas promotes increases histone acetylation prior to tumor development

Since histone acetylation is sensitive to metabolic state and metabolism is altered in cancer cells, we next asked whether oncogene activation could drive changes in histone acetylation *in vivo*. Oncogenic Kras mutations are found in the vast majority of human pancreatic adenocarcinoma (PDA) cases, and recent studies have demonstrated that mutant Kras in pancreatic cancer cells drives extensive metabolic rewiring (Ying et al., 2012, Son et al., 2013). We observed that in the pancreas of healthy wt mice, acinar cells exhibited very low levels of AcH3 and AcH4, as detected by immunohistochemistry (IHC), although ductal cells were strongly positive for these marks (**Figure 8A**). In contrast, in mice expressing oncogenic Kras [LSL-$Kras^{G12D}$; $p53^{L/+}$; Pdx1-Cre (KPC) mice], areas of acinar-to-ductal metaplasia (ADM), precancerous pancreatic intraepithelial neoplasia (PanIN), and PDA exhibited high levels of AcH3 and AcH4 (**Figure 8 A, B**). PDA may arise from acinar cells (Morris et al., 2010), and strikingly, elevated AcH4 was observed in acinar cells even prior to increases in proliferation, as assessed by Ki67 immunostaining (**Figure 8C**), or the appearance of any histological abnormalities (**Figure 9A, B**). Thus histone acetylation levels are elevated upon $Kras^{G12D}$ expression in mouse pancreas early in the process of tumor development.

We next interrogated signaling pathways downstream of Kras to identify those responsible for elevating histone acetylation in primary murine PanIN cells. Reductions in histone acetylation were observed with each of the inhibitors that we tested (**Figure 10A**). PI3K and Akt inhibition also significantly reduced glucose uptake and lactate consumption and suppressed ACLY phosphorylation (**Figure 10A, B**). Phosphorylation

at Ser455 has been shown to increase ACLY's activity (Potapova et al., 2000). On the other hand, the level of AceCS1, which produces nuclear-cytoplasmic acetyl-CoA from acetate, was somewhat suppressed by PI3K, but not by Akt, inhibition in these cells (**Figure 10A**). Acetyl-CoA and acetyl-CoA: CoASH levels were potently suppressed upon Akt inhibition (**Figure 10C**), and histone acetylation levels in Akt inhibitor-treated cells increased upon supplementing cells with acetate (**Figure 10D**). Suppression of histone acetylation by Akt inhibition was comparable to that observed upon either glucose limitation or ACL silencing, both of which were also rescued by acetate (**Figure 10D**). In primary murine PDA cells, we similarly observed suppression of histone acetylation and glucose uptake by PI3K or Akt inhibition, as well as acetate rescue of histone acetylation in Akt inhibitor- or low glucose-treated cells (**Figure 11B-D**). These data indicate that in premalignant and cancerous cells expressing oncogenic Kras, histone acetylation is regulated in part by Akt-dependent regulation of acetyl-CoA metabolism.

Figure 8: Oncogenic Kras Increases Histone Acetylation *In Vivo*

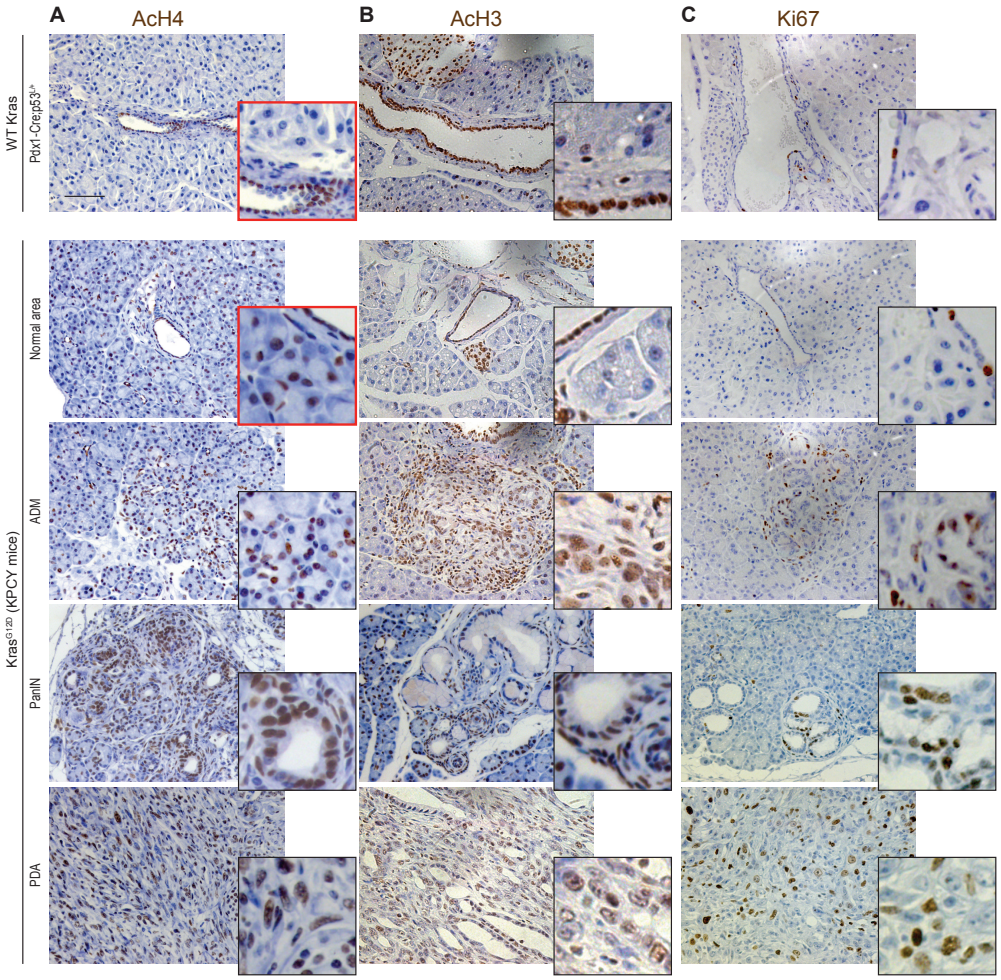

Pancreata from mice expressing Kras-G12D (KPCY) were harvested at either 6 weeks (KPCY-Normal Area), 8 weeks (KPCY-PanIN) or 10 weeks (KPCY-PDA) of age, along with pancreata from control (Kras WT) mice (n≥3, each group). Immunohistochemistry against AcH4 (A), AcH3 (B) or Ki67 (C) was performed on paraffin-embedded tissue sections and nuclei were counterstained with hematoxylin. Representative images are shown, with magnification of areas of interest. Scale bar: 50 μm.

Figure 9: $Kras^{G12D}$ expression increases histone H4 acetylation in pancreatic acinar cells in vivo

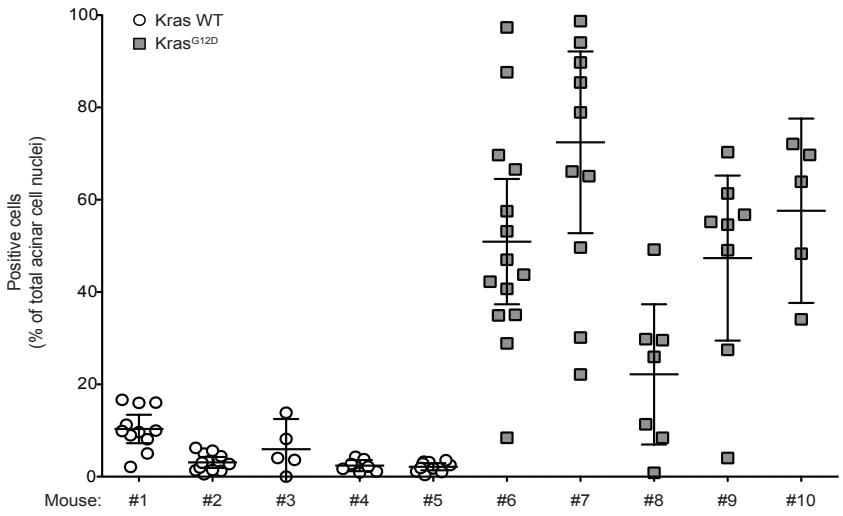

Pancreata from either wild type (Kras WT) or oncogenic Kras (KrasG12D)-expressing mice were harvested at 6 weeks of age (n=5, each group). Acinar cell nuclei positive for acetylated histone H4 (AcH4) were quantified by immunohistochemistry. The scientist who performed the quantitation was blinded to the genotypes of the mice. Percentages of AcH4-positive acinar cell nuclei were calculated in different, non-overlapping microscopic fields and plotted (each dot refers to a different microscopic fields). Each column indicates a different animal. Bars denote means and interquartile ranges.

Figure 10: Oncogenic Kras Enhances Histone Acetylation In Vitro in an Akt- and Acly-Dependent Manner

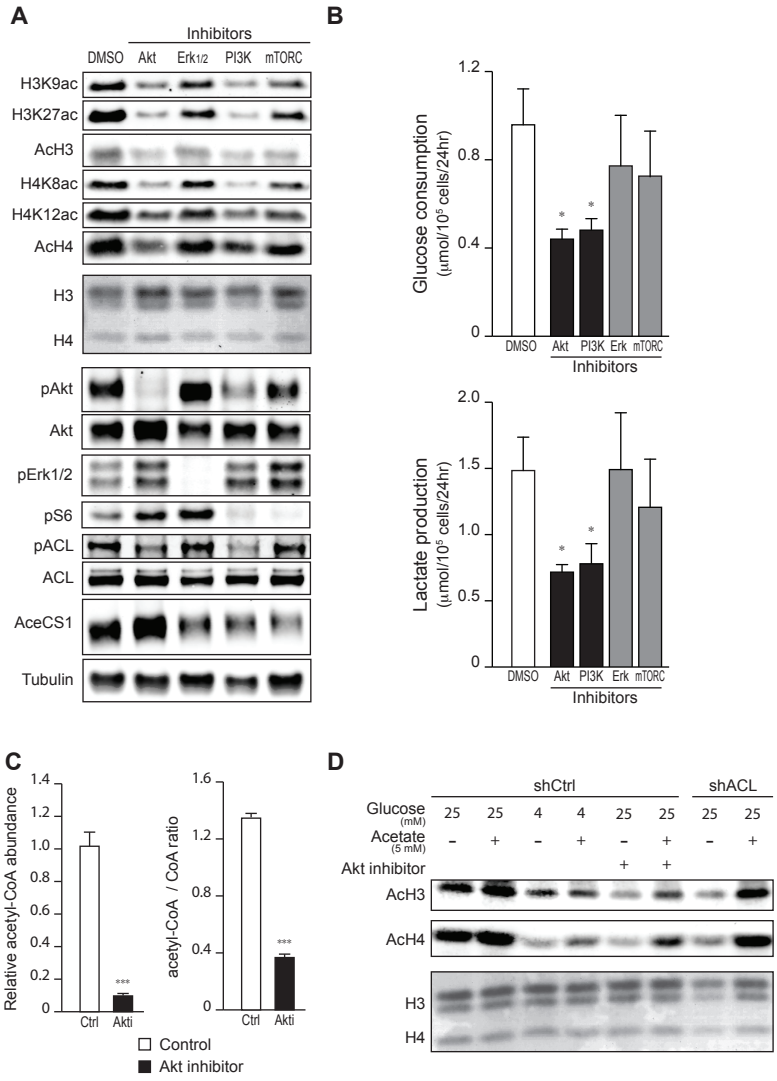

(A) Mouse pancreatic primary cells derived from KPCY mouse PanIN lesions were treated with indicated inhibitors for 24 hours. Acetylation of histones and phosphorylation of signaling proteins were assessed by Western Blot in acid extracts and RIPA lysates, respectively. Ponceau staining is shown as loading control for histones. (B) Glucose consumption and Lactate production were measured in PanIN-derived primary mouse cells treated as in (A), mean +/− SD of triplicates (*, $p<0.05$). (C) Acetyl-CoA and CoASH levels were measured in PanIN cells, +/− Akt inhibitor, mean +/− SD of triplicates (***, $p<0.001$). (D) PanIN-derived primary cells were transduced with control (shCtrl) or ACL-targeting (shACL) short hairpin RNA. Cells were cultivated under indicated glucose concentrations, +/− Akt inhibitor, +/− 5 mM acetate for 24 hours. Histones were acid-extracted and analyzed by Western Blot. Ponceau staining is shown as loading control for histones.

Figure 11: Akt regulates histone acetylation in PanIN and PDA cells

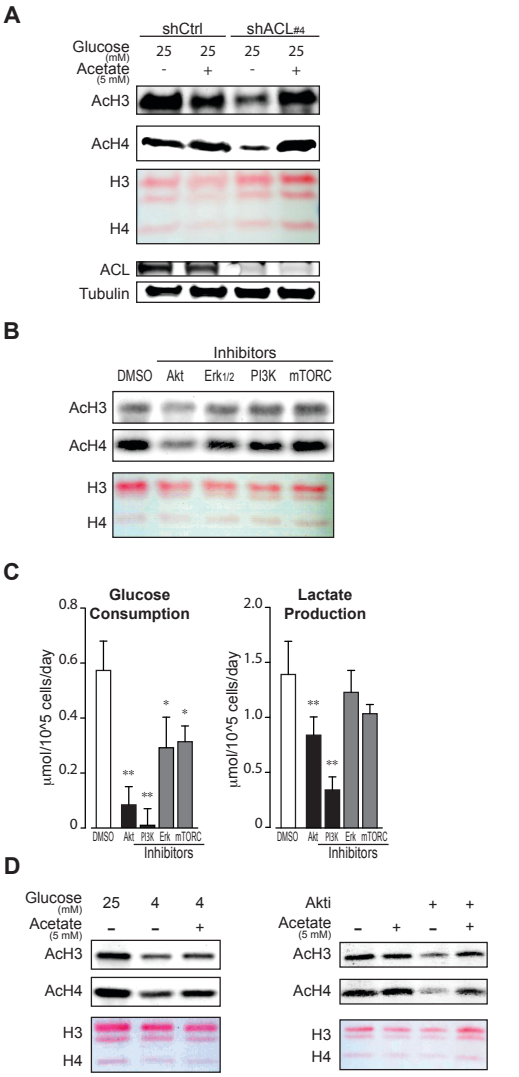

(A) PanIN-derived primary cells were transduced with control (shCtrl) or Acly-targeting (shAcly #4) short hairpin RNA. Cells were cultivated under indicated glucose concentrations, with or without 5 mM acetate for 24 hours. Histones were acid-extracted and analyzed by Western Blot. Ponceau staining is shown as loading control for histones. (B) Mouse PDA-lesion derived cells from KPCY mice were cultured and either mock-treated (DMSO) or treated with the indicated inhibitors for 24 hours. Acetylation of acid-extracted histones was assessed by Western Blot. (C) Glucose consumption and Lactate production were measured in PDA-derived primary mouse cells treated as in part A, mean +/- SD of triplicates (**, $p<0.005$; *, $p<0.05$). (D) PDA-derived primary cells were cultured in high (25 mM) or low (4 mM) glucose conditions, with or without Akt inhibitor and with or without 5 mM acetate for 24 hours. Histone acetylation levels were assessed by Western Blot. Ponceau staining for total histones is shown as loading control.

3.2.4 Akt activation sustains histone acetylation in nutrient-limited conditions

To probe further into the mechanism whereby Akt regulates histone acetylation, we examined the effects of constitutive Akt activation in cancer cells by comparing parental LN229 cells with LN229 cells in which a constitutively active form of Akt, myristoylated Akt (myrAkt), was stably expressed. LN229-myrAkt cells have been shown to consume more glucose but maintain a similar proliferation rate as parental cells (Elstrom et al., 2004a). Levels of histone acetylation in high glucose conditions were not markedly different between the two cell lines. However, when cultured in low glucose, LN229-myrAkt cells sustained a significantly higher level of histone acetylation than parental cells (**Figure 12A**). Similar results were also obtained in SF188 and SF188-myrAkt cells (**Figure 13A**). Time course analysis indicated that myrAkt expression extended the timeframe over which cells could maintain histone acetylation levels in low glucose (**Figure 13B**).

Glucose deprivation results in depletion of ACLY's substrate citrate in LN229 cells (**Figure 14A**). In myrAkt-expressing cells, citrate levels were lower than in the parental cells, even in high glucose conditions, and loss of citrate was accelerated upon glucose deprivation (**Figure 14A**). *In vitro* studies of ACLY enzymatic activity have demonstrated that phosphorylation at Ser455 increases the enzymatic activity of ACLY, resulting in a 6-fold increase in V(max) (Potapova et al., 2000). Hence, increased phosphorylation of ACLY by Akt could potentially enable sustained acetyl-CoA production and thereby histone acetylation even if availability of the ACLY substrate citrate is reduced. To test whether ACLY phosphorylation is sufficient to sustain high levels of histone acetylation in low glucose, we expressed WT-ACLY and ACLY Ser455

phospho-mimetic (S455D) and phospho-mutant (S455A) proteins in LN229 cells. Expression of ACLY-S455D enabled high levels of histone acetylation to be sustained in low glucose, similar to that observed with myrAkt expression (**Figure 12B**). A trend towards higher histone acetylation in low glucose was also noted with expression of WT-ACLY. These results suggest that ACLY is a key downstream effector of Akt in promoting histone acetylation, particularly when nutrients are limited.

This result raised the question of where cells obtain the carbon for histone acetylation in cells with constitutive Akt/ACLY activation but limited glucose. Recent studies have shown that under certain conditions such as hypoxia, glutamine can be reductively carboxylated to generate citrate and supply lipogenic acetyl-CoA and that depletion of citrate or an elevated α-ketoglutarate: citrate ratio is necessary for this effect (Fendt et al., 2013, Gameiro et al., 2013). We hypothesized that citrate depletion observed with myrAkt expression might stimulate glutamine reductive carboxylation. However, analysis of citrate isotopologues following exposure to [$^{13}C_5$ $^{15}N_2$]-glutamine revealed that glutamine continues to be oxidized in myrAkt-expressing cells and that little to no reductive carboxylation occurred in either high or low glucose conditions (**Figure 14B**). On the other hand, acetyl-CoA, though significantly depleted in control or wt ACL-expressing cells in low glucose, retained a comparable percent enrichment from glucose (M+2 acetyl-CoA) when cultured in either 1 mM or 10 mM [U-$^{13}C_6$]-glucose (**Figure 12C**). Moreover, in ACLY-S455D-expressing cells, both total and M+2 acetyl-CoA resisted depletion in low glucose (**Figure 12C**), suggesting that even when glucose is limited, it remains a major source of acetyl-CoA in this context.

Hence, the data indicate that Akt promotes acetyl-CoA production and histone acetylation through combined effects on 1) promoting the uptake and metabolism of glucose and 2) promoting phosphorylation and activation of ACLY to facilitate continued acetyl-CoA production even when its substrate citrate is limited.

3.2.5 Akt activation acutely promotes histone acetylation in vivo

To directly test whether acute activation of Akt regulates histone acetylation *in vivo*, we exploited a doxycycline-inducible mouse model of breast cancer, in which myrAkt is activated in mammary epithelial cells upon administration of doxycycline to mice through the drinking water (Gunther et al., 2002). pAkt and pACLY levels increased with myrAkt expression, as expected (**Figure 12D**). In control animals, relatively weak staining for AcH4 was detected in ductal epithelial cells. Remarkably, however, upon induction of Akt, pronounced increases in histone acetylation were detected within 96 hours of doxycycline administration (**Figure 12D**). On the other hand, another activating mark, H3K4me1, was not obviously regulated, suggesting that histone acetylation - not histone marks in general- may be specifically impacted by Akt activation. Hence, acute activation of Akt *in vivo* increases global histone acetylation levels.

These data indicate that activation of Akt acutely promotes histone acetylation. We next investigated whether Akt activation is associated with histone acetylation in established human tumors.

Figure 12: Akt Activation Allows Sustained Histone Acetylation in Glucose-Limited Conditions

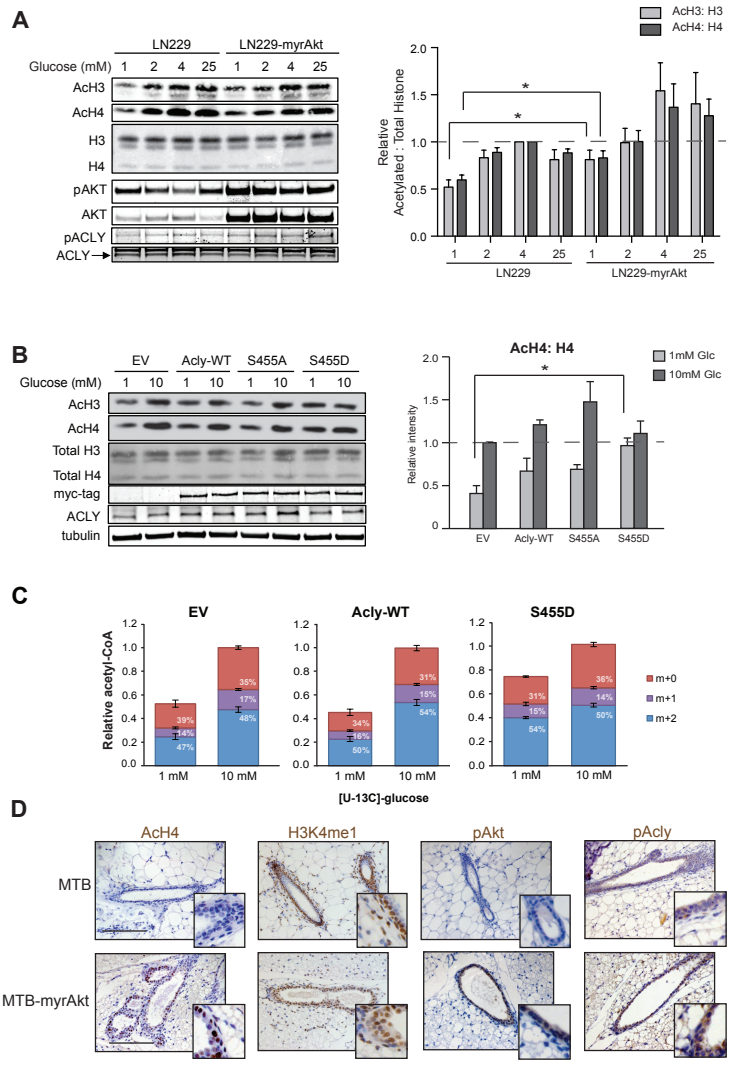

(A) Western blot analysis of proteins and histones from LN229 and LN229-myrAkt cells. Quantitation represents 5 independent experiments with LN229 4mM samples set to 1, mean +/− SEM (*, p ≤0.05). (B) Western blot analysis of histone acid extracts from LN229 cells stably expressing vector (EV), wt ACL, ACL-S455A, or ACL-S455D. Cells were treated with 1 or 10mM glucose for 24 hours before lysis. Quantitation represents the ratio of acetylated to total histones in four independent experiments with EV 10 mM set to 1, mean +/− SEM (*, p≤0.05) (C) Relative acetyl-CoA concentrations and percent enrichment after treatment in 1 mM or 10 mM [U-$^{13}C_6$]-glucose for 20 hours, mean +/− SEM of triplicates. Total acetyl-CoA levels as well as M+2 acetyl-CoA (enriched from glucose) were significantly suppressed (p≤0.05) in 1 mM as compared to 10 mM glucose in EV and WT-ACL cells, but not ACL-S455D cells. (D) Control (MTB) and transgenic (MTB-tAkt) mice were administered doxycyclin for 96 hours (n≥5, each group). Immunohistochemistry was performed on paraffin-embedded mammary tissue sections. Representative images are shown, along with magnification of areas of interest. Scale bar: 50 μm.

Figure 13: Akt promotes histone acetylation under glucose limited conditions.

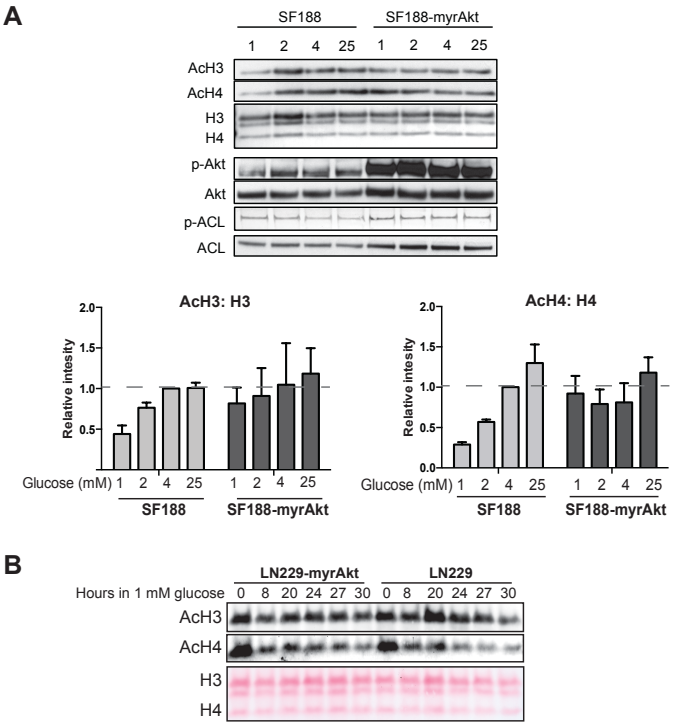

(A) Western blot analysis of proteins and histones from SF188 cells with or without myrAkt. Quantitation represents 3 independent experiments, mean +/- SEM, with SF188 4mM samples set to 1. (B) LN229 and LN229-myrAkt cells were incubated in 1 mM glucose for indicated times. Histones were extracted and analyzed by Western blot.

Figure 14: Activated Akt-ACLY pathway does not stimulate glutamine reductive carboxylation

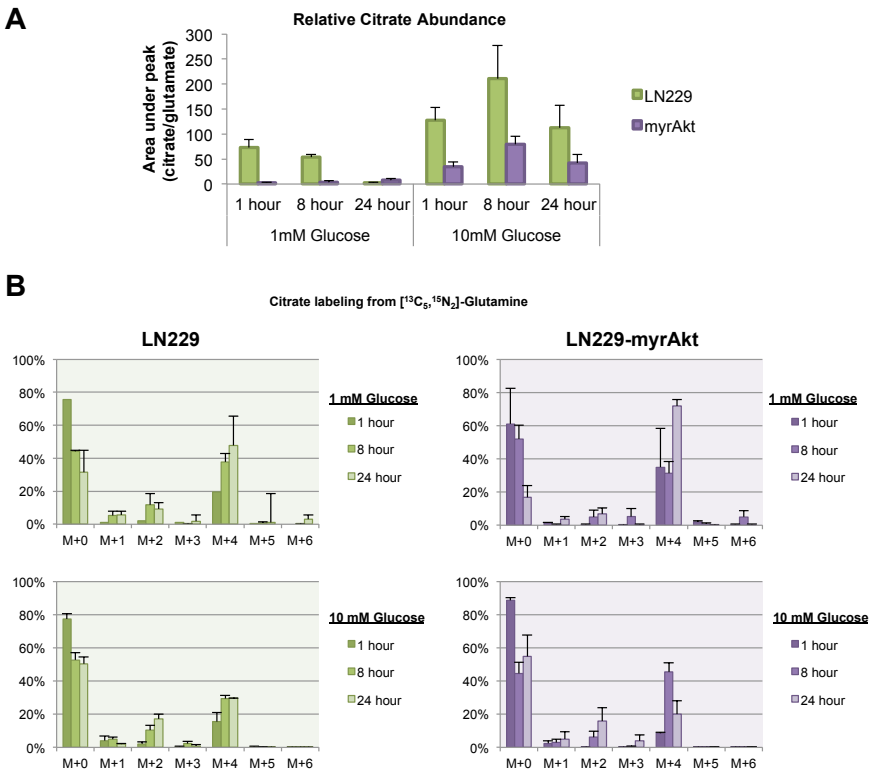

A) Comparison of citrate levels in LN229 cells and LN229-myrAkt cells treated with 2mM [$^{13}C_5{}^{15}N_2$]-glutamine and 1mM or 10mM glucose for the indicated times. The graph depicts total citrate normalized to total glutamate. The total of each metabolite was calculated as the summation of isotopologues generated for the metabolite. (B) Comparison of citrate isotopologues in LN229 and LN229-myrAkt cells treated with 2 mM [$^{13}C_5{}^{15}N_2$]-glutamine and 1 mM or 10 mM glucose for the indicated times. The graph indicates the percent of carbons contributed by glutamine for each isotopologue. m+4 citrate is generated through glutamine oxidative metabolism while m+5 citrate is generated by reductive carboxylation.

3.2.6 Histone acetylation levels correlate with pAkt in human glioma

The PI3K/Akt pathway is frequently activated in GBM as a result of mutations resulting in activation of EGFR or PI3K or loss of PTEN (Lino and Merlo, 2011). We examined a diverse panel of human gliomas to determine whether AcH4 is associated with pAkt levels. A total of 56 samples on a tumor tissue microarray (TMA) were analyzed for pAkt and AcH4 (**Figure 15A**). Each tumor sample was scored in a blinded manner by a neuropathologist and given a combined score for percent of positive cells and intensity of staining (H-score) for both pAkt and AcH4. A statistically significant positive correlation was found between pAkt and AcH4, indicating that Akt activation is associated with increased histone acetylation in human tumors (**Figure 15B**). pAkt levels tended to increase with tumor grade, particularly in astrocytomas, although no significant relationship was observed between tumor grade and AcH4 (**Figure 15C**). The relationship between pAkt and AcH4 is therefore not secondary to effects of tumor grade. IDH mutations occur frequently in gliomas and alter both cell metabolism and epigenetics (Losman and Kaelin, 2013). Of particular relevance, IDH mutations cause hypermethylation of histones (Lu et al., 2012), suggesting the possibility that histone acetylation might be altered secondarily to methylation effects in IDH mutant tumors. H3K9me3 was previously shown to be elevated in IDH mutant tumors in this patient set (Venneti et al., 2013a), and we found no significant relationship between H3K9me3 and pAkt levels (not shown). Moreover, AcH4 levels were not different between IDH wt and IDH mutant tumors (**Figure 15D**).

Figure 15: pAKT Correlates with Histone Acetylation in Human Glioma

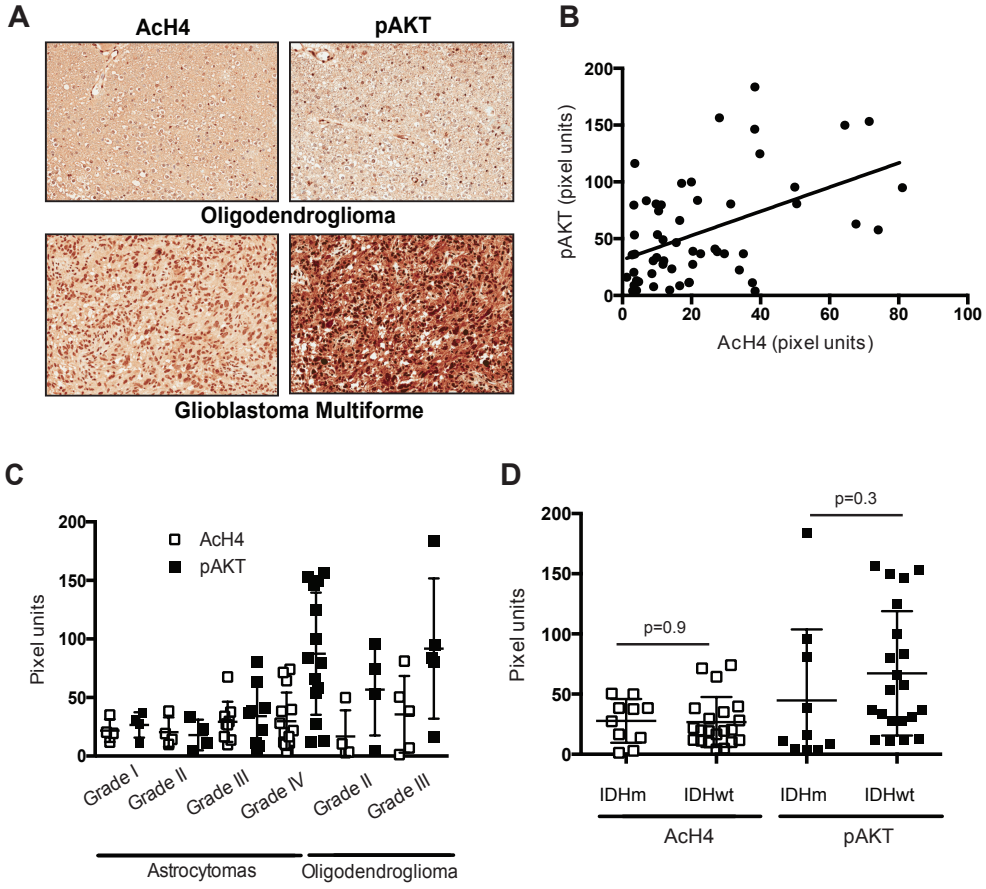

(A) Representative images (20X) of pAkt and AcH4 in a grade IV GBM and a grade II oligodendroglioma. (B) pAkt expression showed a significant correlation with AcH4 levels in 56 human glioma samples (r=0.4721, p=0.0002). (C) pAkt and AcH4 in astrocytic tumors (grade IV astrocytomas = GBM) and oligodendrogliomas, mean +/−SD. (D) pAkt and AcH4 levels in 10 IDH mutant and 21 IDH wt gliomas, mean +/− SD.

3.2.7 Histone acetylation levels correlate with pAkt in human prostate cancer

In human prostate tumors, significant correlations have been reported between levels of histone acetylation marks with tumor grade (H3K18ac and H4K12ac), as well as with the risk of tumor recurrence (H3K18ac, H3K9ac, H4K12ac) (Bianco-Miotto et al., 2010, Seligson et al., 2005). The PI3K-Akt pathway is frequently activated in prostate cancer due to PTEN loss or other mutations, and inhibition of Akt in the PTEN null prostate cancer cell lines PC-3 and C4-2 reduced overall levels of histone acetylation (**Figure 17A**). We investigated levels of three histone acetylation marks- H3K18ac, H3K9ac, and H4K12ac- and their association with pAkt(Ser473) in a panel of human prostate tumors (**Figure 16A**). The cohort consisted of patients with either metastatic or localized disease, with primary tumor grades ranging from 3-5 on the Gleason scale. Tumors were scored for both the percentage of positive cells and the intensity of staining. A striking positive correlation was observed between pAkt and each of the histone acetylation marks (**Figure 16B**). Levels of each histone acetylation mark were also strongly correlated with one another in tumors (**Figure 17B**). Percentages of nuclei positive for H3K18ac were similar between patients with metastatic as compared to localized disease, while H3K9ac and particularly H4K12ac scored positive in a higher percentage of nuclei in patients with metastatic disease (**Figure 17C**). H4K12ac was also higher in Gleason 4 and 5 tumors than Gleason 3 samples (**Figure 17D**). Together the data from human prostate cancer and glioma suggest that Akt activation is a major determinant of histone acetylation levels in tumors.

3.2.8 Histone acetylation as a predictive biomarker for therapeutic failure

For 10 of the prostate cancer patients with localized disease, biochemical failure (PSA recurrence) data was available. Strikingly, levels of histone acetylation were highly predictive of which patients would later exhibit biochemical failure. The five patients with the lowest levels of H4K12ac, H3K18ac, and H3K9ac developed biochemical failure, whereas the five with the highest levels of these marks did not (**Figure 16C**). These findings agree with those of Seligson and colleagues, showing that low levels of histone modifications such as H3K18ac are associated with a poor prognosis in prostate cancer (Seligson et al., 2005). Within these 10 samples, the relationship between pAkt and each histone acetylation mark held (**Figure 17E**), although pAkt levels did not predict biochemical failure in these 10 samples (**Figure 16C**). Hence, histone acetylation levels might be a valuable biomarker to predict tumor relapse.

Figure 16: pAKT Correlates with Histone Acetylation Levels in Human Prostate Cancer

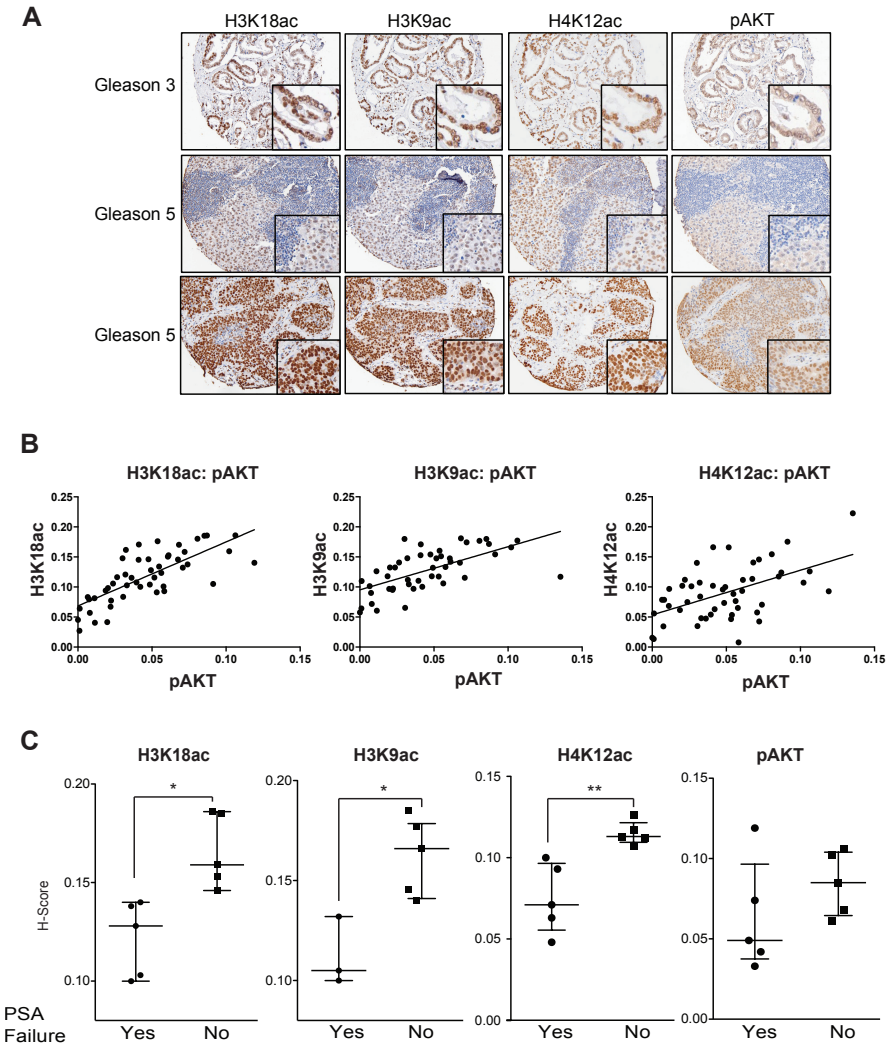

(A) Representative images of H3K18ac, H3K9ac, H4K12ac, and pAkt expression detected by immunohistochemistry in Gleason grade 3–5, metastatic (n=25) and non-metastatic (n=24) prostate cancer tumors. (B) H-scores were determined and correlations between marks determined. pAkt expression showed a significant correlation with: H3K18ac levels (r=0.7452, $p \leq 0.0001$); H3K9Ac (r=0.6283, $p \leq 0.0001$); and H4K12ac (r=0.5276, $p \leq 0.0001$). (C) Box plot showing H-scores for H4K12ac, H3K18ac, H3K9ac, and pAkt in prostate cancer tumors in patients who developed PSA failure (Yes) or not (No) (**, p<0.005, *, p<0.05).

Figure 17: Histone acetylation marks correlate with one another in human prostate tumors

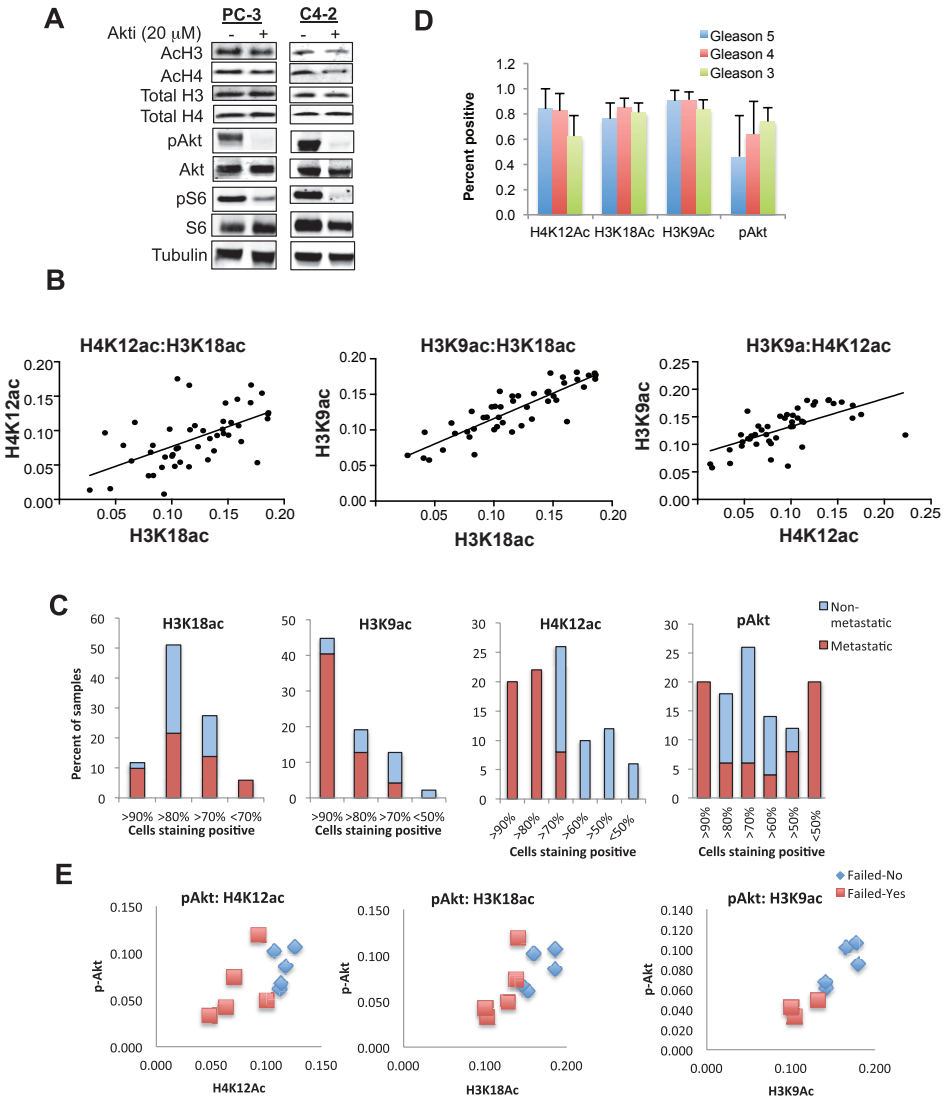

A) Prostate cancer cells C4-2 and PC-3 were cultured in 10mM glucose in RPMI medium and were either mock-treated (EtOH) or treated with Akt inhibitor for 24 hours. Whole cell lysates were analyzed by Western blot. B) Levels of histone acetylation marks (H3K18ac, H4K12ac and H3K9ac) strongly correlated with one another in tumors (H3K18ac and H4K12ac: r=0.58, p<0.0001, H3K18ac and H3K9ac: r=0.866, p<0.0001; H3K9ac and H4K12ac: r=0.6412, p<0.0001). C) Percentage distribution of positive nuclei for select histone marks (H3K18ac, H4K12ac and H3K9ac) between metastatic and non-metastatic tumors. D) Distribution of percent positivity for select histone marks (H3K18ac, H4K12ac and H3K9ac) in tumors based on Gleason score, mean +/ SD. E) Relationship between pAKT and histone acetylation marks in the 10 patients with biochemical failure data shown in Figure 16C.

3.3 Discussion

We report that oncogenic Akt activation is a key determinant of global histone acetylation levels in cancer cells. We provide evidence that this occurs through Akt-dependent metabolic reprogramming to promote high acetyl-CoA production. Akt ensures continuous acetyl-CoA production even during nutrient limitation by promoting the phosphorylation and activation of ACLY. To our knowledge, this is the first report that implicates metabolic reprogramming mediated by oncogenic activation of a signal transduction pathway as a major factor underlying tumor epigenomic regulation.

Elucidating the regulation of tumor histone acetylation levels is important clinically, and the mechanisms that control tumor histone acetylation are currently poorly understood. Our data suggest that metabolic effects contribute to determining histone acetylation levels in tumors. Other relevant factors in addition to acetyl-CoA metabolism include levels of KATs and HDACs, as well as tumor pH. The significance of global histone acetylation levels is not yet fully clear. Several studies have examined the relationship between histone acetylation levels and tumor recurrence and patient survival in various cancer types [reviewed in (Chervona and Costa, 2012, Kurdistani, 2007)]. Significant correlations have been shown in several studies, although high histone acetylation has been associated with both better and worse prognoses, likely reflecting differences in types of cancer, tumor grade, therapeutic approaches, and sample stratification. Our data suggest that low levels of histone acetylation may predict poor patient outcome in prostate cancer, similar to the findings of Seligson et al (Seligson et al., 2005). Further study is needed to understand how global histone acetylation levels impact tumor growth and progression, as well as treatment responses.

It will be crucial to further investigate the functions of metabolic control of acetylation, as well as the role of ACLY levels and phosphorylation, in regulating gene expression and promoting tumorigenesis. ACLY silencing is known to inhibit cancer cell proliferation and suppress tumor growth (Hatzivassiliou et al., 2005, Bauer et al., 2005, Migita et al., 2008). While suppression of de novo lipogenesis in the absence of ACLY is certainly a key component of this anti-tumor effect, a growing literature indicates that acetylation also plays a crucial role in promoting anabolic metabolism and growth. Acetyl-CoA has been shown to promote growth and proliferation in yeast, through histone acetylation at genes involved in these processes (Cai et al., 2011). Moreover, acetyl-CoA and acetylation regulate many metabolic enzymes (Guan and Xiong, 2011), and a role for acetyl-CoA in suppressing autophagy has also recently been uncovered (Eisenberg et al., 2014, Marino et al., 2014). We show here that many proliferation-related genes are acetyl-CoA-regulated in glioblastoma cells, correlating with overall histone acetylation levels, as well as histone acetylation at these genes. Thus, our study adds to a growing literature that implicates acetyl-CoA in providing pro-growth cues to the cell.

We have focused this study on the role of the PI3K/Akt pathway in regulation of acetyl-CoA production and histone acetylation. Many oncogenes and tumor suppressors are now recognized to regulate cellular metabolism. Microenvironmental conditions such as hypoxia also potently reprogram cellular metabolism. Moreover, in addition to acetyl-CoA, metabolites such as UDP-GlcNAc, S-adenosylmethionine (SAM), and α-ketoglutarate are also required by chromatin modifying enzymes and could potentially impact the epigenome if their levels are altered in tumors (Lu and Thompson, 2012a). It

is therefore conceivable that altered metabolite utilization substantially alters chromatin in many or most cancer cells.

Intense effort is currently aimed at targeting both cancer cell metabolism and cancer epigenetics (Dawson and Kouzarides, 2012, Vander Heiden, 2011). If metabolism is indeed a critical mediator of cancer cell epigenetic deregulation, it is possible that epigenetic alterations could be reversed through therapeutics directed at metabolic targets. Improved understanding of metabolic regulation of the epigenome could point towards contexts in which existing epigenetic therapies such as HDAC inhibitors would be most effective or could open doors to development of more specific therapeutics targeting the intersection of metabolism and epigenetics. The finding that the PI3K/Akt pathway is a key determinant of histone acetylation levels in tumors represents an important step forward in understanding the extent to which oncogenic metabolic reprogramming could control the epigenome.

CHAPTER 4:

ACETYL-COA COORDINATES CALCIUM-NFAT1 SIGNALING FOR CELL MIGRATION

4.1 Introduction

Metabolic reprogramming in cancer cells facilitates the acquisition and utilization of nutrients necessary for proliferation and survival within the tumor microenvironment, which is often nutrient-limited. In addition to direct roles in metabolic processes, certain metabolites are substrates of enzymes that carry out post-translational modifications and thus serve parallel functions as signaling molecules. Altered levels of such intracellular metabolites can result in distinct changes in gene expression, cellular differentiation, and interaction with the tumor microenvironment (Metallo and Vander Heiden, 2010, Pavlova and Thompson, 2016, Vander Heiden et al., 2009, Wellen and Thompson, 2012).

One metabolic intermediate that has emerged as a key link between metabolism, signaling, and the epigenome is acetyl-coenzyme A (acetyl-CoA), the acetyl donor for acetylation reactions (Kinnaird et al., 2016, Pietrocola et al., 2015). Histone acetylation levels are highly sensitive to acetyl-CoA abundance (Cai et al., 2011, Cluntun et al., 2015)(Chapter 3), and in many types of mammalian cells the acetyl-CoA producing enzyme ATP-citrate lyase (ACLY) regulates histone acetylation levels (Wellen et al., 2009, Zhao et al., 2016, Wong et al., 2017, Covarrubias et al., 2016, Donohoe et al., 2012). ACLY is localized in both the cytosol and nucleus and generates acetyl-CoA from citrate exported from mitochondria, thus directly linking mitochondrial metabolism to nuclear processes such as histone acetylation and cytosolic processes such as lipid biosynthesis. We previously established that nutrient-dependent fluctuations in acetyl-

CoA abundance impact gene expression profiles in glioblastoma cells (Chapter 3). Although such changes in gene expression correlate with global histone acetylation levels, the specific mechanisms through which acetyl-CoA abundance impacts gene expression are poorly elucidated.

Recent studies have identified roles of metabolic enzymes in gene regulation. For example, acyl-CoA synthetase short-chain family member 2 (ACSS2), which uses acetate as a substrate to generate acetyl-CoA, is recruited to specific loci to regulate site-specific histone acetylation in the hippocampus to facilitate memory formation or in cells under nutrient stress to enable induction of autophagy and lysosome biogenesis genes(Li et al., 2017, Mews et al., 2017). ACSS2 has also been shown to be required for acetylation of the transcription factor HIF-2α (Xu et al., 2014).

Among genes responsive to acetyl-CoA abundance in glioblastoma cells are many genes involved in cell adhesion, extracellular matrix (ECM) interaction, cytoskeleton, and integrin signaling (Chapter 3). The most common brain tumor, glioblastoma (GBM), is highly invasive, limiting the efficacy of surgical resection (Furnari et al., 2007, Jhanwar-Uniyal et al., 2015). In this study, we aimed to define the specific mechanisms through which acetyl-CoA abundance regulates expression of cell adhesion and migration genes, since such insights could suggest new therapeutic strategies to limit the invasive characteristics of this lethal cancer. We identified NFAT1 as a key acetyl-CoA-responsive transcription factor that promotes glioblastoma cell adhesion to the ECM and migration. Unexpectedly, we found that acetyl-CoA abundance impacts NFAT nuclear localization via regulation of calcium signaling (Furnari et al., 2007, Jhanwar-Uniyal et

al., 2015). These data identify a link between cellular metabolism and gene regulation that modulates cancer cell phenotypes.

4.2 Results

4.2.1 Acetyl-CoA availability regulates expression of genes involved in cell migration and adhesion in glioblastoma cells.

Histone acetylation levels decline when glucose is limited, correlating with acetyl-CoA abundance, and can be restored upon supplementation of acetate, which enters the cell and is directly converted to acetyl-CoA by acetyl-CoA synthetase enzymes (ACSS1-3). In the previous chapter, we profiled gene expression in high and low glucose conditions, in the presence and absence of acetate (**Figure 4**). Among gene sets enriched in "acetyl-CoA-high" conditions (enriched in both high glucose and low glucose plus acetate) were cell adhesion, migration, and cytoskeleton pathways (PANTHER: Integrin signaling pathway; KEGG: Regulation of actin cytoskeleton; KEGG: Cell adhesion molecules; REACTOME: Integrin cell surface interactions; KEGG: ECM-receptor interaction)(**Figure 4**). Expression patterns for select genes within these sets were validated by qPCR (**Figure 18A**). H3K27 acetylation (H3K27ac) correlated with gene expression at glucose- and acetate-regulated genes, as shown by ChIP-qPCR (**Figure 19A**). To test if cell migration was functionally impacted under these conditions, we employed wound healing and transwell migration assays. In both, cell migration was impaired in low glucose and rescued with acetate supplementation (**Figure 18B, C**). Importantly, acetate rescued cell migration without altering doubling time (**Figure 4**), indicating that its effects on migration are not secondary to enhanced proliferation.

Integrin-mediated adhesion to the extracellular matrix (ECM) is a crucial component of cancer cell migration and invasion (Pickup et al., 2014). To test the impact of acetyl-CoA abundance on glioblastoma cell adhesion to the ECM, we employed a brain-inspired biomaterial platform comprised of 50% fibronectin, 25% vitronectin, 20% tenascin C, and 5% laminin (Barney et al., 2015). After incubating cells in high or low glucose, with or without acetate supplementation, cells were seeded onto the ECM and their adhesion was recorded over time. Both glucose and acetate enhanced cell adhesion to the brain ECM (**Figure 18D**). Enhanced adhesion by glucose and acetate was also observed using a simplified adhesion assay with fibronectin only, and these findings were consistent in three other glioblastoma cell lines tested (**Figure 18E-G**). To test whether the timing for acetyl-CoA dependent cell adhesion is consistent with a transcriptional process, we performed a time course analysis of adhesion following glucose and acetate supplementation. Cells were incubated overnight in low glucose and then high glucose or acetate added back and adhesion examined. Improved capacity to adhere to fibronectin was observed beginning 4 hours after glucose or acetate addback and was most pronounced after 24 hours (**Figure 18H**), consistent with a role for gene transcription rather than an acute signaling event.

Regulation of adhesion and migration by glucose and acetate could be directly reliant on acetyl-CoA itself, or indirectly mediated through a metabolic pathway that employs acetyl-CoA, such as fatty acid, cholesterol, or hexosamine synthesis. For example, fatty acids are required for cell migration by contributing to invadopodia formation and lipid rafts (Scott et al., 2012, Byon et al., 2009). Fatty acid supplementation, however, was unable to restore adhesion under low glucose conditions (**Figure 19B**). Likewise, mevalonate, an intermediate in the synthesis of sterols and

isoprenoids, which also contributes to migration (Mullen et al., 2016), failed to significantly rescue adhesion (**Figure 19C**). N-acetyl-glucosamine (GlcNAc), which rescues the hexosamine pathway and is important for receptor membrane localization (Wellen et al., 2010), resulted in a modest enhancement (**Figure 19C**). This suggested that the ability for cells to generate lipids, sterols, and glycan-chain was not as limiting as acetyl-CoA itself. Acetate can also be converted to acetyl-CoA in mitochondria, and consistent with this, citrate levels were suppressed in low glucose and partially restored by acetate supplementation (**Figure 19D**). Moreover, pyruvate supplementation enhanced cell adhesion to a similar extent as acetate under low glucose conditions (**Figure 19E**). Glucose, acetate, and pyruvate all can supply mitochondrial acetyl-CoA to support citrate production and use in the TCA cycle. Mitochondrial citrate can also be exported for ACLY-dependent acetyl-CoA production in the cytosol and nucleus. Notably, inhibition of the lysine acetyltransferase p300 using C646 suppressed the effects of glucose and acetate in enhancing H3K27ac levels and cell adhesion (**Figure 19F, G**), further supporting roles acetyl-CoA as a signaling molecule. Collectively, these data indicate that glioblastoma cell adhesion and migration is impaired when intracellular acetyl-CoA levels are low.

4.2.2 Nutrient-regulated cell adhesion and migration requires ACLY.

As evidenced by the increase in citrate after the addition of acetate, we next asked whether ACLY is required for nutrient-dependent adhesion and migration. Upon silencing of *ACLY,* both wound healing and adhesion to fibronectin were impaired (**Figure 20A, B**). Similarly, pharmacological inhibition of ACLY potently suppressed adhesion and transwell migration, as well as expression of adhesion and migration

related genes (**Figure 20B, C,** and **Figure 21A).** Nutrient-dependent adhesion and expression of *ITGA2B* were also suppressed upon genetic deletion of ACLY in LN229 cells (**Figure 20E, F**). Moreover, xenograft tumor growth was markedly impaired in the absence of ACLY (**Figure 21B, C**), and several adhesion- and migration-related genes exhibited lower expression in tumors generated from ACLY-deficient cells (**Figure 20G**), supporting the relevance of ACLY in modulating expression of these genes *in vivo*.

Figure 18: Acetyl-CoA promotes cell adhesion and migration in glioblastoma cells

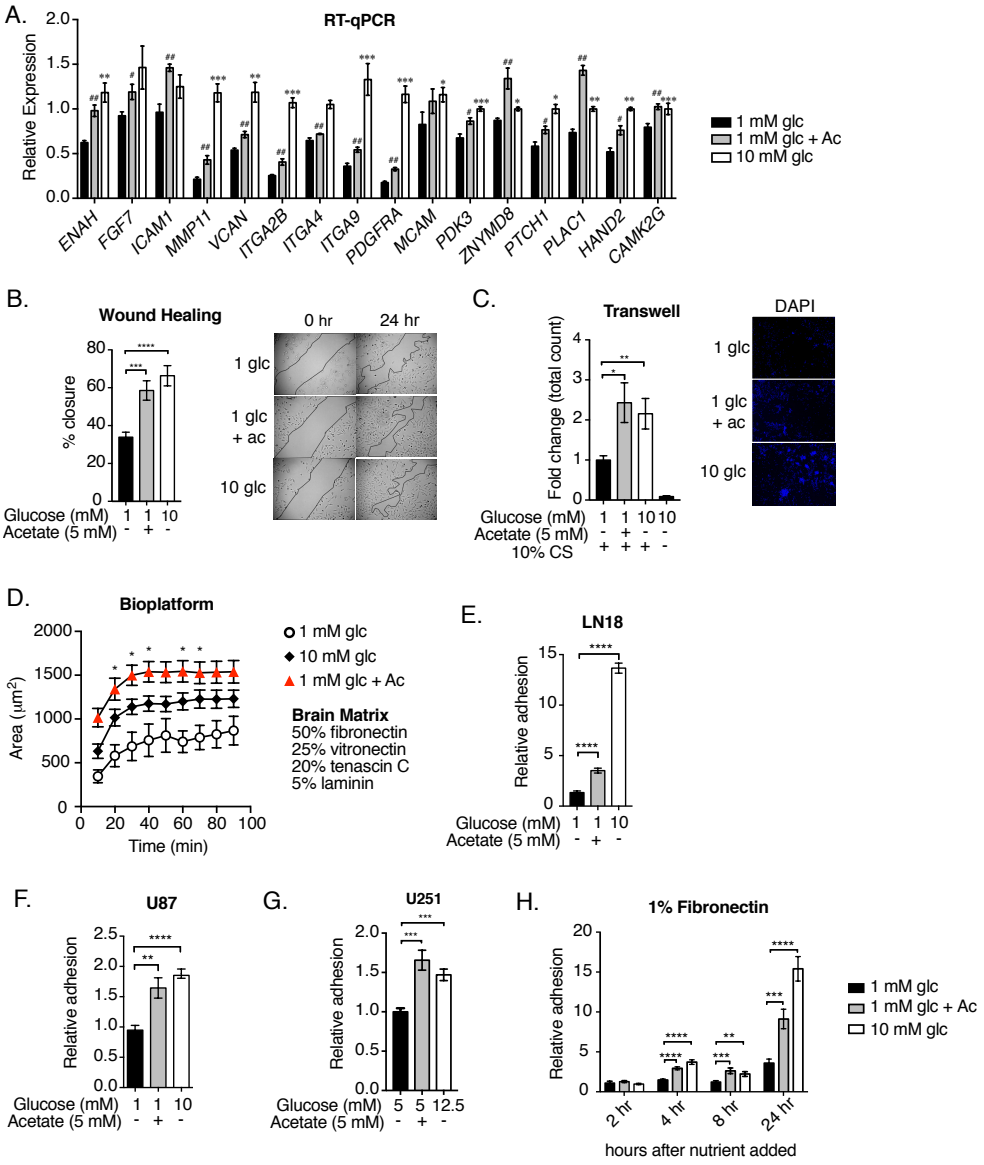

(A) Relative mRNA levels of acetyl-CoA up-regulated genes in LN229 cells. Significance of acetate treated over 1 mM glucose denoted # (#, p<0.05; ##, p<0.01). Significance of 10 mM glucose treated over 1 mM glucose denoted * (**, p<0.01; ***, p<0.001). (B) Wound healing assay in LN229 cells. (***, p<0.001, ****, p<0.0001). Right panel: Lines indicate boundary of scratch. Photos captured at 0 hours and after 24 hours. (C) Transwell migration of LN229 across 8.0 µm polycarbonate membrane. (*, p<0.05; **, p<0.01). Right panel: cells were stained with Hoechst and photos were captured 24 hours after seeding. (D) Adhesion quantified on biomaterial platform with ECM components of the brain. Area covered by cells were measured over time. Turkey Post Test *, p<0.05. (E-G) Relative adhesion to 1% fibronectin after 24 hours of indicated treatments in (E) LN18, (F) U87, and (G) U251 cells ** p<0.01,*** p<0.001, **** p<0.0001. (H) LN229 cells were treated after overnight starvation. Quantification of adhesion to 1% fibronectin after indicated hours of treatment ** p<0.01,*** p<0.001, **** p<0.0001. For all panels: mean +/- SEM of triplicates

Figure 19: Acetyl-CoA promotes local histone acetylation and supports citrate production

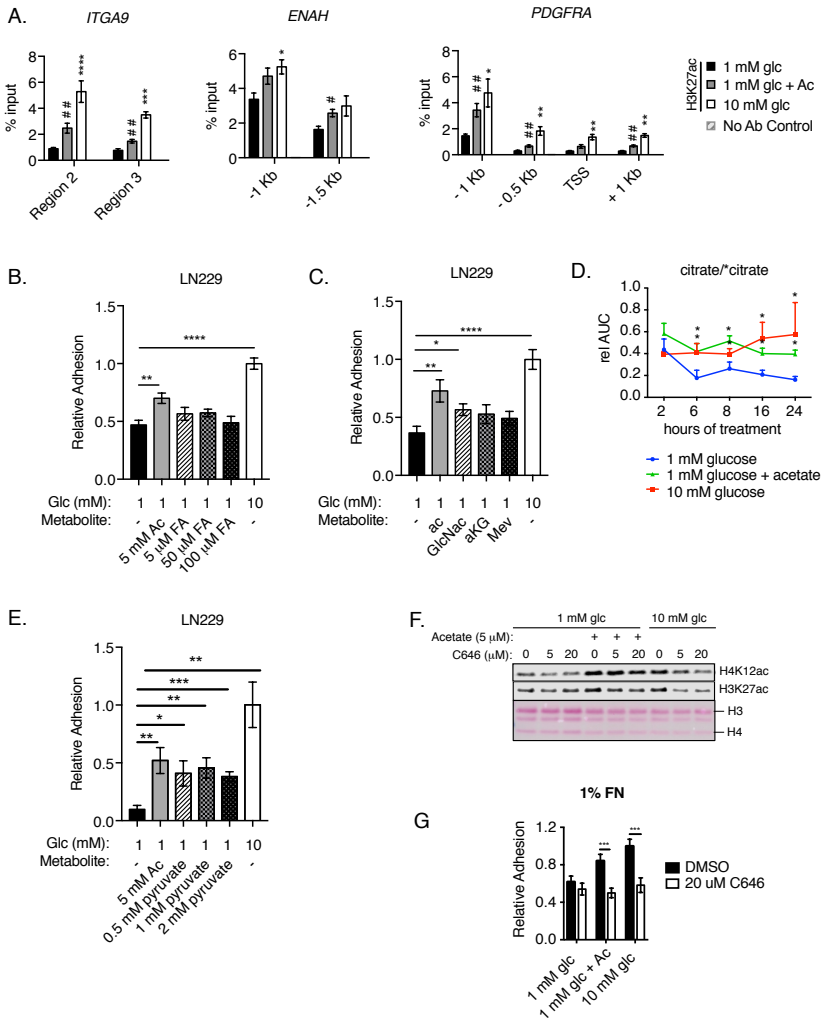

(A) H3K27ac analysis of several regions of indicated genes. Significance of acetate treated over 1 mM glucose denoted with # (#, p<0.05; ##, p<0.01). Significance of 10 mM glucose treated over 1 mM glucose denoted with * (*, p<0.05; **, p<0.01; ***, p<0.001). (B-C) Relative adhesion after 24 hours of treatment (*, p<0.05; **, p<0.01; ****, p<0.0001). (D) relative amount of citrate detected by LCMS, normalized to U-13C-citrate as internal control (*citrate) Mean, error bars represent SD triplicates (p<0.05). (E) Relative adhesion to 1% fibronectin after 24 hours of treatment (*, p<0.05; **, p<0.01; ***, p<0.001). (F) Detection of acetylation as determined by western blot after 24 hours of indicated treaments. (G) Relative adhesion onto 1% fibronectin after 24 hours of treatment with C646 or vehicle control (DMSO) (***, p<0.001). Unless otherwise indicated, all panels: mean +/- SEM triplicates.

Figure 20: Acetyl-CoA regulation of cell adhesion and migration requires ACLY

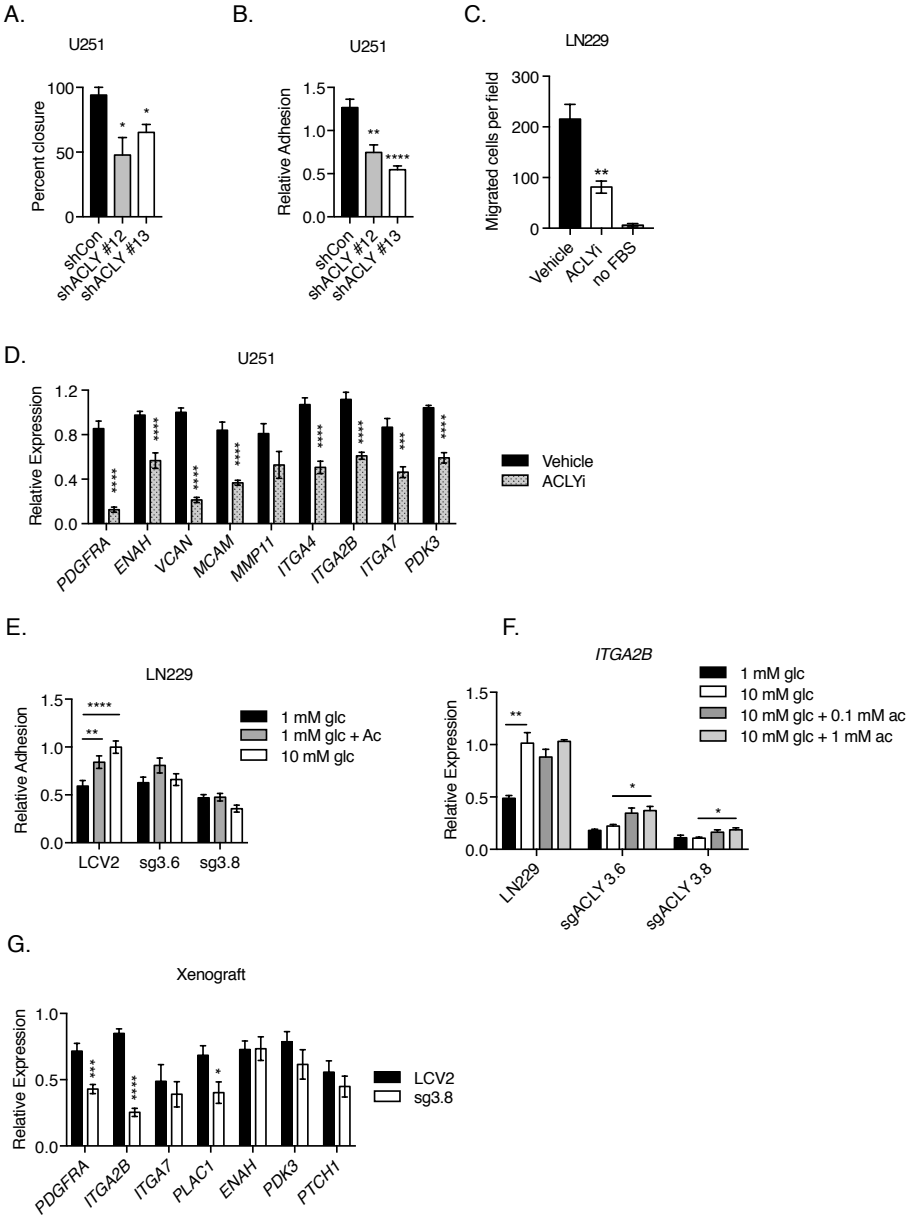

A) Wound healing assay in U251 with stable knockdown of ACLY(*, p<0.05) (B) Relative adhesion in U251 cells with stable knockdown of ACLY. (**, p<0.01; ***, p<0.001) (C) Transwell migration of LN229 cells after treatment with ACLi or vehicle; no FBS is a control. (**, p<0.01). All conditions were in 10 mM glucose. (D) Relative mRNA expression of acetyl-CoA regulated genes in U251 cells treated with 50 μM ACLY inhibitor (ACLi; BMS303141) in 10 mM glucose. (***, p<0.001; ****, p<0.0001). (E) Relative adhesion in two different ACLY-KO clones (sg3.6 and sg3.8) on 1% fibronectin. Parental cells (LCV2) were infected with Cas9 but without guide RNA. (**, p<0.01; ****, p<0.0001). (F) Relative expression of *ITGA2B* in cells described in panel E (*, p<0.05; **, p<0.01). (G) Relative mRNA expression of acetyl-CoA up-regulated genes in xenograft derived tumors (*, p<0.05; **** p<0.0001). All panels: mean+/- SEM

Figure 21: ACLY is required for cell adhesion and xenograft tumor growth

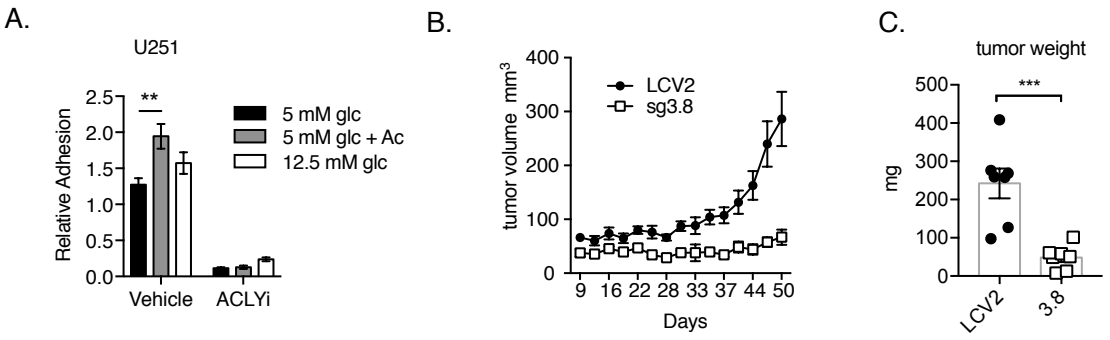

(A) Relative adhesion in U251 cells on 1% fibronectin after 24 hours with 50 μM ACLYi. (**, $p<0.01$). (B) Tumor volume. For each condition, n = 7. (C) Tumor weight (***, $p<0.001$) For each condition, n = 7.

4.2.3 Cellular adhesion and migration genes are regulated by NFAT family transcription factors.

While expression of cell migration and adhesion genes correlates with histone acetylation (**Figure 18A** and **Figure 19A**), we postulated that specificity of acetyl-CoA dependent gene expression might be achieved through regulation of one or more transcription factor. To gain initial insight into transcription factors that might be responsive to acetyl-CoA abundance, we queried the Broad Institute molecular signatures database (MSigDB) to identify top enriched transcription factor motifs (Subramanian et al., 2005, Mootha et al., 2003). The NFAT binding consensus motif TGGAAA(Badran et al., 2002) was the most highly enriched transcription factor motif within 2 kb upstream and downstream of the TSS of "acetyl-CoA up" genes (**Figure 22A,** and **Figure 23A, B**).

NFAT isoforms 1-4 are calcium-responsive transcription factors involved in a wide range of cellular processes in different cell types (Muller and Rao, 2010, Mancini and Toker, 2009). Notably, substantial evidence links NFAT to the regulation of cell migration and invasion in cancer (Qin et al., 2014), including in glioblastoma (Chigurupati et al., 2010, Tie et al., 2013, Wang et al., 2015). Ca^{2+} homeostasis is tightly controlled in the cell. When Ca^{2+} is released from endoplasmic reticulum stores into the cytosol, calcium-sensitive calmodulin activates the phosphatase calcineurin, which dephosphorylates NFAT. Dephosphorylation exposes the nuclear localization signal that allows NFAT to enter the nucleus and bind to its canonical motif (Muller and Rao, 2010, Mancini and Toker, 2009). NFAT requires the coactivator p300 for its transcriptional activity (Garcia-Rodriguez and Rao, 1998), making it a likely candidate for regulating

acetyl-CoA-responsive genes. However, the majority of NFAT regulated genes in glioma have not been defined, nor is NFAT known to be responsive to acetyl-CoA availability.

To investigate whether NFAT is involved in acetyl-CoA-dependent adhesion, we inhibited calcineurin with cyclosporine A (CsA) (Schreiber and Crabtree, 1992). CsA potently suppressed cell adhesion to fibronectin in the presence of either glucose or acetate (**Figure 22B** and **Figure 23C**). Reciprocally, we tested whether increasing cytosolic calcium could promote cell adhesion. Treatment of cells with ionomycin for 4 hours rescued cell adhesion under low glucose conditions, as well as after treatment with ACLYi (Fig 3C and 3**D**). Using quantitative PCR, we determined that NFAT1 (NFATC2) is the most highly expressed NFAT isoform in LN229 cells (**Figure. 23D**). RNA-mediated silencing of NFAT1 (**Figure 23E**) suppressed both canonical NFAT target genes such as *PTGS2*, as well as selected "acetyl-CoA-up" genes predicted to be NFAT targets (**Figure 22E** and **Figure 23F**). Additionally, NFAT1 silencing reduced wound healing and adhesion (**Figure 22G**). Thus, is most likely that NFAT1 is required for acetyl-CoA dependent cell adhesion.

Figure 22: The transcription factor NFAT1 mediates acetyl-CoA dependent cell adhesion and migration

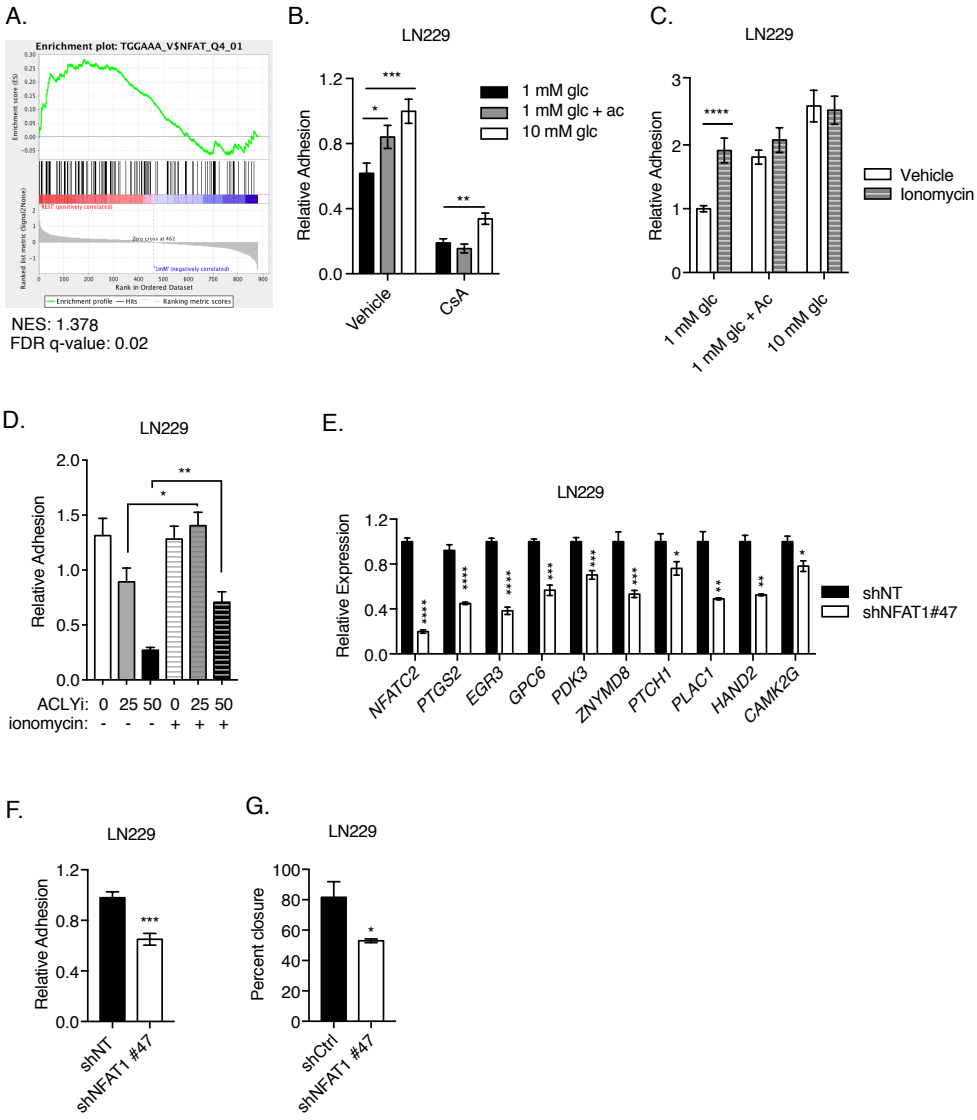

(A) Gene set enrichment analysis (GSEA) of acetyl-CoA up-regulated genes. (B) LN229 cell adhesion onto 1% fibronectin after 24 hours of 10 μM cyclosporin A (CsA) or vehicle control.(*p<0.05; **, p<0.01; ***p<0.001). (C) LN229 cell adhesion onto 1% fibronectin after 20 hours of nutrient treatment followed by 4 hours of treatment with 0.5 μM ionomycin or vehicle control. (****, p<0.0001) (D) Relative adhesion after 20 hours of treatment with ACLYi followed by 4 hour of treatment with 0.5 μM ionomycin or vehicle control. *, p<0.05; ** p<0.01. (E) Relative mRNA expression of acetyl-CoA up-regulated genes after short-hairpin mediated knockdown of NFAT1 in LN229 cells. Representative genes from list generated in from GSEA in panel A. (F) Relative adhesion onto 1% fibronectin after 24 hours of indicated nutrient conditions after knockdown of NFAT1 in LN229 cells (***, p<0.001). (G) Wound healing assay in LN229 cells after knockdown of NFAT1 (*, p<0.05). All panels: mean +/- SEM

Figure 23: NFAT1 is the top predicted transcription factor to regulate acetyl-CoA genes

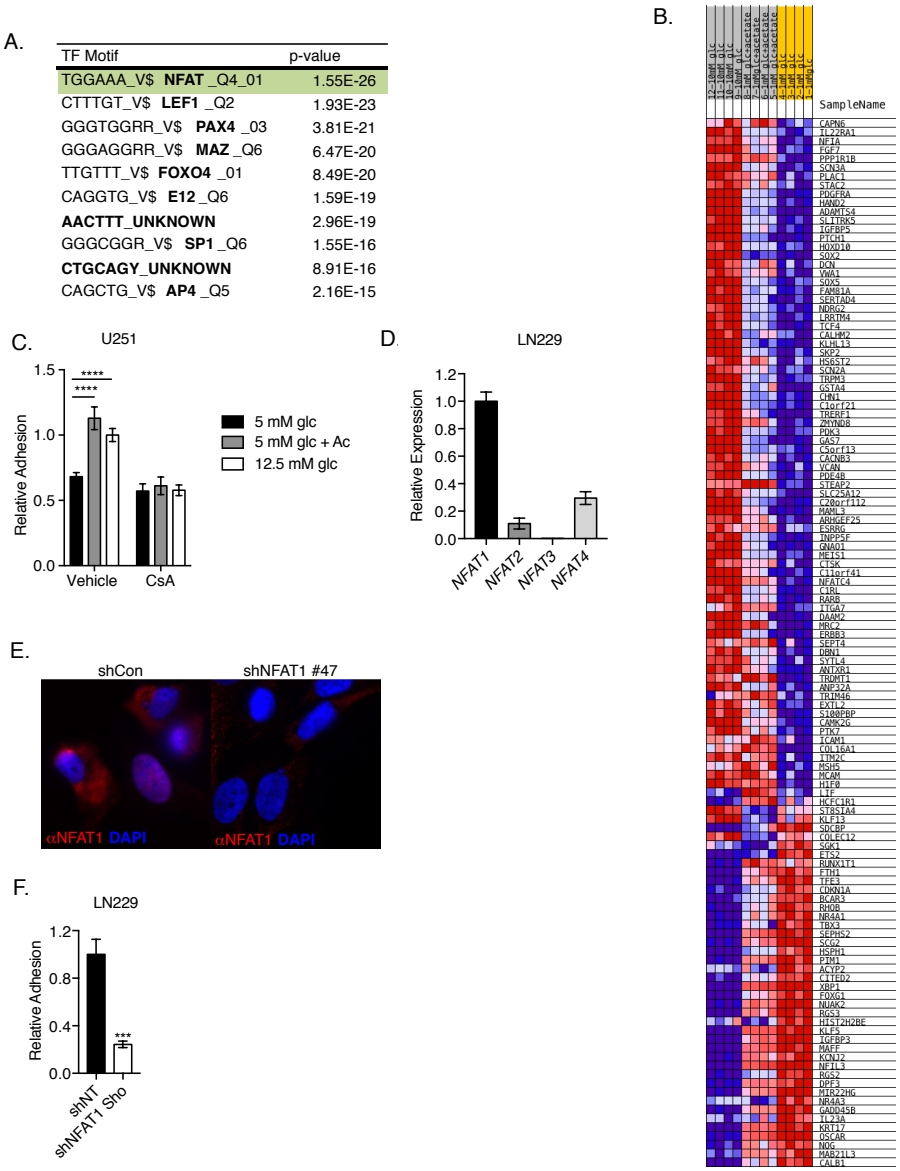

(A) Top motifs predicted to regulate acetyl-CoA genes. (B) Heatmap representation of genes identified in Figure 22A. (C) Relative adhesion onto 1% fibronectin after 24hour treatment with CsA (20μM). (****, p<0.0001). (D) Relative mRNA levels of each NFAT family member in LN229. (E) Representative image of immunofluorescent staining of NFAT1 in red demonstrating knockdown efficiency. (F) Relative adhesion onto 1% fibronectin after knockdown of NFAT1 using previously published hairpin sequence (Shoshan et al, 2016)

4.4.4 Calcium dynamics and NFAT1 localization is acetyl-CoA dependent.

Since ionomycin rescued cell adhesion in low glucose (**Figure 22C**), acetyl-CoA may be acting upstream of calcium release to control NFAT. To investigate if acetyl-CoA impacts calcium dynamics, we sought to visualize and measure cytoplasmic calcium using an ultra-sensitive protein calcium sensor, GCaMP6f (Chen et al., 2013a). Cells were starved overnight in 1 mM glucose and then medium replaced, containing 1 mM glucose, 10 mM glucose, or 1 mM glucose + 5 mM acetate. Calcium bursts were monitored over time, and both glucose and acetate were found to enhance the frequency of Ca^{2+} release (**Figure 24A**). These "Ca2+ bursts" are thought to promote local focal adhesion proteins disassembly which is required for migration (Tsai and Meyer, 2012, Wei et al., 2009). Notably, previous literature demonstrated that glucose promotes Ca2+-NFAT signaling, via phosphoenolpyruvate (PEP)-dependent inhibition of SERCA reuptake of cytosolic calcium (Ho et al., 2015). In the glioblastoma cells, high glucose raised PEP levels, but acetate did not, (**Figure 25**), suggesting that acetate impacts Ca^{2+} homeostasis via a distinct mechanism.

If acetyl-CoA abundance impacts intracellular Ca^{2+}, it would be expected to promote NFAT1 dephosphorylation and nuclear localization. Indeed, using immunofluorescent imaging, we observed that NFAT1 nuclear localization is reduced under low glucose conditions and rescued in the presence of acetate (**Figure 24B, 24C**). Ionomycin treatment induced a shift in NFAT mobility in gel, consistent with reduced phosphorylation (**Figure 24D**). Both glucose and acetate similarly increased NFAT mobility, and no further effect was observed in the presence of ionomycin (**Figure 24D**). Furthermore, ACLY-deficient cells demonstrated NFAT1 nuclear exclusion, and

nuclear localization was restored upon reintroduction of murine ACLY (**Figure 26B, 26C**). Biochemical inhibition of ACLY also reduced NFAT mobility (consistent with hyperphosphorylation) and suppressed NFAT nuclear localization (**Figure 24E, F**). In the presence of ionomycin, ACLY inhibition failed to reduce NFAT mobility (**Figure 24F**), consistent with ACLY acting upstream of calcium release. The addition of a phosphomutant (Wang, J Pathol 2009) constitutively active NFAT1 rescued adhesion under low glucose compared to exogenous WT-NFAT1. (**Figure 24G**). Together, these data indicate that acetyl-CoA abundance facilitates cell adhesion and migration in glioblastoma cells via promoting Ca^{2+}-NFAT signaling.

Figure 24: Nuclear localization of NFAT1 and calcium signaling are acetyl-CoA dependent

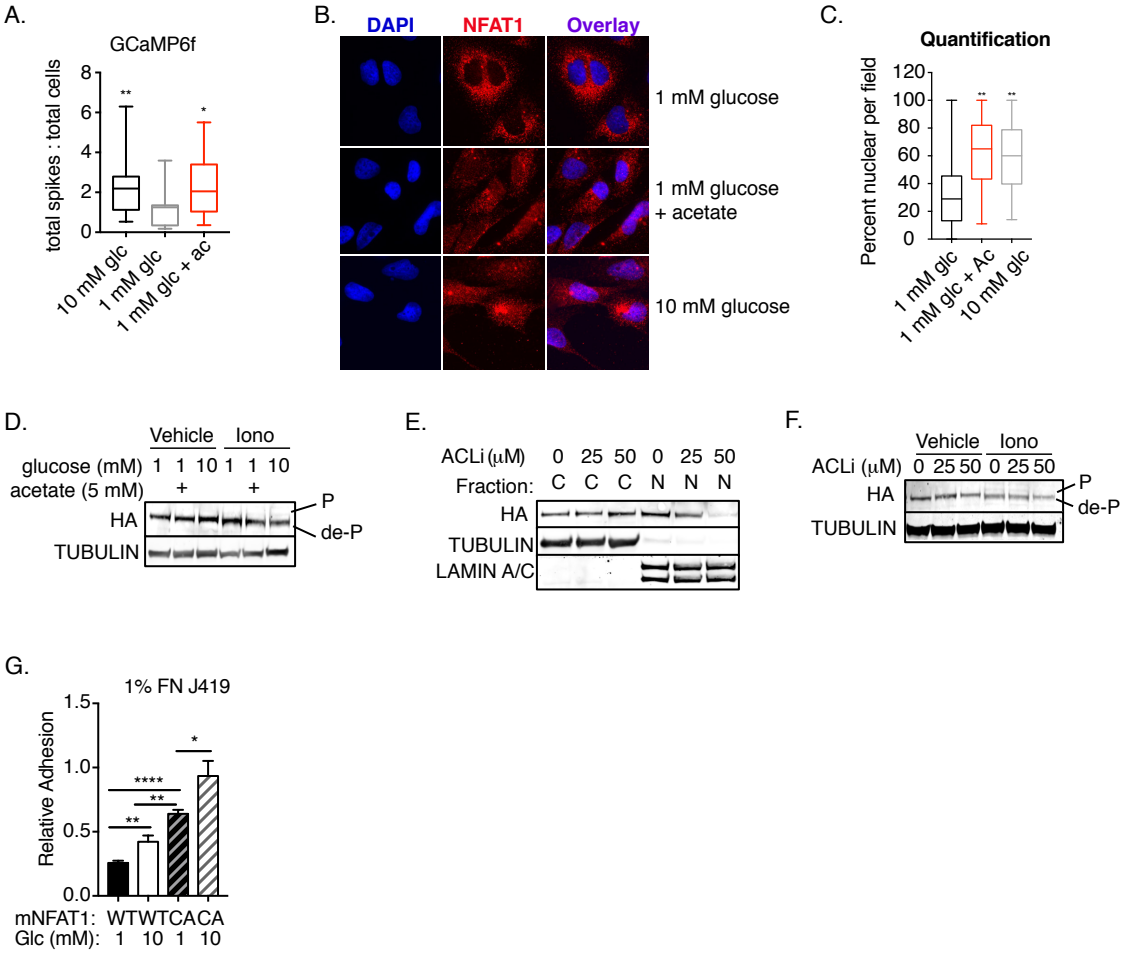

(A) Quantification of fluorescent spikes after nutrient addback. At least 116 cells counted per condition. Blinded scoring of number of spikes per field per cell. **, p<0.01; *,p<0.05. (B) Immunofluorescent detection of endogenous NFAT1 localization in LN229 cells. (C) Quantification of NFAT1 detected in the nucleus as percentage per field. **, p<0.01 (D) Western blot of phosphorylation state of exogenously expressed HA-tagged NFAT1 after 16 hours of treatment followed by 15 minutes of treatment with ionomycin (Iono) or vehicle before harvest. (E) Western blot depicting NFAT1 localization after cellular fractionation. Cells were treated for 24 hours in 10 mM glucose with indicated concentrations of ACLYi or with ethanol vehicle control. (F) Western blot of phosphorylation state of exogenously expressed HA-tagged NFAT1 after 16 hours of treatment in 10 mM glucose and indicated concentrations of ACLYi followed by 15 minutes of treatment with ionomycin or vehicle before harvest. (G) Relative adhesion in LN229 cells stably expressing WT-NFAT1 or CA-NFAT1. *, p<0.05; ** p<0.01; ****, p<0.0001. All panels: mean+/- SEM

Figure 25: PEP concentrations are regulated by glucose and cannot be rescued with acetate under low glucose

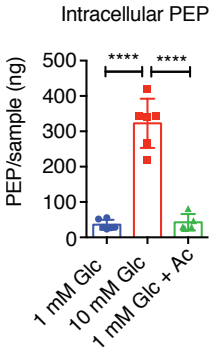

LCMS quantification of phosphoenolpyruvate (PEP). ****, p<0.0001, Mean +/- SD

Figure 26: NFAT1 nuclear localization is dependent on presence of ACLY

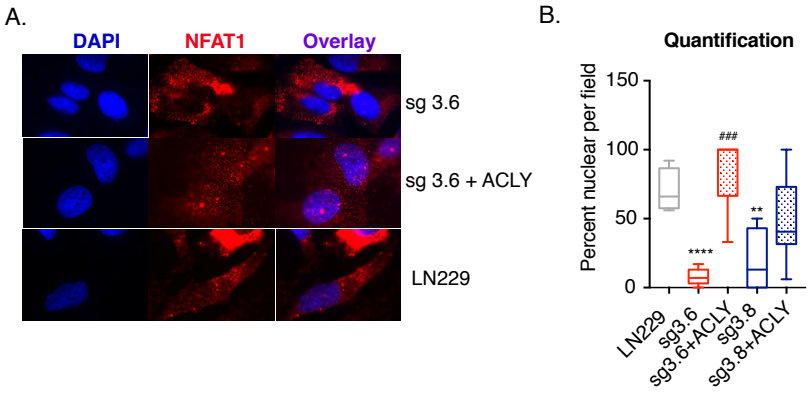

(A) Immunofluorescent detection of endogenous NFAT1 localization in LN229 and LN229 sgACLY cells (clone 3.6) with or without expression of CRISPR resistant mouse ACLY. (B) Quantification of NFAT1 detected in the nucleus as percentage per field in LN229 and LN229 sgACLY cells (clones 3.6 and 3.8). * denotes significance of knockout compared to LN229 (**, p<0.01, ****, p<0.0001). # denotes significance of knockout compared to ACLY addback (###, p<0.001).

4.3 Discussion

A growing body of work demonstrates that metabolism can regulate cellular decisions. These decisions are made in part through the regulation of gene expression. In these studies, we chose to alter glucose and acetate in cell culture media to determine the effects of acetyl-CoA abundance in the cell on the expression of genes involved in cell migration and adhesion in glioblastoma cells. We found that the expression of these genes is in part mediated through the regulation of Ca^{2+}-NFAT1 signaling. While NFAT has been previously shown to be regulated in response to glucose availability (Ho et al., 2015, Koenig et al., 2010, Lawrence et al., 2002), acetyl-CoA as a product of glucose metabolism has not been previously linked to Ca^{2+} homeostasis or NFAT function.

Calcium is a critical signaling molecule that needs to be tightly controlled. In non-excitable cells and in cancer, changes in cytosolic calcium are transient and tend to follow an oscillatory pattern (Dupont et al., 2011). These dynamics are important for signaling and activate important downstream proteins in the nucleus. Both calcium oscillations and NFAT transcription factors have established roles in cancer cell migration and invasion (Qin et al., 2014, Cui et al., 2017). In glioblastoma, Ca2+ oscillations trigger migration by modulating focal adhesion dynamics (Giannone et al., 2002). These calcium oscillations are controlled in part by store-operated calcium channel proteins, STIM1 and Orai1, which were found to be critical for glioblastoma invasion (Motiani et al., 2013). Similarly, TRPC6, a receptor-activated calcium channel in the cell membrane, expression increases under hypoxia and promotes elevated intracellular calcium and NFAT activation; knockdown of TRPC6 or NFAT inhibition suppressed invasive phenotypes in glioblastoma cells (Chigurupati et al., 2010).

Consistently, inhibition of IP3R-mediated Ca2+ release, with caffeine, reduced glioblastoma cell migration and extended survival in a mouse glioblastoma xenograft model (Kang et al., 2010).

The deregulation of calcium oscillations by metabolism is underexplored. The current study identifies that high acetyl-CoA abundance promotes Ca^{2+}-NFAT signaling. Dysfunctional calcium homeostasis is proposed to be associated with metabolic pathological conditions (Arruda and Hotamisligil, 2015), and our data suggests that cancer metabolism can feed forward to promote transient calcium release that can signal downstream to initiate many processes, such as NFAT nuclear localization. NFAT overexpression and aberrant nuclear localization have been reported in other cancers, such as pancreatic cancer (Koenig et al., 2010, Buchholz et al., 2006); thus, it is tempting to speculate that our model may hold true in a broad range of solid tumors with demonstrated Ca2+-NFAT signaling. Future experiments will be needed to elucidate the precise mechanisms through which acetyl-CoA promotes calcium dynamics for NFAT activation.

Acetyl-CoA continues to provide a layer of regulation on epigenetics and gene expression. In establishing acetyl-CoA regulation of glioblastoma cell migration, our study provides a previously unrecognized link between metabolism and calcium homeostasis. We are only beginning to understand how tumor metabolism signals to the cell to control malignant phenotypes.

CHAPTER 5:

CONCLUSIONS/FUTURE DIRECTIONS

5.1 Conclusions

Cancer cells exhibit substantial epigenetic alterations that contribute to the acquisition of all hallmarks of cancer (Jones and Baylin, 2007, Hanahan and Weinberg, 2011). In this thesis, we explored how extensively metabolic reprogramming contribute could contribute to this epigenetic deregulation. Several studies over the past several years provide compelling evidence that acetylation of histones is dependent on the availability of acetyl-CoA [reviewed in (Kinnaird et al., 2016). Prior to the work presented in this thesis, the field of cancer metabolism and epigenetics speculated on the possibility that concentrations of acetyl-CoA could be limiting and the concentrations could impact histone acetylation. In this work, we present evidence that mammalian concentrations of acetyl-CoA are between 6-13 μM in the cell and the ratio of acetyl-CoA:CoA are regulated dynamically by glucose availability, which impacts overall histone acetylation levels.

We further explored the oncogenic control of acetyl-CoA as a major contributor to deregulated global histone acetylation. We found that constitutive activation of the PI3 kinase-AKT pathway promotes elevated histone acetylation, both in vitro in cancer cell lines and in vivo in 2 different mouse models. Remarkably, although histone acetylation levels are regulated by glucose, phosphorylation of ACLY downstream of AKT allows histone acetylation to be sustained during glucose limitation (**Figure 12, Figure 27**). Such a mechanism could potentially enable tumor cells to maintain histone acetylation in a heterogeneous microenvironment. In support of this possibility, global

histone acetylation levels were found to correlate significantly with pAKT(Ser473) in human gliomas and prostate tumors (**Figure 15, Figure 16**).

Secondly, we addressed the impact of acetyl-CoA availability on tumor-promoting phenotypes. In glioblastoma cells, genes favored in the presence of high acetyl-CoA include those with roles in cell cycle, DNA replication, and cell migration (Figure 4). During glucose limitation, supplementing cells with acetate (increasing acetyl-CoA levels) stimulated expression of these genes, promoted migration (**Figure 18**), but did not promote proliferation unless other glucose-dependent metabolites were provided (Figure 4). Thus, acetyl-CoA may provide a pro-growth signal to the cell by regulating relevant gene expression programs. Notably, elevated histone acetylation is observed upon oncogene activation in mice prior to the appearance of tumors (**Figure 8**). Studies exploring the possibility that oncogene-induced metabolic regulation of histone acetylation might promote a favorable epigenetic context for malignant transformation are currently in progress in the lab.

The results from the work in Chapter 3 led us to further investigate mechanisms of acetyl-CoA dependent gene expression. Like the growth-related genes, histone acetylation near the promoter regions of several migration genes were significantly higher under conditions that promoted acetyl-CoA formation (**Figure 5**). But to understand whether other forms of transcriptional regulation are at play, we investigated our acetyl-CoA gene set to uncover potential transcription factors that might control cell migration. Notably, NFAT family proteins were predicted to regulate our gene set (**Figure 22**). Many studies demonstrate NFAT proteins in tumorigenesis and tumor cell migration (Mognol et al., 2016, Muller and Rao, 2010). Furthermore, glioma samples display high levels of NFAT1 nuclear staining (Tie et al., 2013). We discovered that low

acetyl-CoA conditions can reduce NFAT nuclear accumulation and mechanistically, this is through loss of acetyl-CoA regulation of calcium oscillations. Our study points to an undescribed metabolic regulation of NFAT nuclear localization and also connects together previous studies that have implicated acetyl-CoA (Chen et al., 2015), NFAT (Mancini and Toker, 2009), and calcium independently to cell migration (Chen et al., 2013b) (**Figure 28**).

Of note, we find a requirement for ACLY to initiate cell adhesion and migration and provision of acetate in ACLY-deficiency does not rescue adhesion. Others have observed similar phenomena that acetate induction of T cell activation requires ACLY (Balmer et al., 2016). Indeed, when ^{13}C-acetate was monitored in human patients with glioblastoma by ^{13}C- NMR, glioma cells incorporated acetate derived carbons into the TCA cycle metabolites, including citrate. In ACLY-deficient settings, cell proliferation (Zhao et al., 2016) and homologous recombination DNA damage repair (Sivanand et al., 2017), acetate is not able to full compensate for the loss of the phenotype. Reasons for why acetate cannot rescue certain phenotypes under ACLY-deficiency remains to be explored.

Acetyl-CoA and acetylation thus represent crucial components of the cell's nutrient-sensing repertoire. The functional consequences of high acetyl-CoA might be diverse depending on the cell-type and future studies will need to be done to address how broadly the described mechanisms regulate cancer cell phenotypes. Importantly, these studies provide evidence for how nutrient availability is assimilated to coordinate a transcriptional response.

Figure 27: AKT promotes tumor cell histone acetylation

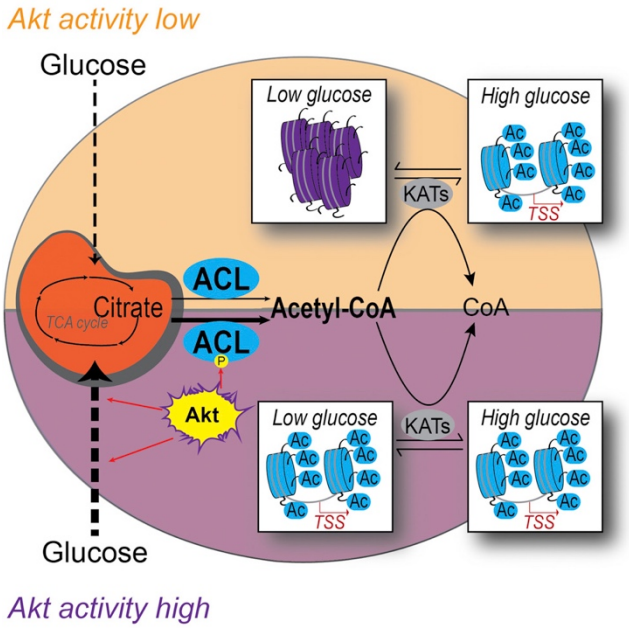

Model for findings in Chapter 3: Oncogenic AKT expression promotes elevated histone acetylation through ACLY phosphorylation, enabling sustained histone acetylation in low glucose.

Figure 28: Acetyl-CoA promotes adhesion and migration through histone acetylation and NFAT1 nuclear localization

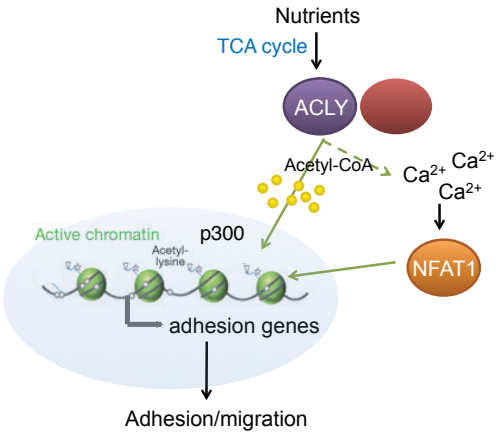

Model for findings in Chapter 4: acetyl-CoA availability via ACLY and ACSS2 increases histone acetylation at adhesion and migration related genes and also increases cytosolic calcium to allow NFAT1 to localize in the nucleus. Collectively, this results in gene expression and migration of glioblastoma cells.

5.2 Future Directions

5.2.1 Acetyl-CoA and organelle calcium-store crosstalk?

Our data points to acetyl-CoA production being upstream of calcium signaling. The addition of ionomycin, an artificial stimulation of calcium release, can rescue adhesion in acetyl-CoA depleted conditions. It remains to be explored how acetyl-CoA communicates with organelles for calcium release into the cytosol. The mitochondria and the endoplasmic reticulum (ER) are two potential sources of intracellular calcium.

Many studies on mitochondria calcium regulation have been linked to cell migration [reviewed in (Paupe and Prudent, 2017)]. Acetate uptake by the cell under low glucose conditions may reduce mitochondria calcium overload. Mitochondrial matrix Ca2+ overload enhances generation of reactive oxygen species, triggers the permeability transition pore, and releases cytochrome c, which ultimately causes cell apoptosis. Notably, calcium is required for proper TCA enzymatic reactions [reviewed in (Denton, 2009)]. Perhaps acetate supplementation supports the balance of calcium in the mitochondria, preventing accumulation of calcium in the mitochondria and presumably more in the cytosol. MICU1 is the molecular gatekeeper preventing mitochondria Ca2+ overload (Mallilankaraman et al., 2012). In endothelial cells, silencing MICU1 impaired cell migration by scratch assay and a basal increase of mitochondrial Ca2+. Experiments designed to test whether MICU1 knockdown impedes acetate rescue of cell migration could help us understand this delicate relationship between acetyl-CoA and mitochondrial calcium.

Alternatively, acetyl-CoA could communicate with the endoplasmic reticulum (ER). This relationship is plausible because: 1) the ER largest store of calcium in the cell and 2) the ER membrane has an acetyl-CoA transporter (AT-1). AT-1 deficient animals develop early onset of neurological problems, suggesting that changes in ER acetyl-CoA homeostasis is linked to disease (Peng et al., 2014). Perhaps nutrient-derived acetyl-CoA is required for rapid nutrient-sensitive acetylation in the ER that allows for release of calcium. Acetyl-proteomics analysis after subcellular fractionation of organelles from cells given a short treatment of U-^{13}C-glucose could help us identify proteins that are acetylated in a nutrient dependent manner and related to calcium regulatory processes.

Notably, it was previously reported in T cells that glycolysis supports calcium signaling through production of PEP, which inhibits the cytosolic calcium uptake transporter sarcoplasmic endoplasmic reticulum calcium antiporter (SERCA) (Ho et al., 2015). PEP is proposed to inhibit SERCA by oxidizing cysteine 675, a known modification that reduces SERCA activity (Sharov et al., 2006). This allows for sustained calcium release (Ho et al., 2015). Similar to PEP, acetate itself might also promote cysteine oxidation on SERCA. We would examine the redox state of the cell under low glucose + acetate conditions to further delineate mechanisms for acetate regulation of calcium. If we see an effect by acetate, knockdown of ACSS1 and/or ACSS2 would further confirm the effects were dependent on acetate derived acetyl-CoA.

5.2.2 Defining nutrient sensitive histone acetylation in glioblastoma

In low glucose conditions, acetyl-CoA levels decrease and become limiting for histone acetylation. Concomitant decreases in expression of pro-growth genes mirror the

reduction in global and promoter-specific histone acetylation. Importantly, supplementation of acetate can rescue intracellular pools of acetyl-CoA, histone acetylation, and restore growth promoting gene expression. These findings suggest that acetyl-CoA provides a layer of regulation of gene expression in tumors. However, whether the histone acetylation occurs at relevant regions of the genome and plays a role in the transcription isn't clear. Determination of the precise location nutrient-sensitive acetylation at a genome-wide level could further inform us of functional consequences of high histone acetylation.

Few studies have completed a full characterization of metabolite availability and paired it with assessment of genome-wide changes. As mentioned in the introduction, histone acetylation in yeast displayed nutrient regulated histone acetylation. Of note, while H3K9ac appeared at promoters concurrently with expression as determined by RNA-seq, H3K14ac and H4K5ac presented at the promoters about an hour before the RNA peak appeared (Kuang et al., 2014), suggesting that different KATs may respond to different levels of acetyl-CoA. In cancer, methionine restriction indeed reduced H3K4me3 globally (Mentch et al., 2015). Pairing the information on H3K4me3 as determined by ChIP-seq to RNA-seq expression data, the authors found that the regions of the genome that responded to methionine corresponded with changes in gene expression from RNA-seq in colon cancer cells. These changes were 2 Kb upstream and downstream of the TSS. However, neither of these studies reported the number of gene promoters that were sensitive and the degree of overlap with changes in gene expression. How much histone acetylation is part of gene regulation versus buffering (McBrian et al., 2013) or storage [reviewed in (Fan et al., 2015)]?

We could contribute to this question through using our glioblastoma cells, where we have already defined a system where acetyl-CoA availability can be controlled. Future work should expand on identifying the genomic regions that are sensitive to acetyl-CoA in this system. Traditional ChIP-seq methods do not allow for direct comparison of signal amplitude between samples. In order to achieve quantitative comparisons of histone acetylation genome-wide, this work should be completed using ChIP-Rx (Orlando et al., 2014), which will identify graded epigenomic changes following treatment. These studies will help us understand the consequences of histone acetylation and understand how transient these programs are.

Furthermore, definition of nutrient sensitive sites on the genome may offer some insight on specificity of glucose versus acetate dependent histone acetylation. It is curious why mammalian cells evolved with the expression of two very important nuclear-cytoplasmic acetyl-CoA producing enzymes, ACLY and ACSS2. As mentioned in the introduction, both enzymes are highly relevant in many different types of cancer and both contribute to histone acetylation under various conditions [reviewed in (Carrer and Wellen, 2015, Kinnaird et al., 2016)]. In fact, nuclear ACSS2 binds near regions of H3K9ac, H5K4ac, and H4K12ac and is required for memory formation in the hippocampus (Mews et al., 2017). Our studies could complement these findings in a cancer setting.

5.2.3 Therapeutic implications

Targeting ACLY will be challenging as cells will likely find alternative sources of acetyl-CoA. As demonstrated in this thesis, under low glucose conditions, acetate can

rescue cell migration. However, it is encouraging that in ACLY-knockout cells, acetate does is not sufficient to rescue adhesion, indicating that there may be conditions that allow for ACLY to be targeted therapeutically. It is possible that development of a better ACLY inhibitor can be used to slow down glioma cell migration in combination with current glioblastoma therapies designed to slow down cell growth. Additionally, targeting NFAT regulated genes related to cell migration may provide another method to target glioblastoma. Lastly, it would be interesting to understand whether therapeutics targeting acetyl-CoA metabolism also impact chromatin modifications and perhaps can be used in combination with current epigenetic therapies.

Table 1: cDNA Primers

ENAH_F	GGACCATCAGGTCGTGATAAA
ENAH_R	CCATACACCTGTCTAGCATCTC
FGF7_F	GGCCTCCATCCCTCTTACTC
FGF7_R	AGCTGCGTGACCTTAGGTGT
ICAM1_F	GTCATCATCACTGTGGTAGC
ICAM1_R	GGCCTGTTGTAGTCTGTATTT
MMP11_F	GGCAGAGGCCCTAAAGGTAT
MMP11 _R	CGAAGTCGATCATGATGTCAG
VCAN_F	GGCACCTGTTATCCTACTGAAA
VCAN_R	GCTCCATTACGACAGGGATTAG
ITGA2B_F	CCCTGGAAGAAGATGATGAAGAG
ITGA2B_R	GGAGGCAACTTGTTGGAGAA
ITGA4_F	GCCACCCTGAGTCAGTAAATAG
ITGA4_R	CTGGAACTTCCTTGCCCTTAT
ITGA9_F	ACCAGGAATTTCTTGCCTAAC
ITGA9_R	CTGTGTTCAGCAGCATGTA
PDGFRA_F	GAAGAAGAGAGCTCCGATGTG
PDGFRA_R	TAGCAAGTGTACAACCCTGTG
MCAM_F	CTGTTGGAGACAGGTGTTGAA
MCAM_R	CTGGTGTGAGGGTGGTTAAAT
PDK3_F	ATACCAACCGCATCTCTTTC
PDK3_R	GGTGGGATCGATACTTCCTA
ZMYND8_F	CGCAGGACACATCAACAA
ZMYND8_R	GTGAGTGGCTGCTTCATATAG
PTCH1_F	GTTGTGGGCCTCCTCATATT
PTCH1_R	GACTTACTCGTCCTCCAACTTC
PLAC1_F	GCCCAGAAGGATGAGAAATG
PLAC1_R	ACCTGGGTATGCTCTTCTT
HAND2_F	TACATCGCCTACCTCATGGA
HAND2_R	TCCTTCTTCCTCTTCTCCTCTT
CAMK2G_F	CGCAGGTGTGTGAAGAAA
CAMK2G_R	CGTTCTAGTTTCTGGTGATCC

RPL19_F	CAAGAAGGAGGAGATCATCAAG
RPL19_R	ATCACAGAGGCCAGTATGTA
PTGS2_F	TTGACAGTCCACCAACTTAC
PTGS2_R	GGAGGAAGGGCTCTAGTATAA
NFATC2_F	GTGGCAGAATCGTCTCTTTAC
NFATC2_R	GCTGTCTGTGTCTTGTCTTT
GPC6_F	GTCAGCATTACCCTACACTATC
GPC6_R	AGGCAAGTATCTGGCTTTG
E2F2_F	TTTACCTCCTGAGCGAGTCA
E2F2_R	AGCACGTTGGTGATGTCATAG
MCM10_F	CGGAACAAACCTAGTGGGATAA
MCM10_R	AGAAGGCTTCCACACAGATG
SERPINA5_F	TGGTCCCACACTTATCAGCA
SERPINA5_R	GTCCCAATGTCACACAGCAC

BIBLIOGRAPHY

ALBAUGH, B. N., ARNOLD, K. M. & DENU, J. M. 2011. KAT(ching) metabolism by the tail: insight into the links between lysine acetyltransferases and metabolism. *Chembiochem : a European journal of chemical biology,* 12**,** 290-8.

ARRUDA, A. P. & HOTAMISLIGIL, G. S. 2015. Calcium Homeostasis and Organelle Function in the Pathogenesis of Obesity and Diabetes. *Cell Metab,* 22**,** 381-97.

AZAD, N., ZAHNOW, C. A., RUDIN, C. M. & BAYLIN, S. B. 2013. The future of epigenetic therapy in solid tumours--lessons from the past. *Nature reviews. Clinical oncology,* 10**,** 256-66.

BADRAN, B. M., WOLINSKY, S. M., BURNY, A. & WILLARD-GALLO, K. E. 2002. Identification of three NFAT binding motifs in the 5'-upstream region of the human CD3gamma gene that differentially bind NFATc1, NFATc2, and NF-kappa B p50. *J Biol Chem,* 277**,** 47136-48.

BALMER, M. L., MA, E. H., BANTUG, G. R., GRAHLERT, J., PFISTER, S., GLATTER, T., JAUCH, A., DIMELOE, S., SLACK, E., DEHIO, P., KRZYZANIAK, M. A., KING, C. G., BURGENER, A. V., FISCHER, M., DEVELIOGLU, L., BELLE, R., RECHER, M., BONILLA, W. V., MACPHERSON, A. J., HAPFELMEIER, S., JONES, R. G. & HESS, C. 2016. Memory CD8(+) T Cells Require Increased Concentrations of Acetate Induced by Stress for Optimal Function. *Immunity,* 44**,** 1312-24.

BARNEY, L. E., DANDLEY, E. C., JANSEN, L. E., REICH, N. G., MERCURIO, A. M. & PEYTON, S. R. 2015. A cell-ECM screening method to predict breast cancer metastasis. *Integr Biol (Camb),* 7**,** 198-212.

BASU, S. S. & BLAIR, I. A. 2012. SILEC: a protocol for generating and using isotopically labeled coenzyme A mass spectrometry standards. *Nature protocols,* 7**,** 1-12.

BASU, S. S., MESAROS, C., GELHAUS, S. L. & BLAIR, I. A. 2011. Stable isotope labeling by essential nutrients in cell culture for preparation of labeled coenzyme A and its thioesters. *Analytical chemistry,* 83**,** 1363-9.

BAUER, D. E., HATZIVASSILIOU, G., ZHAO, F., ANDREADIS, C. & THOMPSON, C. B. 2005. ATP citrate lyase is an important component of cell growth and transformation. *Oncogene,* 24**,** 6314-22.

BERGER, S. L. 2007. The complex language of chromatin regulation during transcription. *Nature,* 447**,** 407-12.

BERGER, S. L. & SASSONE-CORSI, P. 2016. Metabolic Signaling to Chromatin. *Cold Spring Harb Perspect Biol,* 8.

BIANCO-MIOTTO, T., CHIAM, K., BUCHANAN, G., JINDAL, S., DAY, T. K., THOMAS, M., PICKERING, M. A., O'LOUGHLIN, M. A., RYAN, N. K., RAYMOND, W. A., HORVATH, L. G., KENCH, J. G., STRICKER, P. D., MARSHALL, V. R., SUTHERLAND, R. L., HENSHALL, S. M., GERALD, W. L., SCHER, H. I., RISBRIDGER, G. P., CLEMENTS, J. A., BUTLER, L. M., TILLEY, W. D., HORSFALL, D. J. & RICCIARDELLI, C. 2010. Global levels of specific histone modifications and an epigenetic gene signature predict prostate cancer progression and development. *Cancer epidemiology, biomarkers & prevention : a publication of the American Association for Cancer Research, cosponsored by the American Society of Preventive Oncology,* 19**,** 2611-22.

BUCHHOLZ, M., SCHATZ, A., WAGNER, M., MICHL, P., LINHART, T., ADLER, G., GRESS, T. M. & ELLENRIEDER, V. 2006. Overexpression of c-myc in pancreatic cancer caused by ectopic activation of NFATc1 and the Ca2+/calcineurin signaling pathway. *EMBO J,* 25**,** 3714-24.

BYON, C. H., HARDY, R. W., REN, C., PONNAZHAGAN, S., WELCH, D. R., MCDONALD, J. M. & CHEN, Y. 2009. Free fatty acids enhance breast cancer cell migration through plasminogen activator inhibitor-1 and SMAD4. *Lab Invest,* 89**,** 1221-8.

CAI, L., SUTTER, B. M., LI, B. & TU, B. P. 2011. Acetyl-CoA induces cell growth and proliferation by promoting the acetylation of histones at growth genes. *Mol Cell,* 42**,** 426-37.

CARRER, A. & WELLEN, K. E. 2015. Metabolism and epigenetics: a link cancer cells exploit. *Curr Opin Biotechnol,* 34**,** 23-9.

CHEN, R., XU, M., NAGATI, J. S., HOGG, R. T., DAS, A., GERARD, R. D. & GARCIA, J. A. 2015. The acetate/ACSS2 switch regulates HIF-2 stress signaling in the tumor cell microenvironment. *PLoS One,* 10**,** e0116515.

CHEN, T. W., WARDILL, T. J., SUN, Y., PULVER, S. R., RENNINGER, S. L., BAOHAN, A., SCHREITER, E. R., KERR, R. A., ORGER, M. B., JAYARAMAN, V., LOOGER, L. L., SVOBODA, K. & KIM, D. S. 2013a. Ultrasensitive fluorescent proteins for imaging neuronal activity. *Nature,* 499**,** 295-300.

CHEN, Y. F., CHEN, Y. T., CHIU, W. T. & SHEN, M. R. 2013b. Remodeling of calcium signaling in tumor progression. *J Biomed Sci,* 20**,** 23.

CHERVONA, Y. & COSTA, M. 2012. Histone modifications and cancer: biomarkers of prognosis? *Am J Cancer Res,* 2**,** 589-97.

CHIGURUPATI, S., VENKATARAMAN, R., BARRERA, D., NAGANATHAN, A., MADAN, M., PAUL, L., PATTISAPU, J. V., KYRIAZIS, G. A., SUGAYA, K., BUSHNEV, S., LATHIA, J. D., RICH, J. N. & CHAN, S. L. 2010. Receptor channel TRPC6 is a key mediator of Notch-driven glioblastoma growth and invasiveness. *Cancer Res,* 70**,** 418-27.

CHOCARRO-CALVO, A., GARCIA-MARTINEZ, J. M., ARDILA-GONZALEZ, S., DE LA VIEJA, A. & GARCIA-JIMENEZ, C. 2013. Glucose-induced beta-catenin acetylation enhances Wnt signaling in cancer. *Mol Cell,* 49**,** 474-86.

CHOUDHARY, C., KUMAR, C., GNAD, F., NIELSEN, M. L., REHMAN, M., WALTHER, T. C., OLSEN, J. V. & MANN, M. 2009. Lysine acetylation targets protein complexes and co-regulates major cellular functions. *Science,* 325**,** 834-40.

CHYPRE, M., ZAIDI, N. & SMANS, K. 2012. ATP-citrate lyase: a mini-review. *Biochem Biophys Res Commun,* 422**,** 1-4.

CLUNTUN, A. A., HUANG, H., DAI, L., LIU, X., ZHAO, Y. & LOCASALE, J. W. 2015. The rate of glycolysis quantitatively mediates specific histone acetylation sites. *Cancer Metab,* 3**,** 10.

COMERFORD, S. A., HUANG, Z., DU, X., WANG, Y., CAI, L., WITKIEWICZ, A. K., WALTERS, H., TANTAWY, M. N., FU, A., MANNING, H. C., HORTON, J. D., HAMMER, R. E., MCKNIGHT, S. L. & TU, B. P. 2014. Acetate dependence of tumors. *Cell,* 159**,** 1591-602.

COVARRUBIAS, A. J., AKSOYLAR, H. I., YU, J., SNYDER, N. W., WORTH, A. J., IYER, S. S., WANG, J., BEN-SAHRA, I., BYLES, V., POLYNNE-STAPORNKUL, T., ESPINOSA, E. C., LAMMING, D., MANNING, B. D., ZHANG, Y., BLAIR, I. A. & HORNG, T. 2016. Akt-mTORC1 signaling regulates Acly to integrate metabolic input to control of macrophage activation. *Elife,* 5.

CUI, C., MERRITT, R., FU, L. & PAN, Z. 2017. Targeting calcium signaling in cancer therapy. *Acta Pharm Sin B,* 7**,** 3-17.

DAWSON, M. A. & KOUZARIDES, T. 2012. Cancer epigenetics: from mechanism to therapy. *Cell,* 150**,** 12-27.

DEBERARDINIS, R. J., LUM, J. J., HATZIVASSILIOU, G. & THOMPSON, C. B. 2008. The biology of cancer: metabolic reprogramming fuels cell growth and proliferation. *Cell Metab,* 7**,** 11-20.

DENTON, R. M. 2009. Regulation of mitochondrial dehydrogenases by calcium ions. *Biochim Biophys Acta,* 1787**,** 1309-16.

DONOHOE, D. R., COLLINS, L. B., WALI, A., BIGLER, R., SUN, W. & BULTMAN, S. J. 2012. The Warburg effect dictates the mechanism of butyrate-mediated histone acetylation and cell proliferation. *Molecular cell,* 48**,** 612-26.

DUPONT, G., COMBETTES, L., BIRD, G. S. & PUTNEY, J. W. 2011. Calcium oscillations. *Cold Spring Harb Perspect Biol,* 3.

EISENBERG, T., SCHROEDER, S., ANDRYUSHKOVA, A., PENDL, T., KUTTNER, V., BHUKEL, A., MARINO, G., PIETROCOLA, F., HARGER, A., ZIMMERMANN, A.,

MOUSTAFA, T., SPRENGER, A., JANY, E., BUTTNER, S., CARMONA-GUTIERREZ, D., RUCKENSTUHL, C., RING, J., REICHELT, W., SCHIMMEL, K., LEEB, T., MOSER, C., SCHATZ, S., KAMOLZ, L. P., MAGNES, C., SINNER, F., SEDEJ, S., FROHLICH, K. U., JUHASZ, G., PIEBER, T. R., DENGJEL, J., SIGRIST, S. J., KROEMER, G. & MADEO, F. 2014. Nucleocytosolic depletion of the energy metabolite acetyl-coenzyme a stimulates autophagy and prolongs lifespan. *Cell metabolism,* 19**,** 431-44.

ELSTROM, R. L., BAUER, D. E., BUZZAI, M., KARNAUSKAS, R., HARRIS, M. H., PLAS, D. R., ZHUANG, H., CINALLI, R. M., ALAVI, A., RUDIN, C. M. & THOMPSON, C. B. 2004a. Akt stimulates aerobic glycolysis in cancer cells. *Cancer research,* 64**,** 3892-9.

ELSTROM, R. L., BAUER, D. E., BUZZAI, M., KARNAUSKAS, R., HARRIS, M. H., PLAS, D. R., ZHUANG, H., CINALLI, R. M., ALAVI, A., RUDIN, C. M. & THOMPSON, C. B. 2004b. Akt stimulates aerobic glycolysis in cancer cells. *Cancer Res,* 64**,** 3892-9.

EVERTTS, A. G., ZEE, B. M., DIMAGGIO, P. A., GONZALES-COPE, M., COLLER, H. A. & GARCIA, B. A. 2013. Quantitative dynamics of the link between cellular metabolism and histone acetylation. *The Journal of biological chemistry,* 288**,** 12142-51.

FAN, J., KRAUTKRAMER, K. A., FELDMAN, J. L. & DENU, J. M. 2015. Metabolic regulation of histone post-translational modifications. *ACS Chem Biol,* 10**,** 95-108.

FENDT, S. M., BELL, E. L., KEIBLER, M. A., OLENCHOCK, B. A., MAYERS, J. R., WASYLENKO, T. M., VOKES, N. I., GUARENTE, L., VANDER HEIDEN, M. G. & STEPHANOPOULOS, G. 2013. Reductive glutamine metabolism is a function of the alpha-ketoglutarate to citrate ratio in cells. *Nature communications,* 4**,** 2236.

FRIIS, R. M., WU, B. P., REINKE, S. N., HOCKMAN, D. J., SYKES, B. D. & SCHULTZ, M. C. 2009. A glycolytic burst drives glucose induction of global histone acetylation by picNuA4 and SAGA. *Nucleic Acids Res,* 37**,** 3969-80.

FURNARI, F. B., FENTON, T., BACHOO, R. M., MUKASA, A., STOMMEL, J. M., STEGH, A., HAHN, W. C., LIGON, K. L., LOUIS, D. N., BRENNAN, C., CHIN, L., DEPINHO, R. A. & CAVENEE, W. K. 2007. Malignant astrocytic glioma: genetics, biology, and paths to treatment. *Genes Dev,* 21**,** 2683-710.

GAMEIRO, P. A., YANG, J., METELO, A. M., PEREZ-CARRO, R., BAKER, R., WANG, Z., ARREOLA, A., RATHMELL, W. K., OLUMI, A., LOPEZ-LARRUBIA, P., STEPHANOPOULOS, G. & ILIOPOULOS, O. 2013. In vivo HIF-mediated reductive carboxylation is regulated by citrate levels and sensitizes VHL-deficient cells to glutamine deprivation. *Cell metabolism,* 17**,** 372-85.

GAO, X., LIN, S. H., REN, F., LI, J. T., CHEN, J. J., YAO, C. B., YANG, H. B., JIANG, S. X., YAN, G. Q., WANG, D., WANG, Y., LIU, Y., CAI, Z., XU, Y. Y., CHEN, J., YU, W., YANG, P. Y. & LEI, Q. Y. 2016. Acetate functions as an epigenetic metabolite to promote lipid synthesis under hypoxia. *Nat Commun,* 7**,** 11960.

GARCIA-RODRIGUEZ, C. & RAO, A. 1998. Nuclear factor of activated T cells (NFAT)-dependent transactivation regulated by the coactivators p300/CREB-binding protein (CBP). *J Exp Med,* 187**,** 2031-6.

GIANNONE, G., RONDE, P., GAIRE, M., HAIECH, J. & TAKEDA, K. 2002. Calcium oscillations trigger focal adhesion disassembly in human U87 astrocytoma cells. *J Biol Chem,* 277**,** 26364-71.

GOLDBERG, A. D., ALLIS, C. D. & BERNSTEIN, E. 2007. Epigenetics: a landscape takes shape. *Cell,* 128**,** 635-8.

GRONROOS, E., HELLMAN, U., HELDIN, C. H. & ERICSSON, J. 2002. Control of Smad7 stability by competition between acetylation and ubiquitination. *Mol Cell,* 10**,** 483-93.

GUAN, K. L. & XIONG, Y. 2011. Regulation of intermediary metabolism by protein acetylation. *Trends in biochemical sciences,* 36**,** 108-16.

GUNTHER, E. J., BELKA, G. K., WERTHEIM, G. B., WANG, J., HARTMAN, J. L., BOXER, R. B. & CHODOSH, L. A. 2002. A novel doxycycline-inducible system for the transgenic analysis of mammary gland biology. *FASEB journal : official publication of the Federation of American Societies for Experimental Biology,* 16**,** 283-92.

HALLOWS, W. C., LEE, S. & DENU, J. M. 2006. Sirtuins deacetylate and activate mammalian acetyl-CoA synthetases. *Proc Natl Acad Sci U S A,* 103**,** 10230-5.

HANAHAN, D. & WEINBERG, R. A. 2011. Hallmarks of cancer: the next generation. *Cell,* 144**,** 646-74.

HATZIVASSILIOU, G., ZHAO, F., BAUER, D. E., ANDREADIS, C., SHAW, A. N., DHANAK, D., HINGORANI, S. R., TUVESON, D. A. & THOMPSON, C. B. 2005. ATP citrate lyase inhibition can suppress tumor cell growth. *Cancer Cell,* 8**,** 311-21.

HO, P. C., BIHUNIAK, J. D., MACINTYRE, A. N., STARON, M., LIU, X., AMEZQUITA, R., TSUI, Y. C., CUI, G., MICEVIC, G., PERALES, J. C., KLEINSTEIN, S. H., ABEL, E. D., INSOGNA, K. L., FESKE, S., LOCASALE, J. W., BOSENBERG, M. W., RATHMELL, J. C. & KAECH, S. M. 2015. Phosphoenolpyruvate Is a Metabolic Checkpoint of Anti-tumor T Cell Responses. *Cell,* 162**,** 1217-28.

HOUTKOOPER, R. H., PIRINEN, E. & AUWERX, J. 2012. Sirtuins as regulators of metabolism and healthspan. *Nat Rev Mol Cell Biol,* 13**,** 225-38.

JAENISCH, R. & BIRD, A. 2003. Epigenetic regulation of gene expression: how the genome integrates intrinsic and environmental signals. *Nat Genet,* 33 Suppl, 245-54.

JAIN, M., NILSSON, R., SHARMA, S., MADHUSUDHAN, N., KITAMI, T., SOUZA, A. L., KAFRI, R., KIRSCHNER, M. W., CLISH, C. B. & MOOTHA, V. K. 2012. Metabolite profiling identifies a key role for glycine in rapid cancer cell proliferation. *Science,* 336, 1040-4.

JENUWEIN, T. & ALLIS, C. D. 2001. Translating the histone code. *Science,* 293, 1074-80.

JHANWAR-UNIYAL, M., LABAGNARA, M., FRIEDMAN, M., KWASNICKI, A. & MURALI, R. 2015. Glioblastoma: molecular pathways, stem cells and therapeutic targets. *Cancers (Basel),* 7, 538-55.

JONES, P. A. & BAYLIN, S. B. 2007. The epigenomics of cancer. *Cell,* 128, 683-92.

JONES, P. A., ISSA, J. P. & BAYLIN, S. 2016. Targeting the cancer epigenome for therapy. *Nat Rev Genet,* 17, 630-41.

KAELIN, W. G., JR. & MCKNIGHT, S. L. 2013. Influence of metabolism on epigenetics and disease. *Cell,* 153, 56-69.

KANG, S. S., HAN, K. S., KU, B. M., LEE, Y. K., HONG, J., SHIN, H. Y., ALMONTE, A. G., WOO, D. H., BRAT, D. J., HWANG, E. M., YOO, S. H., CHUNG, C. K., PARK, S. H., PAEK, S. H., ROH, E. J., LEE, S. J., PARK, J. Y., TRAYNELIS, S. F. & LEE, C. J. 2010. Caffeine-mediated inhibition of calcium release channel inositol 1,4,5-trisphosphate receptor subtype 3 blocks glioblastoma invasion and extends survival. *Cancer Res,* 70, 1173-83.

KATADA, S., IMHOF, A. & SASSONE-CORSI, P. 2012. Connecting threads: epigenetics and metabolism. *Cell,* 148, 24-8.

KILLIAN, J. K., KIM, S. Y., MIETTINEN, M., SMITH, C., MERINO, M., TSOKOS, M., QUEZADO, M., SMITH, W. I., JR., JAHROMI, M. S., XEKOUKI, P., SZAREK, E., WALKER, R. L., LASOTA, J., RAFFELD, M., KLOTZLE, B., WANG, Z., JONES, L., ZHU, Y., WANG, Y., WATERFALL, J. J., O'SULLIVAN, M. J., BIBIKOVA, M., PACAK, K., STRATAKIS, C., JANEWAY, K. A., SCHIFFMAN, J. D., FAN, J. B., HELMAN, L. & MELTZER, P. S. 2013. Succinate dehydrogenase mutation underlies global epigenomic divergence in gastrointestinal stromal tumor. *Cancer discovery,* 3, 648-57.

KIM, S. C., SPRUNG, R., CHEN, Y., XU, Y., BALL, H., PEI, J., CHENG, T., KHO, Y., XIAO, H., XIAO, L., GRISHIN, N. V., WHITE, M., YANG, X. J. & ZHAO, Y. 2006. Substrate and functional diversity of lysine acetylation revealed by a proteomics survey. *Mol Cell,* 23, 607-18.

KINNAIRD, A., ZHAO, S., WELLEN, K. E. & MICHELAKIS, E. D. 2016. Metabolic control of epigenetics in cancer. *Nat Rev Cancer,* 16**,** 694-707.

KOENIG, A., LINHART, T., SCHLENGEMANN, K., REUTLINGER, K., WEGELE, J., ADLER, G., SINGH, G., HOFMANN, L., KUNSCH, S., BUCH, T., SCHAFER, E., GRESS, T. M., FERNANDEZ-ZAPICO, M. E. & ELLENRIEDER, V. 2010. NFAT-induced histone acetylation relay switch promotes c-Myc-dependent growth in pancreatic cancer cells. *Gastroenterology,* 138**,** 1189-99 e1-2.

KUANG, Z., CAI, L., ZHANG, X., JI, H., TU, B. P. & BOEKE, J. D. 2014. High-temporal-resolution view of transcription and chromatin states across distinct metabolic states in budding yeast. *Nat Struct Mol Biol,* 21**,** 854-63.

KURDISTANI, S. K. 2007. Histone modifications as markers of cancer prognosis: a cellular view. *Br J Cancer,* 97**,** 1-5.

LANGER, M. R., FRY, C. J., PETERSON, C. L. & DENU, J. M. 2002. Modulating acetyl-CoA binding in the GCN5 family of histone acetyltransferases. *The Journal of biological chemistry,* 277**,** 27337-44.

LAWRENCE, M. C., BHATT, H. S. & EASOM, R. A. 2002. NFAT regulates insulin gene promoter activity in response to synergistic pathways induced by glucose and glucagon-like peptide-1. *Diabetes,* 51**,** 691-8.

LEE, J. V., CARRER, A., SHAH, S., SNYDER, N. W., WEI, S., VENNETI, S., WORTH, A. J., YUAN, Z. F., LIM, H. W., LIU, S., JACKSON, E., AIELLO, N. M., HAAS, N. B., REBBECK, T. R., JUDKINS, A., WON, K. J., CHODOSH, L. A., GARCIA, B. A., STANGER, B. Z., FELDMAN, M. D., BLAIR, I. A. & WELLEN, K. E. 2014. Akt-dependent metabolic reprogramming regulates tumor cell histone acetylation. *Cell Metab,* 20**,** 306-319.

LETOUZE, E., MARTINELLI, C., LORIOT, C., BURNICHON, N., ABERMIL, N., OTTOLENGHI, C., JANIN, M., MENARA, M., NGUYEN, A. T., BENIT, P., BUFFET, A., MARCAILLOU, C., BERTHERAT, J., AMAR, L., RUSTIN, P., DE REYNIES, A., GIMENEZ-ROQUEPLO, A. P. & FAVIER, J. 2013. SDH mutations establish a hypermethylator phenotype in paraganglioma. *Cancer cell,* 23**,** 739-52.

LI, H., WITTWER, T., WEBER, A., SCHNEIDER, H., MORENO, R., MAINE, G. N., KRACHT, M., SCHMITZ, M. L. & BURSTEIN, E. 2012. Regulation of NF-kappaB activity by competition between RelA acetylation and ubiquitination. *Oncogene,* 31**,** 611-23.

LI, M., LUO, J., BROOKS, C. L. & GU, W. 2002. Acetylation of p53 inhibits its ubiquitination by Mdm2. *J Biol Chem,* 277**,** 50607-11.

LI, X., YU, W., QIAN, X., XIA, Y., ZHENG, Y., LEE, J. H., LI, W., LYU, J., RAO, G., ZHANG, X., QIAN, C. N., ROZEN, S. G., JIANG, T. & LU, Z. 2017. Nucleus-

Translocated ACSS2 Promotes Gene Transcription for Lysosomal Biogenesis and Autophagy. *Mol Cell,* 66**,** 684-697 e9.

LINO, M. M. & MERLO, A. 2011. PI3Kinase signaling in glioblastoma. *Journal of neuro-oncology,* 103**,** 417-27.

LONDONO GENTILE, T., LU, C., LODATO, P. M., TSE, S., OLEJNICZAK, S. H., WITZE, E. S., THOMPSON, C. B. & WELLEN, K. E. 2013. DNMT1 Is Regulated by ATP-Citrate Lyase and Maintains Methylation Patterns during Adipocyte Differentiation. *Molecular and cellular biology,* 33**,** 3864-78.

LOSMAN, J. A. & KAELIN, W. G., JR. 2013. What a difference a hydroxyl makes: mutant IDH, (R)-2-hydroxyglutarate, and cancer. *Genes & development,* 27**,** 836-52.

LU, C. & THOMPSON, C. B. 2012a. Metabolic regulation of epigenetics. *Cell metabolism,* 16**,** 9-17.

LU, C. & THOMPSON, C. B. 2012b. Metabolic regulation of epigenetics. *Cell Metab,* 16**,** 9-17.

LU, C., WARD, P. S., KAPOOR, G. S., ROHLE, D., TURCAN, S., ABDEL-WAHAB, O., EDWARDS, C. R., KHANIN, R., FIGUEROA, M. E., MELNICK, A., WELLEN, K. E., O'ROURKE, D. M., BERGER, S. L., CHAN, T. A., LEVINE, R. L., MELLINGHOFF, I. K. & THOMPSON, C. B. 2012. IDH mutation impairs histone demethylation and results in a block to cell differentiation. *Nature,* 483**,** 474-8.

LUO, J., MANNING, B. D. & CANTLEY, L. C. 2003. Targeting the PI3K-Akt pathway in human cancer: rationale and promise. *Cancer Cell,* 4**,** 257-62.

LUO, W. & SEMENZA, G. L. 2012. Emerging roles of PKM2 in cell metabolism and cancer progression. *Trends in endocrinology and metabolism: TEM,* 23**,** 560-6.

MALLILANKARAMAN, K., DOONAN, P., CARDENAS, C., CHANDRAMOORTHY, H. C., MULLER, M., MILLER, R., HOFFMAN, N. E., GANDHIRAJAN, R. K., MOLGO, J., BIRNBAUM, M. J., ROTHBERG, B. S., MAK, D. O., FOSKETT, J. K. & MADESH, M. 2012. MICU1 is an essential gatekeeper for MCU-mediated mitochondrial Ca(2+) uptake that regulates cell survival. *Cell,* 151**,** 630-44.

MANCINI, M. & TOKER, A. 2009. NFAT proteins: emerging roles in cancer progression. *Nat Rev Cancer,* 9**,** 810-20.

MARINO, G., PIETROCOLA, F., EISENBERG, T., KONG, Y., MALIK, S. A., ANDRYUSHKOVA, A., SCHROEDER, S., PENDL, T., HARGER, A., NISO-SANTANO, M., ZAMZAMI, N., SCOAZEC, M., DURAND, S., ENOT, D. P., FERNANDEZ, A. F., MARTINS, I., KEPP, O., SENOVILLA, L., BAUVY, C., MORSELLI, E., VACCHELLI, E., BENNETZEN, M., MAGNES, C., SINNER, F., PIEBER, T., LOPEZ-OTIN, C., MAIURI, M. C., CODOGNO, P., ANDERSEN, J. S.,

HILL, J. A., MADEO, F. & KROEMER, G. 2014. Regulation of autophagy by cytosolic acetyl-coenzyme A. *Molecular cell,* 53**,** 710-25.

MARTINEZ-PASTOR, B., COSENTINO, C. & MOSTOSLAVSKY, R. 2013. A tale of metabolites: the cross-talk between chromatin and energy metabolism. *Cancer Discov,* 3**,** 497-501.

MASHIMO, T., PICHUMANI, K., VEMIREDDY, V., HATANPAA, K. J., SINGH, D. K., SIRASANAGANDLA, S., NANNEPAGA, S., PICCIRILLO, S. G., KOVACS, Z., FOONG, C., HUANG, Z., BARNETT, S., MICKEY, B. E., DEBERARDINIS, R. J., TU, B. P., MAHER, E. A. & BACHOO, R. M. 2014. Acetate is a bioenergetic substrate for human glioblastoma and brain metastases. *Cell,* 159**,** 1603-14.

MCBRIAN, M. A., BEHBAHAN, I. S., FERRARI, R., SU, T., HUANG, T. W., LI, K., HONG, C. S., CHRISTOFK, H. R., VOGELAUER, M., SELIGSON, D. B. & KURDISTANI, S. K. 2013. Histone acetylation regulates intracellular pH. *Mol Cell,* 49**,** 310-21.

MENTCH, S. J., MEHRMOHAMADI, M., HUANG, L., LIU, X., GUPTA, D., MATTOCKS, D., GOMEZ PADILLA, P., ABLES, G., BAMMAN, M. M., THALACKER-MERCER, A. E., NICHENAMETLA, S. N. & LOCASALE, J. W. 2015. Histone Methylation Dynamics and Gene Regulation Occur through the Sensing of One-Carbon Metabolism. *Cell Metab,* 22**,** 861-73.

METALLO, C. M. & VANDER HEIDEN, M. G. 2010. Metabolism strikes back: metabolic flux regulates cell signaling. *Genes Dev,* 24**,** 2717-22.

MEWS, P., DONAHUE, G., DRAKE, A. M., LUCZAK, V., ABEL, T. & BERGER, S. L. 2017. Acetyl-CoA synthetase regulates histone acetylation and hippocampal memory. *Nature,* 546**,** 381-386.

MIGITA, T., NARITA, T., NOMURA, K., MIYAGI, E., INAZUKA, F., MATSUURA, M., USHIJIMA, M., MASHIMA, T., SEIMIYA, H., SATOH, Y., OKUMURA, S., NAKAGAWA, K. & ISHIKAWA, Y. 2008. ATP citrate lyase: activation and therapeutic implications in non-small cell lung cancer. *Cancer research,* 68**,** 8547-54.

MOGNOL, G. P., CARNEIRO, F. R., ROBBS, B. K., FAGET, D. V. & VIOLA, J. P. 2016. Cell cycle and apoptosis regulation by NFAT transcription factors: new roles for an old player. *Cell Death Dis,* 7**,** e2199.

MOOTHA, V. K., LINDGREN, C. M., ERIKSSON, K. F., SUBRAMANIAN, A., SIHAG, S., LEHAR, J., PUIGSERVER, P., CARLSSON, E., RIDDERSTRALE, M., LAURILA, E., HOUSTIS, N., DALY, M. J., PATTERSON, N., MESIROV, J. P., GOLUB, T. R., TAMAYO, P., SPIEGELMAN, B., LANDER, E. S., HIRSCHHORN, J. N., ALTSHULER, D. & GROOP, L. C. 2003. PGC-1alpha-responsive genes involved in oxidative phosphorylation are coordinately downregulated in human diabetes. *Nat Genet,* 34**,** 267-73.

MORENO-SANCHEZ, R., RODRIGUEZ-ENRIQUEZ, S., MARIN-HERNANDEZ, A. & SAAVEDRA, E. 2007. Energy metabolism in tumor cells. *FEBS J,* 274**,** 1393-418.

MORRIS, J. P. T., WANG, S. C. & HEBROK, M. 2010. KRAS, Hedgehog, Wnt and the twisted developmental biology of pancreatic ductal adenocarcinoma. *Nature reviews. Cancer,* 10**,** 683-95.

MOTIANI, R. K., HYZINSKI-GARCIA, M. C., ZHANG, X., HENKEL, M. M., ABDULLAEV, I. F., KUO, Y. H., MATROUGUI, K., MONGIN, A. A. & TREBAK, M. 2013. STIM1 and Orai1 mediate CRAC channel activity and are essential for human glioblastoma invasion. *Pflugers Arch,* 465**,** 1249-60.

MULLEN, P. J., YU, R., LONGO, J., ARCHER, M. C. & PENN, L. Z. 2016. The interplay between cell signalling and the mevalonate pathway in cancer. *Nat Rev Cancer,* 16**,** 718-731.

MULLER, M. R. & RAO, A. 2010. NFAT, immunity and cancer: a transcription factor comes of age. *Nat Rev Immunol,* 10**,** 645-56.

ORLANDO, D. A., CHEN, M. W., BROWN, V. E., SOLANKI, S., CHOI, Y. J., OLSON, E. R., FRITZ, C. C., BRADNER, J. E. & GUENTHER, M. G. 2014. Quantitative ChIP-Seq normalization reveals global modulation of the epigenome. *Cell Rep,* 9**,** 1163-70.

PARLO, R. A. & COLEMAN, P. S. 1984. Enhanced rate of citrate export from cholesterol-rich hepatoma mitochondria. The truncated Krebs cycle and other metabolic ramifications of mitochondrial membrane cholesterol. *J Biol Chem,* 259**,** 9997-10003.

PAUPE, V. & PRUDENT, J. 2017. New insights into the role of mitochondrial calcium homeostasis in cell migration. *Biochem Biophys Res Commun*.

PAVLOVA, N. N. & THOMPSON, C. B. 2016. The Emerging Hallmarks of Cancer Metabolism. *Cell Metab,* 23**,** 27-47.

PENG, Y., LI, M., CLARKSON, B. D., PEHAR, M., LAO, P. J., HILLMER, A. T., BARNHART, T. E., CHRISTIAN, B. T., MITCHELL, H. A., BENDLIN, B. B., SANDOR, M. & PUGLIELLI, L. 2014. Deficient import of acetyl-CoA into the ER lumen causes neurodegeneration and propensity to infections, inflammation, and cancer. *J Neurosci,* 34**,** 6772-89.

PICKUP, M. W., MOUW, J. K. & WEAVER, V. M. 2014. The extracellular matrix modulates the hallmarks of cancer. *EMBO Rep,* 15**,** 1243-53.

PIETROCOLA, F., GALLUZZI, L., BRAVO-SAN PEDRO, J. M., MADEO, F. & KROEMER, G. 2015. Acetyl coenzyme A: a central metabolite and second messenger. *Cell Metab,* 21**,** 805-21.

PLAS, D. R., TALAPATRA, S., EDINGER, A. L., RATHMELL, J. C. & THOMPSON, C. B. 2001. Akt and Bcl-xL promote growth factor-independent survival through distinct effects on mitochondrial physiology. *J Biol Chem,* 276**,** 12041-8.

POTAPOVA, I. A., EL-MAGHRABI, M. R., DORONIN, S. V. & BENJAMIN, W. B. 2000. Phosphorylation of recombinant human ATP:citrate lyase by cAMP-dependent protein kinase abolishes homotropic allosteric regulation of the enzyme by citrate and increases the enzyme activity. Allosteric activation of ATP:citrate lyase by phosphorylated sugars. *Biochemistry,* 39**,** 1169-79.

QIN, J. J., NAG, S., WANG, W., ZHOU, J., ZHANG, W. D., WANG, H. & ZHANG, R. 2014. NFAT as cancer target: mission possible? *Biochim Biophys Acta,* 1846**,** 297-311.

RATHMELL, J. C., FOX, C. J., PLAS, D. R., HAMMERMAN, P. S., CINALLI, R. M. & THOMPSON, C. B. 2003. Akt-directed glucose metabolism can prevent Bax conformation change and promote growth factor-independent survival. *Mol Cell Biol,* 23**,** 7315-28.

RHIM, A. D., MIREK, E. T., AIELLO, N. M., MAITRA, A., BAILEY, J. M., MCALLISTER, F., REICHERT, M., BEATTY, G. L., RUSTGI, A. K., VONDERHEIDE, R. H., LEACH, S. D. & STANGER, B. Z. 2012. EMT and dissemination precede pancreatic tumor formation. *Cell,* 148**,** 349-61.

SABARI, B. R., ZHANG, D., ALLIS, C. D. & ZHAO, Y. 2017. Metabolic regulation of gene expression through histone acylations. *Nat Rev Mol Cell Biol,* 18**,** 90-101.

SCHREIBER, S. L. & CRABTREE, G. R. 1992. The mechanism of action of cyclosporin A and FK506. *Immunol Today,* 13**,** 136-42.

SCHUG, Z. T., PECK, B., JONES, D. T., ZHANG, Q., GROSSKURTH, S., ALAM, I. S., GOODWIN, L. M., SMETHURST, E., MASON, S., BLYTH, K., MCGARRY, L., JAMES, D., SHANKS, E., KALNA, G., SAUNDERS, R. E., JIANG, M., HOWELL, M., LASSAILLY, F., THIN, M. Z., SPENCER-DENE, B., STAMP, G., VAN DEN BROEK, N. J., MACKAY, G., BULUSU, V., KAMPHORST, J. J., TARDITO, S., STRACHAN, D., HARRIS, A. L., ABOAGYE, E. O., CRITCHLOW, S. E., WAKELAM, M. J., SCHULZE, A. & GOTTLIEB, E. 2015. Acetyl-CoA synthetase 2 promotes acetate utilization and maintains cancer cell growth under metabolic stress. *Cancer Cell,* 27**,** 57-71.

SCOTT, K. E., WHEELER, F. B., DAVIS, A. L., THOMAS, M. J., NTAMBI, J. M., SEALS, D. F. & KRIDEL, S. J. 2012. Metabolic regulation of invadopodia and invasion by acetyl-CoA carboxylase 1 and de novo lipogenesis. *PLoS One,* 7**,** e29761.

SELIGSON, D. B., HORVATH, S., SHI, T., YU, H., TZE, S., GRUNSTEIN, M. & KURDISTANI, S. K. 2005. Global histone modification patterns predict risk of prostate cancer recurrence. *Nature,* 435**,** 1262-6.

SHAROV, V. S., DREMINA, E. S., GALEVA, N. A., WILLIAMS, T. D. & SCHONEICH, C. 2006. Quantitative mapping of oxidation-sensitive cysteine residues in SERCA in vivo and in vitro by HPLC-electrospray-tandem MS: selective protein oxidation during biological aging. *Biochem J,* 394**,** 605-15.

SHEN, H. & LAIRD, P. W. 2013. Interplay between the Cancer Genome and Epigenome. *Cell,* 153**,** 38-55.

SHOSHAN, E., BRAEUER, R. R., KAMIYA, T., MOBLEY, A. K., HUANG, L., VASQUEZ, M. E., VELAZQUEZ-TORRES, G., CHAKRAVARTI, N., IVAN, C., PRIETO, V., VILLARES, G. J. & BAR-ELI, M. 2016. NFAT1 Directly Regulates IL8 and MMP3 to Promote Melanoma Tumor Growth and Metastasis. *Cancer Res,* 76**,** 3145-55.

SIVANAND, S., RHOADES, S., JIANG, Q., LEE, J. V., BENCI, J., ZHANG, J., YUAN, S., VINEY, I., ZHAO, S., CARRER, A., BENNETT, M. J., MINN, A. J., WELJIE, A. M., GREENBERG, R. A. & WELLEN, K. E. 2017. Nuclear Acetyl-CoA Production by ACLY Promotes Homologous Recombination. *Mol Cell,* 67**,** 252-265 e6.

SON, J., LYSSIOTIS, C. A., YING, H., WANG, X., HUA, S., LIGORIO, M., PERERA, R. M., FERRONE, C. R., MULLARKY, E., SHYH-CHANG, N., KANG, Y., FLEMING, J. B., BARDEESY, N., ASARA, J. M., HAIGIS, M. C., DEPINHO, R. A., CANTLEY, L. C. & KIMMELMAN, A. C. 2013. Glutamine supports pancreatic cancer growth through a KRAS-regulated metabolic pathway. *Nature,* 496**,** 101-5.

SUBRAMANIAN, A., TAMAYO, P., MOOTHA, V. K., MUKHERJEE, S., EBERT, B. L., GILLETTE, M. A., PAULOVICH, A., POMEROY, S. L., GOLUB, T. R., LANDER, E. S. & MESIROV, J. P. 2005. Gene set enrichment analysis: a knowledge-based approach for interpreting genome-wide expression profiles. *Proc Natl Acad Sci U S A,* 102**,** 15545-50.

TAKAHASHI, H., MCCAFFERY, J. M., IRIZARRY, R. A. & BOEKE, J. D. 2006. Nucleocytosolic acetyl-coenzyme a synthetase is required for histone acetylation and global transcription. *Mol Cell,* 23**,** 207-17.

TIE, X., HAN, S., MENG, L., WANG, Y. & WU, A. 2013. NFAT1 is highly expressed in, and regulates the invasion of, glioblastoma multiforme cells. *PLoS One,* 8**,** e66008.

TSAI, F. C. & MEYER, T. 2012. Ca2+ pulses control local cycles of lamellipodia retraction and adhesion along the front of migrating cells. *Curr Biol,* 22**,** 837-42.

ULANOVSKAYA, O. A., ZUHL, A. M. & CRAVATT, B. F. 2013. NNMT promotes epigenetic remodeling in cancer by creating a metabolic methylation sink. *Nature chemical biology,* 9**,** 300-6.

VANDER HEIDEN, M. G. 2011. Targeting cancer metabolism: a therapeutic window opens. *Nature reviews. Drug discovery,* 10**,** 671-84.

VANDER HEIDEN, M. G., CANTLEY, L. C. & THOMPSON, C. B. 2009. Understanding the Warburg effect: the metabolic requirements of cell proliferation. *Science,* 324**,** 1029-33.

VENNETI, S., FELICELLA, M. M., COYNE, T., PHILLIPS, J. J., GOROVETS, D., HUSE, J. T., KOFLER, J., LU, C., TIHAN, T., SULLIVAN, L. M., SANTI, M., JUDKINS, A. R., PERRY, A. & THOMPSON, C. B. 2013a. Histone 3 lysine 9 trimethylation is differentially associated with isocitrate dehydrogenase mutations in oligodendrogliomas and high-grade astrocytomas. *Journal of neuropathology and experimental neurology,* 72**,** 298-306.

VENNETI, S., GARIMELLA, M. T., SULLIVAN, L. M., MARTINEZ, D., HUSE, J. T., HEGUY, A., SANTI, M., THOMPSON, C. B. & JUDKINS, A. R. 2013b. Evaluation of Histone 3 Lysine 27 Trimethylation (H3K27me3) and Enhancer of Zest 2 (EZH2) in Pediatric Glial and Glioneuronal Tumors Shows Decreased H3K27me3 in H3F3A K27M Mutant Glioblastomas. *Brain pathology,* 23**,** 558-64.

WADDINGTON, C. H. 1957. The Strategy of the Genes; a Discussion of Some Aspects of Theoretical Biology.

WANG, L., WANG, Z., LI, J., ZHANG, W., REN, F. & YUE, W. 2015. NFATc1 activation promotes the invasion of U251 human glioblastoma multiforme cells through COX-2. *Int J Mol Med,* 35**,** 1333-40.

WARBURG, O. 1956. On the origin of cancer cells. *Science,* 123**,** 309-14.

WARD, P. S. & THOMPSON, C. B. 2012. Metabolic reprogramming: a cancer hallmark even warburg did not anticipate. *Cancer Cell,* 21**,** 297-308.

WEI, C., WANG, X., CHEN, M., OUYANG, K., SONG, L. S. & CHENG, H. 2009. Calcium flickers steer cell migration. *Nature,* 457**,** 901-5.

WELLEN, K. E., HATZIVASSILIOU, G., SACHDEVA, U. M., BUI, T. V., CROSS, J. R. & THOMPSON, C. B. 2009. ATP-citrate lyase links cellular metabolism to histone acetylation. *Science,* 324**,** 1076-80.

WELLEN, K. E., LU, C., MANCUSO, A., LEMONS, J. M., RYCZKO, M., DENNIS, J. W., RABINOWITZ, J. D., COLLER, H. A. & THOMPSON, C. B. 2010. The hexosamine biosynthetic pathway couples growth factor-induced glutamine uptake to glucose metabolism. *Genes Dev,* 24**,** 2784-99.

WELLEN, K. E. & THOMPSON, C. B. 2012. A two-way street: reciprocal regulation of metabolism and signalling. *Nat Rev Mol Cell Biol,* 13**,** 270-6.

WONG, B. W., WANG, X., ZECCHIN, A., THIENPONT, B., CORNELISSEN, I., KALUCKA, J., GARCIA-CABALLERO, M., MISSIAEN, R., HUANG, H., BRUNING, U., BLACHER, S., VINCKIER, S., GOVEIA, J., KNOBLOCH, M., ZHAO, H., DIERKES, C., SHI, C., HAGERLING, R., MORAL-DARDE, V., WYNS,

S., LIPPENS, M., JESSBERGER, S., FENDT, S. M., LUTTUN, A., NOEL, A., KIEFER, F., GHESQUIERE, B., MOONS, L., SCHOONJANS, L., DEWERCHIN, M., EELEN, G., LAMBRECHTS, D. & CARMELIET, P. 2017. The role of fatty acid beta-oxidation in lymphangiogenesis. *Nature,* 542**,** 49-54.

XIAO, M., YANG, H., XU, W., MA, S., LIN, H., ZHU, H., LIU, L., LIU, Y., YANG, C., XU, Y., ZHAO, S., YE, D., XIONG, Y. & GUAN, K. L. 2012. Inhibition of alpha-KG-dependent histone and DNA demethylases by fumarate and succinate that are accumulated in mutations of FH and SDH tumor suppressors. *Genes & development,* 26**,** 1326-38.

XU, M., NAGATI, J. S., XIE, J., LI, J., WALTERS, H., MOON, Y. A., GERARD, R. D., HUANG, C. L., COMERFORD, S. A., HAMMER, R. E., HORTON, J. D., CHEN, R. & GARCIA, J. A. 2014. An acetate switch regulates stress erythropoiesis. *Nat Med,* 20**,** 1018-26.

YING, H., KIMMELMAN, A. C., LYSSIOTIS, C. A., HUA, S., CHU, G. C., FLETCHER-SANANIKONE, E., LOCASALE, J. W., SON, J., ZHANG, H., COLOFF, J. L., YAN, H., WANG, W., CHEN, S., VIALE, A., ZHENG, H., PAIK, J. H., LIM, C., GUIMARAES, A. R., MARTIN, E. S., CHANG, J., HEZEL, A. F., PERRY, S. R., HU, J., GAN, B., XIAO, Y., ASARA, J. M., WEISSLEDER, R., WANG, Y. A., CHIN, L., CANTLEY, L. C. & DEPINHO, R. A. 2012. Oncogenic Kras maintains pancreatic tumors through regulation of anabolic glucose metabolism. *Cell,* 149**,** 656-70.

YUN, J., JOHNSON, J. L., HANIGAN, C. L. & LOCASALE, J. W. 2012. Interactions between epigenetics and metabolism in cancers. *Frontiers in oncology,* 2**,** 163.

ZHAO, S., TORRES, A., HENRY, R. A., TREFELY, S., WALLACE, M., LEE, J. V., CARRER, A., SENGUPTA, A., CAMPBELL, S. L., KUO, Y. M., FREY, A. J., MEURS, N., VIOLA, J. M., BLAIR, I. A., WELJIE, A. M., METALLO, C. M., SNYDER, N. W., ANDREWS, A. J. & WELLEN, K. E. 2016. ATP-Citrate Lyase Controls a Glucose-to-Acetate Metabolic Switch. *Cell Rep,* 17**,** 1037-1052.

ZHAO, S., XU, W., JIANG, W., YU, W., LIN, Y., ZHANG, T., YAO, J., ZHOU, L., ZENG, Y., LI, H., LI, Y., SHI, J., AN, W., HANCOCK, S. M., HE, F., QIN, L., CHIN, J., YANG, P., CHEN, X., LEI, Q., XIONG, Y. & GUAN, K. L. 2010. Regulation of cellular metabolism by protein lysine acetylation. *Science,* 327**,** 1000-4.